This dissertation has been
microfilmed exactly as received 66-13,702

FUNKHOUSER, John Gray, 1934-
THE DETERMINATION OF A SERIES OF AGES OF A HAWAIIAN VOLCANO BY THE POTASSIUM-ARGON METHOD.

University of Hawaii, Ph.D., 1966
Geology

University Microfilms, Inc., Ann Arbor, Michigan

THE DETERMINATION
OF A SERIES OF AGES OF A HAWAIIAN VOLCANO
BY THE POTASSIUM-ARGON METHOD

A THESIS SUBMITTED TO THE GRADUATE SCHOOL OF THE

UNIVERSITY OF HAWAII IN PARTIAL FULFILLMENT

OF THE REQUIREMENTS FOR THE DEGREE OF

DOCTOR OF PHILOSOPHY

IN CHEMISTRY

JANUARY 1966

By

John Gray Funkhouser

Thesis Committee:

John J. Naughton, Chairman
Gordon A. Macdonald
Richard G. Inskeep
Harry Zeitlin
Goro Uehara

To my wife, Andrea, and my two Hawaiian souveniers, Sally and ?.

ACKNOWLEDGEMENTS

Many people have assisted in this research in many different ways. Grateful acknowledgement is expressed to the following individuals who have given freely of their time and skills. My apologies to those whom I have inadvertantly omitted.

Dr. John J. Naughton for, above all, his patience.

Dr. Gordon A. Macdonald for the petrographic description, sample donations, assistance in sample collecting, and valuable advice in geologic matters. Dr. Ralph Moberly, Jr. for his advice in mineral separations. Dr. Theodore K. Chamberlain for the Ewa core.

Dr. I. Lynus Barnes for his inestimable help and counsel. Dr. Jay W. Wrathall for photographic advice and assistance.

Ted Bryant and Floyd McCoy for their geological experience during field trips, and Norman Hubbard for many helpful discussions in geology and petrology.

Dale Hammond for sharing his experience in photography and for the preparation of molybdenum crucibles. Clyde Noble for the synthetic mica and aid in the gas extractions. Bruce Finlayson for his reliable efforts in keeping things running.

Charles Yamashiro and his assistants for their extra effort in obtaining equipment and for his advice in mass spectrometric potassium analysis.

Charles Matule for programming a least squares fit for the isochron plot.

All the undergraduate student assistants, John Gramlich, Eric Kwok, Ronald Nakano, Val Tesoro, for their indefatigable help in all

of the dirty work. Judy Kimura for the hand-picked minerals and X-ray diffraction data.

The junior science apprentices, Ken Honzawa who did much of the time-consuming mineral separations, and Paul Shimada, who performed notably well on the solid-source mass spectrometer.

Joan Ohye for her cheerfulness and for typing and worrying the manuscript to completion. Eileen Duesler for a glassblowing chore and who, with her husband, provided timely assistance in the drafting.

ABSTRACT

A mass spectrometer, gas extraction system, and associated apparatus has been assembled in order to perform potassium-argon age determinations on young, low-potassium rocks typically found in the Hawaiian Islands. The Waianae Volcano Range of Oahu, Hawaii, was systematically dated; the results generally corroborating earlier work by other investigators. Discordantly greater ages were found for certain biotite and hornblende fractions obtained from a 2.3 my rhyodacite. It is suggested that the discordant ages result from excess radiogenic argon held in fluid inclusions in the minerals. This belief is substantiated by visual evidence, vacuum crushing experiments, and the synthesis of a fluoromica that contained inclusions.

Apparent ages of 160 to over 3000 my were obtained from olivines, pyroxenes, and a feldspar separated from a number of Hawaiian xenoliths and inclusions. Again, it is believed that these abnormally great ages can be attributed to excess radiogenic argon contained in the many fluid inclusions observed in these rocks.

The results of this research emphasize the need of multiple, yet selective sampling for potassium-argon dating of young volcanic environments in order to preclude any possibility of excess radiogenic argon cognately or accidentally incorporated into random samples.

TABLE OF CONTENTS

ACKNOWLEDGEMENTS iii

ABSTRACT v

LIST OF TABLES xi

LIST OF FIGURES xii

I. INTRODUCTION

A. General Methods of Age Determination 1

1. Uranium and Thorium Methods 4

2. Rubidium-strontium Method 5

3. Carbon-14 Method 6

4. Potassium-argon Method 6

5. Other Methods 7

a) Thermoluminescence 7

b) Paleomagnetism 8

c) Radiation Damage 8

d) Fission Track Method 9

e) Helium Method 10

f) Potassium-calcium Method 10

g) Ionium Method 11

h) Rhenium-osmium Method 11

i) Lutetium-hafnium Method 12

j) Miscellaneous Methods 12

B. Problem 13

C. Background of the Problem 13

1. Age of the Hawaiian Islands 13

2. Description of the Waianae Range 14

D. Background of the Potassium-argon Method of Geochronometry 17

1. Principle of the Method 17

2. Historical Survey 18

a) Physical Constants 18

b) Procedures 20

c) Apparatus 21

d) Techniques 22

e) Sample Selection 23

f) Argon Diffusion 27

g) Excess Radiogenic Argon 28

h) Air Argon Contamination 30

i) Potassium Determination 32

II. EXPERIMENTAL

A. Construction and Description of the Mass Spectrometer 34

B. Operating Parameters of the Mass Spectrometer . . . 39

C. Description of Gas Extraction System 43

1. General Design and Construction 43

2. Description of the Gettering System 45

3. Description of the Fusion Apparatus 47

4. Description of the Bake-out Ovens 49

5. Description of Crushing Apparatus 51

D. Preparation of Argon-38 and Air Argon Spikes . . . 54

1. Source and Purity of Argon-38 54

2. Argon-38 Spike System 54

3. Argon-38 Spike Preparation 55

4. Air Argon Spike Preparation 58

E. Sample Preparation 59

1. Sample Collection 59

2. Preparation of Whole-rock Samples 60

3. Mineral Separation 60

4. Chemical Pretreatment 61

F. Potassium Analysis 62

1. Flame Photometry 62

2. Separation by Ion Exchange 64

3. R_2O_3 Precipitation 67

4. No Separation--Standard Procedure 69

5. Separation by Distillation 74

6. Isotopic Dilution 74

G. Argon Analysis 75

1. Procedure for Argon Extraction 75

2. Crushing Procedure 78

3. Mass Spectrometric Analysis 78

4. Sample Age Calculation 80

H. Summary of Potassium-argon Age Determination . . . 82

I. Miscellaneous Effects Associated with

Experimental Procedures 83

1. Gettering Conditions 83

2. Re-emission of Gases from Titanium Ion Pumps . . 84

3. Ion Gauge Pumping 88

III. RESULTS AND DISCUSSION

A. Age of the Waianae Range 98

B. Discordant Ages of Hawaiian Extrusives 103

1. Excess Radiogenic Argon 107

a) Accidental Contamination 108

b) Fluid Inclusions 109

(i) Visual Evidence of Inclusions in Mauna Kuwale Rhyodacite 111

(ii) Random Occurrence of Inclusions and Discordant Ages 116

(iii) Release of Argon-40 by Crushing . . . 117

(iv) Synthesis of a Mica with Inclusions 119

c) Argon Dissolution 124

2. Conclusions 125

C. Excess Argon in Hawaiian Xenoliths 125

1. Introduction 125

2. Sampling Sites 128

3. Discussion of Results 129

a) Visual Evidence of Fluid Inclusions 129

b) Crushing and Decrepitation Experiments . . . 132

4. Conclusions 132

D. Precision and Accuracy of Potassium-argon Ages . . . 134

1. Potassium Analysis 137

2. Argon Analysis 140

a) Errors in the Physical Constants 140

b) Precision and Accuracy 141

c) Experimental Errors 144

E. Summary of Conclusions 148

IV. SUMMARY 149

APPENDIX 1 151

APPENDIX 2 152

BIBLIOGRAPHY 156

LIST OF TABLES

1. Principle Isotopes Used for Geochronological Studies . . 3

2. Potassium-argon Ages of the Hawaiian Islands 15

3. Effect of Cations on Potassium Emission 72

4. Potassium-argon Ages of Hawaiian Extrusive Rocks . . . 99-100

5. Potassium-argon Age of Mauna Kuwale Rhyodacite 105

6. Argon-40/Argon-36 Ratios of Vacuum-crushed Rhyodacite Minerals 118

7. Potassium-argon Ages of Hawaiian Xenoliths 130

8. Excess Radiogenic Argon in Hawaiian Rocks 133

9. Excess Argon in Rocks and Minerals 135-136

10. Precision and Accuracy of Potassium Analyses 139

LIST OF FIGURES

1. Decay Scheme for K^{40} 19

2. Mass Spectrometer System 35

3. Sampling End of the Mass Spectrometer 37

4. Mass Spectrometer Tube 38

5. Gas Extraction System 44

6. Fusion Apparatus for Melting Rock and Mineral Samples. . 48

7. Gas Extraction System 50

8. "Wiggle-bug" Crusher 52

9. Hammer Crusher 53

10. Argon-38 Spike Preparation System 56

11. Sodium-potassium Separation on Zirconium Phosphate Ion Exchange Column 66

12. The Effect of Hydrochloric Acid Concentration on Potassium Emission 68

13. Gas Evolution from a Titanium Ion Pump 86

14. Argon Pumping and Re-emission by a Titanium Ion Pump . . 87

15. Ion Gauge Pumping of Argon Isotopes 90

16. Induced Re-emission of Argon-40 and Carbon Monoxide in the Mass Spectrometer Tube 94

17. Isochron Plot for Mauna Kuwale Rhyodacite 106

18. Fluid Inclusions in Biotite of Mauna Kuwale Rhyodacite . 112

19. Multiple-phase Inclusion in Biotite Crystal from Mauna Kuwale Rhyodacite 112

20. Fluid Inclusion in Biotite Crystal of Mauna Kuwale Rhyodacite 113

21. Large Fluid Inclusion in Biotite Crystal of Mauna Kuwale Rhyodacite 113

22. Multiple-phase Inclusion in a Biotite of Mauna Kuwale Rhyodacite 114

23. Rhyodacite Biotite Crystal with Multiple Primary Inclusions 114

24. Fluid Inclusions in Hornblende of Mauna Kuwale Rhyodacite 115

25. Inclusion with Liquid Bubble in Hornblende of Rhyodacite 115

26. Inclusion in a Synthetic Fluoromica 120

27. Dendritic Inclusions in a Dunite from Hualalai, Hawaii 120

28. Dendritic Inclusions in a Hualalai Pyroxenite 131

29. Fluid Inclusions in an Olivine Crystal of a Hualalai Xenolith 131

30. Standard Error in Age of Young Rocks as a Function of Air Argon Contamination 143

31. Sample Collection Sites in the Waianae Range 155

I. INTRODUCTION

A. General Methods of Age Determination

Many estimates on the age of the earth have been made. These have been derived from a variety of hypotheses, from divine revelation to thermodynamical considerations regarding the cooling of the earth. However, the systematic study of the earth's rocks and minerals did not become a basis for age determinations until the early 20th century.

As with most scientific discoveries, the methods of geochronology were built upon a burgeoning foundation of new ideas and theories. In the first part of the 19th century, William Smith in England and George Cuvier in France provided a cornerstone by working with successions of strata identified by the distinctive fossils they contained. Thus it became possible to correlate formations of strata in widely separated regions of the world. Here then was a means of determing the relative ages of rocks. Different successions of strata were classified according to a relative time scale (see Appendix 1). Attempts to assign an absolute age to this time scale were derived by several methods. The most common involved the estimation of the thickness of strata and rate of deposition. For example, in 1905, Sollas[1] obtained a figure of 183,000 feet of strata deposited since the beginning of the Cambrian Period. He took an average rate of deposition of 1 foot/century thus arriving at a time lapse of 18 my. Other methods, for the most part equally inaccurate, were based upon denudation and rates of organic evolution. Some idea

of the chaos prevalent during the first part of the 20th century concerning the age of geological periods may be derived by reading the contemporaneous article of J. Barrels, "Rhythms and the measurements of geologic time."[2]

In 1896, the French physicist Becquerel added another cornerstone to the structure of geochronology by his discovery of radioactivity. In 1905, Boltwood suggested that lead was the ultimate product of uranium decay. In 1907, he computed the ages of ten minerals utilizing their lead-uranium ratio.[3] From this first application of the concept of radioactive decay to geologic time measurement have evolved the most important methods of geochronology in use today. In fact, radiometric dating has enabled geologists to place absolute age figures on the relative time scale derived from stratigraphical and paleontological considerations. The most recent revision is that of Kulp[4] (see Appendix 2).

The mass spectrometer, first rendered operational as a practical device by Aston in 1918 and Dempster in 1919, has provided the basis for measuring radionuclides by stable isotopic dilution techniques. The evolution and refinement of radioactive counting techniques has brought about greater accuracy in radiometric dating by defining the basic constants used in age calculations.

The general methods of absolute geochronometry in use at the present time have been recently reviewed by Hamilton,[5] Aldrich and Wetherill,[6] and Knopf[7] and will be dealt with only briefly here. Table 1 summarizes the basis of each of these methods.

Table 1

Principle Isotopes Used for Geochronological Studies

Parent	Daughter	Half-life (yrs)	Isotopic Abundance (atom %)	Useful Age Range (my)
K^{40}	$Ar^{40}(+Ca^{40})$	1.3×10^{10}	0.0119	$\gg 0.1$
Rb^{87}	Sr^{87}	4.7×10^{10}	27.85	$\gg 10$
Th^{232}	Pb^{208}	1.39×10^{10}	100	$\gg 10$
U^{235}	Pb^{207}	7.13×10^{8}	0.710	$\gg 10$
U^{238}	Pb^{206}	4.51×10^{9}	99.285	$\gg 10$
Pb^{207}/Pb^{206}				$\gg 500$
C^{14}	N^{14}	5570	-	< 0.07

1. Uranium and Thorium Methods

Uranium-238, uranium-235, thorium-232 decay to lead-206, lead-207, lead-208 respectively, and helium. The amount of parent and daughter isotope is related to the age of the system by the general equation

$$Pb = U(e^{\lambda t} - 1)$$

where λ = decay constant for the specific isotope. It is related to half-life by $\lambda = .693/t_{\frac{1}{2}}$ where t = time in years.

Boltwood[3] was the first to utilize the uranium-lead ratio of rocks to determine geologic age. However, not until about 1940, with the mass spectrometric analysis of lead by Nier,[8,9] was the uranium-thorium-lead method put on a sound quantitative basis.

Since uranium and thorium generally occur in the same mineral, three independent estimates of the mineral's age may be made. In addition, the ratio of lead-207 to lead-206 can be related to the age of the mineral. Lead-210 is a short-lived intermediate member of the uranium-238 decay scheme and can be used in an equilibrium ratio with lead-206 to determine age. Another variation based on uranium and thorium decay is related to variations in the isotopic composition of common lead (varying ratios of lead-208, 207, 206 and non-radiogenic lead-204) and hence its appellation, "the common lead method".

Uranium and thorium methods of dating can be applied to a number of minerals. The most ubiquitous is zircon which must be concentrated from rocks such as granites and pegmatites.

Uraninite and thorianite, pitchblende, monazite, sphene and other mineral concentrates have also been used for dating purposes. Isotopic dilution methods utilizing mass spectrometry are extensively employed in the quantitative determination of the uranium, thorium, and lead isotopes needed for age work.

2. Rubidium-strontium Method

Rubidium-87 decays by beta emission to strontium-87. In 1938, Hahn and Walling[10] suggested the possibility of using rubidium-87 decay to measure geologic age, and, in 1946, Ahrens[11] first applied this method extensively.

Since the half-life of rubidium-87 is long compared to geologic time, the following equation may be used to calculate age:

$$t_{my} = \frac{(6.8 \times 10^{10})Sr^{87}}{Rb^{87}}$$

No pure rubidium minerals are found in nature; however, it is isomorphic with potassium so that considerable enrichment of rubidium can occur in potassium minerals. Lepidolite is the favored mineral for rubidium-strontium age work, but it is restricted to pegmatites. Useful ages have been determined from some biotites, muscovites, amphiboles, certain feldspars, and glauconite, a sedimentary mineral. Whole-rock volcanics have recently been dated, but the method is not yet sufficiently sensitive for dating young basalts.[12] Both rubidium and strontium are generally determined by mass spectrometry using isotopic dilution techniques.

3. Carbon-14 Method

Libby[13] suggested this method of dating geological events in 1946. It is based upon the production of carbon-14 in the upper atmosphere by the reaction $N^{14}(n,p)C^{14}$. The radiocarbon combines with oxygen to form carbon dioxide which subsequently comes in contact with the surface of the earth and is uniformly incorporated in organic material by photosynthesis. Carbon from living matter today contains sufficient carbon-14 to undergo approximately 15 beta disintegrations per minute per gram. The age of a sample can be calculated from its present rate of decay measured by refined counting techniques. A large variety of carbon-based samples have been analyzed, including wood, peat, grain, shells, bone, cloth, dung, beeswax, corncobs, pollen, and coral.

4. Potassium-argon Method

Potassium-40 decays both to calcium-40 and argon-40. Aldrich and Nier,[14] in 1948, were the first to utilize potassium-argon decay to measure the age of rocks. Today, this method is the most extensively used in geochronology due to the ubiquitous occurrence of potassium in the earth's rocks and minerals. Evaporites with as much as 50% potassium and pyroxenes with as little as 0.02% potassium have yielded significant potassium-argon ages.

Almost all argon determinations are done by isotopic dilution using mass spectrometry. Potassium on the other hand, is determined by a number of methods, two of the most common being flame photometry and isotopic dilution.

5. Other Methods

Many other methods, both physical and chemical have been developed to date terrestrial rocks and minerals, but none have the general applicability or age range that the uranium-thorium, rubidium-strontium, carbon-14, or potassium-argon geochronometers possess. Some of the more commonly used methods are listed below with a brief description and several pertinent, but by no means inclusive, references.

a) Thermoluminescence[15]

Many minerals emit visible light when heated. This phenomenon is attributed to the release of energy by electrons as they fall from a metastable state (an electron trap) to their normal lattice position. The electrons are trapped in crystal dislocations, impurity inclusions and ion vacancies in the host mineral by absorbing energy from random radiation, primarily alpha particles emitted by the decay of uranium and thorium. The amount of energy released as light at a particular temperature is dependent upon the age of the mineral, past thermal history, radioactivity, chemical impurities, sample preparation, and pressure to which the rock has been subjected.

The thermoluminescence method has the potential of dating rocks less than 100,000 years old; for example, several ages have been determined on late Pleistocene limestone[16] while Sabels[17] has reported ages of 900-35,000

years for basaltic lavas. In both studies, however, the uncertainties involved in sampling and analysis preclude the use of this method of age dating except in extremely limited cases.

b) Paleomagnetism

When a lava flow cools, it acquires a weak but stable remanent magnetization parallel to the direction of the earth's geomagnetic field. The study of such rocks has indicated that the earth's magnetic field has periodically changed polarity; i.e., the North Pole has rotated 180°. Potassium-argon geochronology has served to delineate the recent periods of reversal such that, in many cases, paleomagnetism and radiometric geochronology complement each other. Paleomagnetic reversals, per se, cannot be used to date lava flows, but only to categorize them into certain age brackets. Two normal and two reversed epochs have been defined from recent data and these span but the last 4 my,[18] thus any age correlation must be restricted to very young basalts.

c) Radiation Damage

The physical effects associated with atomic displacements of the crystal lattice resulting from radiation damage have been investigated as a geochronometer in several minerals. The density of zircons has been found to be a function of radiation damage, itself a function of time and uranium-thorium content.[19] Interplanar spacings of

the crystal lattice, determined by x-ray diffraction, have also been related to radiation damage in zircons.[20]

The color of pleochroic halos in biotites has been employed to estimate the age of this mineral.[21] The absorbance is apparently quite sensitive to temperature and thus it may be possible to use this method to date metamorphic events; however, little conclusive work has been reported in this respect.

Color centers in fluorite, absorbing at 305 mμ, have been established as particularly stable. The ratio of color center density to α activity has been correlated with the age of a number of specimens.[22]

d) Fission Track Method[23]

A more sophisticated means of age determination utilizing radiation damage has very recently been developed by workers at General Electric Research Laboratories. This method is based on the amount of crystal damage caused by the spontaneous fission of uranium-238 impurity atoms in a mineral. By suitable chemical etching, radiation damage is indicated by tracks that can be observed with an ordinary microscope. The age of the mineral is indirectly related to the number of observed fission tracks per unit area and the total uranium-238 composition in that area.

A wide variety of minerals have been dated by this new technique; eg, micas, hornblende, beryl, apatite,

zircon, glass, uraninite, calcite. Age limitations are imposed by the uranium content of the mineral. Generally, the minimum age that can be determined in micas is about 10 my; hornblendes, 0.3 my; natural glasses, 30,000 yr; and zircons, 100 yr.[24]

e) Helium Method[25]

Helium is the product of the radioactive decay of the uranium and thorium series and, as such, the amount present can be quantitatively related to the amount of uranium and thorium in a rock by its half-life. Strutt,[26] as early as 1908, first employed this relationship to determine the age of several minerals, bones and phosphate nodules.

The major problem with this method of age dating is loss of the relatively small and mobile helium atom from the crystal lattice of the host mineral. Magnetite, zircon and sphene have been found to be the most retentive minerals and consequently are commonly used for dating purposes. Ages as low as 13 my have been determined from magnetite samples.[27] Recently this method has been applied even to the dating of Pleistocene fossil shells and corals.[28]

f) Potassium-calcium Method

Utilization of the branched decay of potassium-40 to calcium-40 in age determinations is severely limited to minerals with exceptionally low common calcium content

since the most abundant isotope of natural calcium is calcium-40. A few geologically significant dates have been obtained on sylvite samples and some work has been performed with lepidolite and pegmatitic muscovite; however, the problems involved have precluded extensive study especially when such samples are more conducive to alternate methods of geochronometry.

g) Ionium Method[29]

The decay of thorium-230 (ionium), itself a decay product of uranium-238, has been used with a moderate degree of success to date marine sediments. The thorium-230 is precipitated with the ocean sediments while uranium remains in solution. The amount of thorium-230 present can be related to the age of the sample. Generally, in order to correct for certain variables, a ratio of thorium-230 with thorium-232, ferric oxide, or proactinium-231 is measured. Such modifications of the ionium method are useful up to 300,000 yr.

An ionium disequilibrium technique utilizing the decay of uranium-234 to thorium-230 has recently been applied to certain corals and oolites as young as 1,000 yr.[30]

h) Rhenium-osmium Method[31]

Rhenium is a rare element occurring only in molybdenite in sufficient concentration for age dating. The basis of the method is the decay of rhenium-187 to osmium-

187 with a half-life of approximately 4.3×10^{10} yr.

i) Lutetium-hafnium Method[32]

Lutetium-containing minerals are quite rare. One mineral, gadolinite, has been dated using the decay of lutetium-176 to hafnium-176 ($t_{\frac{1}{2}} = 2.1 \times 10^{10}$ yr); however, like the rhenium-osmium method, this means of age determination is too limited to be of geological importance.

j) Miscellaneous Methods

A number of other methods have been suggested as possible means of dating specific geologic systems, but such techniques are, at the present time, more in the analytical development stage than in the applied utilization phase.

The use of cosmic ray generated radioactive chlorine-36 has been considered by Davis and Schaeffer[33] in dating Pleistocene rocks. Attempts to employ radioactive beryllium-10 to date marine sediments have experienced considerable difficulty.[34] The disequilibrium ratio of uranium-234 to uranium-238 in marine calcium carbonate deposits has been proposed by Thurber[35] as a potential Pleistocene dating method. An interesting application to archeological dating has involved the relationship between the thickness of the hydration layer of obsidian to time elapsed since the artifact was first quarried by primitive man.[36]

In all methods of geochronometry, certain criteria must be met in order to achieve meaningful results. For example, the utility of the potassium-argon method as a geochronometer is contingent upon the following conditions:

1. No argon-40 was present initially.

2. There has been no loss or gain of parent or daughter.

3. The duration of formation of the geologic system was short compared to its age.

4. The isotopic composition of potassium has remained constant throughout geologic time.

B. Problem

The object of this research was to assemble the apparatus necessary for the determination of potassium-argon ages on young, low-potassium rocks, and then apply specialized analytical techniques in order to systematically date the Waianae Range of Oahu, Hawaii. In so doing, it was hoped that apparent discordant ages previously reported by other investigators could be resolved.

C. Background of the Problem

1. Age of the Hawaiian Islands

The Hawaiian Islands lie at the southeast extremity of a chain of volcanoes extending over 1500 miles across the Pacific Ocean. Geologic evidence supports mythological lore that Pele, the Hawaiian goddess of fire, has moved progressively southeast and now resides on the island of Hawaii. There is little doubt that the relative age of the Hawaiian

Islands decreases from northwest to southeast. Semi-quantitative estimates of absolute age of the various islands had been made as early as 1927 by Wentworth[37] who based his work upon fluvial erosion rates. Only very recently, however, has the age of the islands been determined by radiometric methods. The results of these investigations are summarized in Table 2.

Much of the tabulated data has been used to support the concept of definite epochs of reversed and normal paleomagnetism. In addition to radiogenic dating, two other ages could be added to Table 2: (1) recent denudation studies indicate the Koolau Volcano Range on Oahu is 1.3-5 my old,[41] (2) paleontological examination of a sample of coral dredged from a drowned terrace southwest of Honolulu suggests submergence occurred during the Miocene epoch.[42]

2. Description of the Waianae Range

The island of Oahu is predominantly composed of the remnants of two major volcanoes; the Koolau Range in the eastern portion of the island, and the older Waianae Range in the western part of the island. Stearns and Vaksvik[43] have divided the Waianae flows into lower, middle, and upper members. The ancient volcanic center lay in the vicinity of Kolekole Pass and the old caldera at one time covered much of what is now Lualualei Valley. The lower member of the Waianae series comprises the pre-caldera stage of volcanic activity. It is separated from the caldera-filling middle member in many places by talus breccia that had accumulated

Table 2

Potassium-Argon Ages of the Hawaiian Islands

Island	Volcanic Series	Age Range (my)	Reference
Kauai	Koloa	1.42	38
		0.60, 1.18	39
	Waimea Canyon	3.84 - 5.62	38
		3.34	39
Oahu	Honolulu	0.9	40
	Koolau	2.22 - 2.56	38
		2.2	40
	Waianae	2.76 - 3.46	38
		2.8, 5.4	40
	Mauna Kuwale (biotite)	8.36	38
Molokai	East Molokai	1.31 - 1.48	38
	West Molokai	1.84	38
Maui	Kula (Haleakala)	0.45 - 0.84	38
	Honolua	1.16	38
	Wailuku	1.29	38
Hawaii	Pololu (Kohala)	0	38
		0 - 0.43	39
	Laupahoehoe (Mauna Kea)	0.6	40
	Waawaa (Hualalai)	0.4	40
	Ninole (Mauna Loa)	0.07, 0.53	39

at the base of the cliffs bounding the caldera, and in other places, by ashy soil. The middle member also includes those lavas erupted on the outer slopes of the volcano during the caldera-filling period. After the caldera had been filled, lavas overflowed to cover the outer slopes of the volcano once again. These post-caldera flows are grouped into the upper member of the Waianae volcanic series. The lower Waianae lavas are thin fluid flows of tholeiitic basalt while the middle member comprises massive, horizontal flows petrographically similar to those of the lower member. The upper Waianae flows rest conformably upon the middle member but grade into alkali basalt and hawaiite. The extent of area covered by lower and middle-upper members of the Waianae flows is indicated by the map of northwestern Oahu (Figure 31) in Appendix 2. For a more detailed description of the geology and petrography of the Waianae Range, see reference 44.

Mauna Kuwale lies just west of Kolekole Pass and forms a portion of the northern wall of Lualualei Valley. The thick, almost horizontal flows that comprise most of Kuwale Ridge have long been defined as a trachyte. They are somewhat unusual for an oceanic basalt environment in that hornblende and biotite are quite prevalent. Petrographically, these flows belong with the upper member of the Waianae series, yet topographically, they lie below the middle Waianae.

Stearns and Vaksvik[43] have suggested that Mauna Kuwale might represent the summit of an older volcano buried by Waianae flows. They based their belief on the stratigraphical situation, the dome-like character of the massive, horizontal beds, and on the fact that other Hawaiian trachytes were regarded as end members of the alkalic suite which signifies the declining stages of volcanic activity. This hypothesis is supported by an age of 8.4 my obtained by McDougall[38] on a biotite fraction separated from the trachyte, whereas ages of 2.7-3.5 my were found for the other members of the Waianae series.

Macdonald,[44] on the other hand, found little erosion between the trachyte and overlying flows which strongly resembled lavas elsewhere in the upper member. He believed the Mauna Kuwale flows to have erupted in the caldera of the Waianae Volcano toward the end of the caldera-filling period.[45] Macdonald[46] has recently defined the biotite-hornblende assemblage a rhyodacite and has shown that it is actually the end member of the tholeiitic suite of basalts, thus providing a basis for a contemporaneous origin with the upper Waianae member.

D. Background of the Potassium-argon Method of Geochronometry

1. Principle of the Method

The utility of the potassium-argon method of geochronometry is derived from the radioactive decay of potassium-40, an isotope of natural potassium. The decay scheme for

potassium-40 is shown in Figure 1 with the appropriate constants that are used in this work.

The equation used to determine the age of a sample from the measured potassium-40 and argon-40 content is given below. It can be easily derived from the basic first order decay expression.

$$t = \frac{1}{\lambda_\gamma + \lambda_\beta} \ln\left[1 + \frac{Ar^{40}}{K^{40}}\left(\frac{1 + R}{R}\right)\right]$$

where t = age of mineral, λ_γ and λ_β are the decay constants for electron capture and β -decay respectively, and R = $\lambda_\gamma / \lambda_\beta$, the branching ratio. Substituting the numerical constants given in Figure 1, the following equation is realized:

$$t_{my} = 1887 \ln \left[1 + 9.130 \frac{Ar^{40}}{K^{40}}\right]$$

2. Historical Survey

a) Physical Constants

The radioactivity of potassium was noted by Campbell and Wood[47] in 1906. Thirty-seven years elapsed, however, before Thompson and Rowlands[48] proved that the decay of potassium involved the formation of argon-40, although Von Weizsacker[49] had predicted a dual decay to calcium-40 and argon-40 in 1937. Also in 1937, Smythe and Hemmindinger[50] found potassium-40 to be the radioactive isotope of potassium; its abundance in natural potassium having been determined in 1935 by Nier.[51] The first successful attempt to utilize Ar^{40}/K^{40} as a

Figure 1

DECAY SCHEME FOR POTASSIUM -40

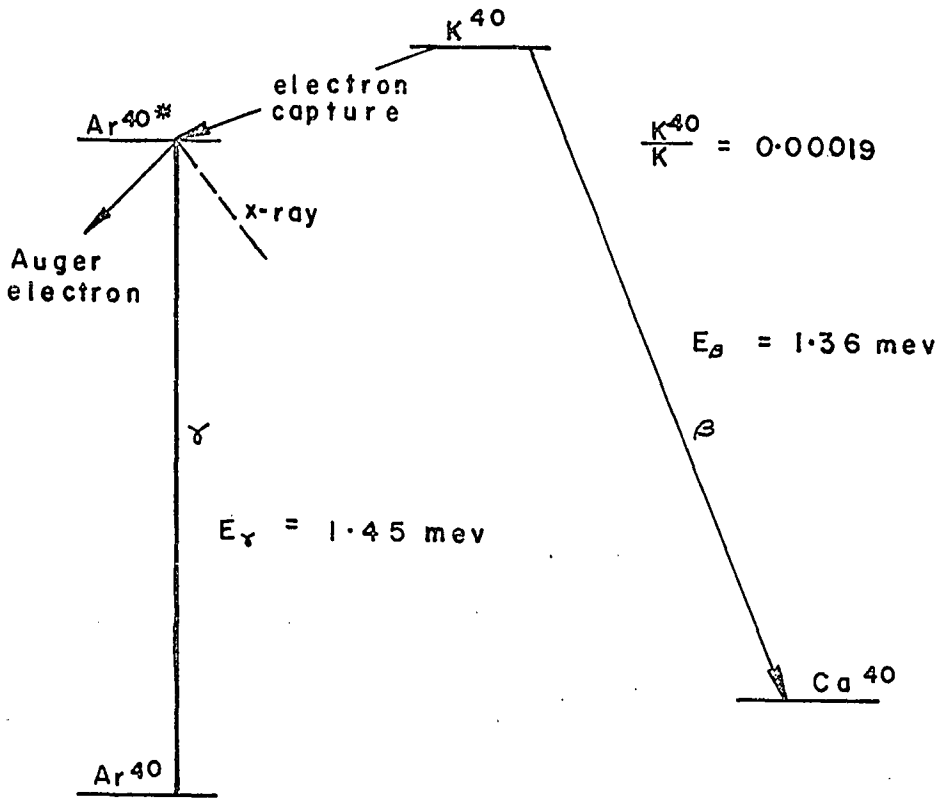

$T_{1/2} = 1 \cdot 30 \times 10^{-9} yr$

$\lambda_\gamma = 0 \cdot 585 \times 10^{-10} yr^{-1}$

$\lambda_\beta = 4 \cdot 72 \times 10^{-10} yr^{-1}$

$R = \frac{\lambda_\gamma}{\lambda_\beta} = 0 \cdot 123$

geochronometer was accomplished by Aldrich and Nier[14] who, in 1948, dated two feldspars and two evaporite minerals.

The determination of the decay constants and thus the branching ratio for potassium decay has been a long and complex affair. The decay of potassium-40 to calcium-40 was relatively easy to follow because of the facility in detecting the emitted electron; however, it had been difficult to quantitatively assess the ejection of Auger electrons from the metastable argon-40. An easier approach was to count the β -rays emitted during the return of argon-40 to ground state energy. Early comparisons of geologically-derived branching ratios with those derived by counting techniques were poor since the samples involved were rocks and minerals of great age and high-potassium content which had lost part of their radiogenic argon by diffusion. There still exists some degree of uncertainty in the basic constants; however, most investigators now use the values given in Figure 1, which are averages derived from the best counting measurements.[6] The isotopic abundance of potassium-40 is taken as 0.0119 atom percent or 0.0122 weight percent.[52]

b) Procedures

The general method of analysis for argon-40 has been the same since 1950, but continuing improvements in instrumentation and experimental techniques have increased analytical sensitivity and thus have broadened

the scope of application of the potassium-argon method of geochronology. The basic procedure is to melt the sample in a vacuum system equilibrate with a known volume of spike, usually argon-38, clean up the extraneous gases by chemical and/or physical methods, and measure isotopic ratios with a mass spectrometer.

Aldrich and Nier[14] used samples of approximately 400 g, heated these to 1000°C, and analyzed the gas with little or no purification. In 1950, Smits and Gentner[53] first applied the potassium-argon method to an undated mineral. They purified the argon by freezing and gettering with calcium. Inghram et al,[54] in 1950, initiated isotopic dilution techniques to measure the amount of radiogenic argon evolved. They used argon-38 as the tracer and employed extensive chemical clean-up of the contaminating gases. A flux of sodium, sodium carbonate, or sodium hydroxide had been widely used in order to melt samples at normal furnace operating temperatures; however, in the mid-1950's, several investigators found incomplete argon release under the conditions of sample melting. Carr and Kulp,[55] in 1955, were among the first to eliminate the flux by utilizing induction heating.

c) Apparatus

The ultra-high vacuum techniques developed by Alpert[56] allowed pressures as low as 10^{-8} mm Hg to be routinely achieved in the extraction and purification

systems. This and improvements in the design of a mass spectrometer by J. H. Reynolds[57] greatly increased sensitivity and accuracy in the quantitative analysis of argon isotopes.

More efficient methods of gas clean-up evolved from much study in this field. (See, for example, reference 58). Some samples of rock can give off up to 200 std cc of gas per gram, most of which is water. Other gases commonly evolved from unaltered rocks and minerals include carbon dioxide, carbon monoxide, hydrogen, nitrogen, chlorine, and fluorine.[59] Getters most commonly employed at the present time are titanium, copper-copper oxide, and calcium. Absorbents such as molecular sieves are used additionally.

d) Techniques

A more thorough study of the techniques of gas extraction and sample preparation has illuminated certain sources of error in argon analysis. Stevens and Shillibeer[60] noted some argon loss after crushing samples of feldspar for extraction preparation, yet Goldich et al[61] found no detectable loss from crushed feldspars even after one year of storage. A rather thorough study by Gerling et al[62] indicated that the mechanical grinding of micas damages their crystal structure, thereby causing loss of radiogenic argon. They suggested the cutting of large flakes to alleviate this hazard.

Carr and Kulp[63] early investigated possible hold-up of argon in extraction and purification systems. They found that quantities of gas as small as 10^{-9} std cc could be circulated without loss in a system containing a rock melt, a radio-frequency glow discharge, a mercury diffusion pump, hot calcium charcoal traps, and even stopcocks. Recent work by Schaeffer and Heymann[64] confirms that no rare gases are driven into the walls of a reactor during glow discharge. Polkanov and Gerling[65] have noted argon hold-up in cold traps when melting fluorine-containing minerals. They postulated the formation of $SiH_4 \cdot 6H_2O$ which crystallizes isomorphically with $Ar \cdot 6H_2O$ at liquid air temperatures. Oxidation of the silane with a copper oxide getter eliminated any such trapping.

e) Sample Selection

As the potassium-argon method of geochronometry gained in sophistication, more thought was given to the selection of rock and mineral samples for analysis. The effect of weathering on potassium-argon ages of granite was studied by Krylov[66] who found that the Ar^{40}/K ratio was generally reduced 10-30% in the initial stages of weathering, but the finer derivatives (river and lake pebbles, sand) maintained the original ratio. He postulated that a natural selection seemed to occur whereby soft and unstable material, a product of initial

weathering, was eliminated by the time the remains were deposited as alluvium. Baadsgaard et al[67] found that biotites lost proportional amounts of argon-40 and potassium such that the age was little affected except in strongly weathered specimens. This work tends to corroborate earlier investigations by Kulp and Engels[68] that up to 50% of the potassium in biotite could be removed without significantly affecting the age, and even after 80% had been removed, the age was lowered only 10%.

Other workers have pointed out types of mineral alteration that may lead to selective argon loss; eg. argillic alteration of glass,[69] devitrification of glass,[39] kaolinization of feldspars,[39] chloritization of pyroxenes.[39] Deuteric alteration of olivine to iddingsite does not appear to affect age.[70] Such investigations have brought about more stringent criteria for the rejection of samples for potassium-argon work.[71] In fact, specific chemical treatment for removing altered or secondary material is sometimes employed in sample preparation.

The particle size of naturally-occurring mineral grains was found to have little effect on potassium-argon ages until the grain size became unmanageably small. Krylov[66] found approximately a 7% lower age in pegmatitic feldspar crystals less than 1 μ in size while Wasserburg and Hayden[73] showed a -80 + 180 mesh sieve

fraction (88-177 μ) of a K-feldspar to have lost about 9% of its radiogenic argon. In both cases, the potassium content of the finer mesh sizes also decreased, but not sufficiently to maintain the age of the larger fractions. The same phenomenon appears to occur with other minerals such as sanidine[74,39] and muscovite;[75] however, Evernden et al[39] obtained the same age on all fractions of a granitic biotite down to -100 + 150 mesh (105-149 μ) and Baadsgaard et al[67] found no loss of apparent age in fractions as small as 270-325 mesh (44-53 μ) for a bentonite biotite.

The significance of metamorphism and thermal contact on argon loss has been assessed by a number of workers.[75-78] Mineral samples were dated at fixed intervals from the contact of an intrusive. As expected, the apparent age of the country rock minerals increased as a function of distance from the intrusive. Two points are worth mentioning, however. One, hornblende showed far less argon loss than did biotite and feldspar; two, there was significant radiogenic argon loss from minerals in rocks presumably too far removed from the thermal zone of contact to experience diffusional loss. These samples exhibited no evidence of disturbance even in thin section examination. Hurley and coworkers,[79] at MIT, found almost complete loss of radiogenic argon from biotite that had experienced temperatures of less than an estimated 100°C.

No petrological evidence implying possible argon loss was noted.[79]

Variations in the diffusional loss of argon in minerals and rocks has plagued workers in the field of geochronology. Wetherill et al,[80] for example, showed that K-feldspars and micas from the same rocks had different argon to potassium ratios. This contributed most to the early confusion of the branching ratio in potassium-40 decay, and brought about the concept of argon retentivity. Some K-feldspars, in old yet fresh samples, were found to retain only 50% radiogenic argon compared to cogenetic micas. From the age data accumulated in the last decade, certain minerals are regarded as sufficiently retentive for selection for potassium-argon dating. Due to the analytical limitations of early methods, only relatively old, high-potassium specimens were sampled. Of these, biotite and muscovite were found to be the most retentive. With the increased sensitivity of modern-day analyses, the utilization of low-potassium minerals has been realized. Hornblende and pyroxenes were found suitable for dating by Hart[81] and McDougall,[82] whereas only certain volcanic feldspars appeared to be retentive enough for reliable age work. It must be realized, however, that retentivity is time dependent in that very young samples (on the order of 10 my) do not, as a rule, lose sufficient argon to affect their age.

The use of whole rock samples in age dating also has been subject to certain criteria. So long as the specimen selected for analysis has remained a closed system, ie, there has been no net loss or gain of potassium and argon, then a valid age should be obtained. The question of how to select such a sample still remains unanswered to a large degree. Judiciously-selected whole-rock basalts were found to yield reliable ages by Erickson[83] and Schaeffer[84] in 1961, and have been much used since. Volcanic glass has been used for age work, but is always suspect due to possible devitrification.[84] Authigenic sedimentary rocks have been dated by the potassium-argon method, although not always reliably (see, for example, references 85 and 86). Sandstones, clays and silts have been dated by Krylov.[66] Shales[87] and their metamorphosed counterparts, slates,[88] have also been analyzed. Preliminary investigations by Lippolt and Gentner[89] indicate that the date of crystallization of "clean" limestones may also be determined by the potassium-argon method.

f) Argon Diffusion

Extensive studies on the diffusion of argon in mineral grains have added surprisingly little to the practical aspects of potassium-argon geochronometry. The difficulty of reproducing natural conditions in the laboratory, the different methods of investigation and

presentation of data, and the complexity of natural diffusion processes have all contributed to the confusing present state of knowledge. Several qualitative generalizations derived from the work of many investigators may be summarized:

1. In many minerals, argon may be held in more than one position, each with a characteristic activation energy, For example; argon held by weak adsorption would have low activation energies, argon-40 located in lattice defects and microcracks would contribute to a medium activation energy, while argon-40 locked in potassium-40 sites in the crystal lattice tends to high energies of activation.

2. Semi-quantitative results indicate the general order of argon retentivity as that found from potassium-argon studies applied to geochronology; ie, hornblende and pyroxene have relatively small diffusion constants, biotite and muscovite also are retentive at surface temperatures while K-feldspars and volcanic glasses exhibit relatively large diffusion rates.

3. Micas lose radiogenic argon rapidly at those temperatures at which structural water is liberated, eg, 400-500°C for biotite, 600-700°C for muscovite.

g) Excess Radiogenic Argon

Earlier, it was mentioned that the validity of the potassium-argon geochronometer depended upon the assump-

tion that no radiogenic argon was initially present in the sample. Little cognizance of this criterion has been manifested until quite recently, although excess argon had been noted in certain minerals unimportant in potassium-argon geochronology.[90,91] Most of the discordantly high potassium-argon ages obtained in the early investigations were dismissed as experimental error, chemical effects pertaining to weathering, or faulty field relationships. However, as the sensitivity of the potassium-argon method has increased and younger, low-potassium rocks are analyzed, the problem of excess argon has had to be recognized.

Anomalously high potassium-argon ages which are attributed to excess argon-40 have been reported for a number of mineral fractions: pyroxenes,[92-96,67] muscovite,[97] biotite,[97] phlogopite,[93,40] albite,[98] plagioclase,[98] and fluorite.[89] It was generally believed that excess argon had been injected into the pyroxene and mica samples during metamorphism. No explanation was given in the case of albite and plagioclase, while Lippolt and Gentner[89] suggested that the excess argon in fluorite was held in fluid inclusions. In fact, a review of the literature reveals the presence of abnormal quantities of argon in fluid and gaseous inclusions of hydrothermal and pneumatolytic minerals[99-101] and in evaporites.[102,103]

h) Air Argon Contamination

Despite the improved sensitivity of argon and potassium analysis, the resolution of the potassium-argon method is limited in young rocks by air argon contamination. Air contains 0.934 volume percent argon, of which 99.600 mole percent is argon-40, 0.063% argon-38, 0.337% argon-36.[104] There is no direct method by which radiogenically-derived argon-40 can be differentiated from air argon-40. In order to correct for contamination by air argon-40, the quantity of argon-36 is measured, multiplied by the natural ratio of argon-40 to argon-36 in air (295.6), and this amount of argon-40 is subtracted from the total argon-40 measured in the sample. Thus any error in the argon-36 reading is magnified 296 times in the measurement of radiogenic argon. By use of the following equation,[105] one can see that a 3% error in the Ar^{36}/Ar^{40} ratio with 50% air argon contamination could cause a 3% uncertainty in radiogenic argon-40. If, in a young, low-potassium rock with very little radiogenic argon-40, the amount of contaminating air argon were 95%, then a 57% error could result in the determination of radiogenic argon.

$$E = \frac{ef}{100 - f}$$

where E = percentage error in the radiogenic argon due to error in Ar^{36}/Ar^{40}, e = percentage error in Ar^{36}/Ar^{40}, f = percentage atmospheric argon in the sample.

Some potassium-argon ages of less than 100,000 yr have been reported in the literature; however, the air argon contamination has been greater than 99%. Even with exceptional accuracy in measuring Ar^{36}/Ar^{40}, uncertainty is so large that only an upper limit to the age of the sample can be set.[106]

Much effort has been expended in order to decrease atmospheric argon contamination without loss of radiogenic argon. Diffusion studies such as those performed by Armikhanov et al[107] have indicated that much of the air argon can be desorbed without loss of radiogenic argon simply by preheating the sample in vacuum. This procedure is commonly employed.

Other methods of decreasing atmospheric contamination have included the use of a traceable argon isotope contained in a solid which is mixed in a known proportion with the sample. A rigorous preheating can then be accomplished even to the extent of losing some radiogenic argon-40 since the amount of radiogenic argon lost can be determined by a standard isotopic dilution calculation. These methods, of course, presume that the diffusion rates for argon in the spike and sample are similar. Naughton[108] has employed a silicate glass that had been irradiated to produce argon-39, while Artemov et al[109] have suggested the use of aluminum chloride containing argon-36.

Naughton has also tried, with varying degrees of success, vacuum crushing to release air argon preferentially,[108] treatment of the sample in a high frequency discharge of mercury,[40] ultrasonic pretreatment of the sample,[110] and crushing and screening the sample under water with subsequent storage under vacuum until ready for use.[40] Evernden and Curtis[72] found that pretreatment of feldspar phenocrysts with dilute hydrofluoric acid reduced air contamination significantly.

Certain minerals have been found to contribute inherently less atmospheric argon during vacuum fusion, eg, less air argon from biotite than plagioclase; thus an indirect means of reducing errors would be to utilize the less gassy portions of the specimen whenever possible.

i) Potassium Determination

Fortunately, improvements in potassium analysis have kept pace with those in argon analysis, yet there still remains much work to be done, especially in the analysis of low potassium rocks and minerals. Generally, the problem of potassium analysis of silicates has been one of either removing or accounting for the effects of interfering elements. To this end, a wide variety of analytical techniques and methods have been employed, eg, gravimetric (chlorplatinate, perchlorate, tetraphenylboron, dipicrylamine), x-ray fluorescence, emission spectroscopy, flame photometry, atomic absorption

spectrophotometry, isotopic dilution by mass spectrometry, neutron activation analysis, different radiometric determinations, and utilization of cation-sensitive electrodes. The most common methods of potassium determination as applied to geochronology are flame photometry and isotopic dilution.

II. EXPERIMENTAL

A. Construction and Description of the Mass Spectrometer

The mass spectrometer used in this research was a glass, 4.5 inch, 60° sector, single-focussing instrument originally designed by J. H. Reynolds.[57] The tube itself was purchased from Nuclide Corporation, State College, Pennsylvania. Vacuum pumps, getters, glass apparatus, and the electronic components were either constructed or purchased.

Figure 2 shows a block diagram of the mass spectrometer. The system can be divided into two sections: (1) the mass spectrometer and (2) the sampling end. The sampling end served as a place to keep the samples and as a reservoir from which aliquots of any sample could be introduced into the mass spectrometer. It also contained a getter by means of which any remaining active gases present in the samples were cleaned up just prior to analysis. The single function of the mass spectrometer section was the isotopic analysis of gas samples.

Figure 3 is a photograph of the sampling end of the mass spectrometer complex. It was constructed from Pyrex tubing. Up to 25 break-offs containing gas samples could be placed onto the manifold. A Bayard-Alpert gauge served as an approximate pressure indicator. The getter originally used (see photograph) was purchased from Amperex Corporation and consisted essentially of a titanium wire wrapped around a tungsten filament. A current of 4-5 amperes was sufficient to evaporate enough titanium to getter the chemically-active gases. After several months of

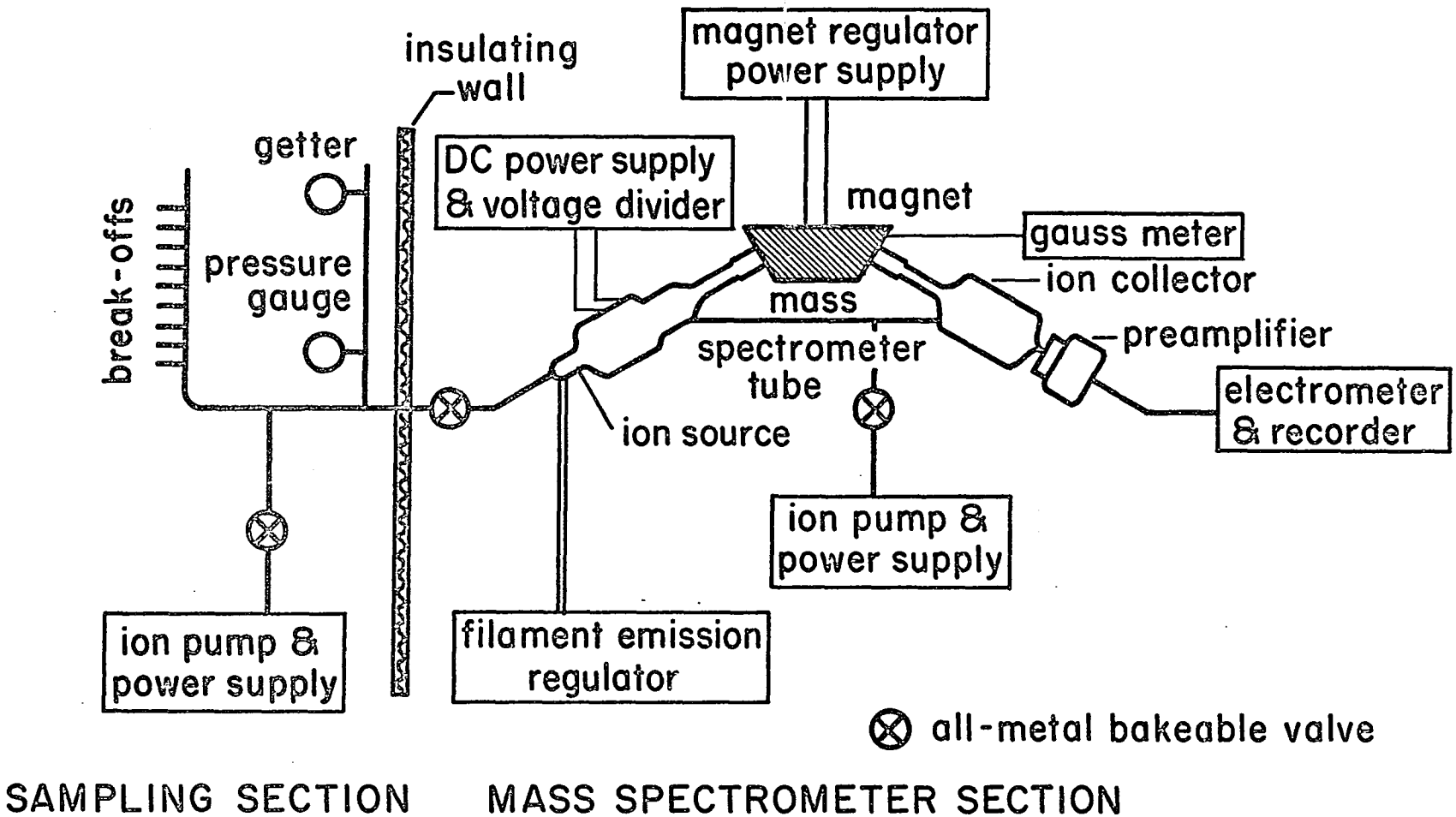

Figure 2

Mass Spectrometer System

operation, the Amperex getter was replaced with one constructed in the laboratory using titanium and tantalum entwined wires wrapped about a tungsten filament and enclosed in a Pyrex tube. The "home-made" getter required 12-18 amperes for rapid clean-up, but was more efficient and lasted longer than the Amperex tube.

There were two outlets from the manifold: one through the vertical magnesite "Maranite" (Johns Manville & Co.) insulation wall to a bakeable, all metal valve (Granville-Phillips Co., Type C) leading into the mass spectrometer; the other through another high vacuum valve and through the Maranite-aluminum support and the table to a titanium getter-ion pump (Varian Associates, "VacIon", 8l/s capacity.

The mass spectrometer tube was constructed of Pyrex and was mounted in a horizontal position (see Figure 4). The tubing leading from the sampling end into the electron bombardment ion source of the mass spectrometer can be seen in the left of the photograph. Another VacIon pump was attached through a high-vacuum valve to the mass spectrometer tube. The ion collector was coated with a graphite paint and enclosed in a grounded steel box in order to prevent stray capacitive currents from contributing to the background noise in the electrometer. The tube was supported on three Maranite blocks with spring clamps.

The filament emission regulator was originally constructed for another type of mass spectrometer and so had to be modified to accomodate the increased load of a larger filament. Accel-

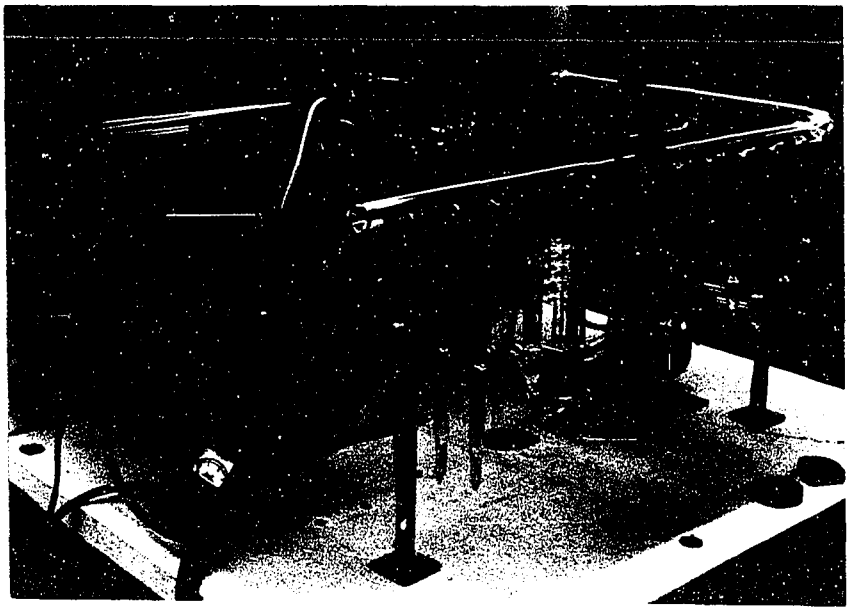

Figure 3

Sampling End of the Mass Spectrometer

Figure 4

Mass Spectrometer Tube

erating and focusing potentials were maintained by a voltage divider fed from a 2 KV DC power supply (John Fluke and Co.). Scanning the mass range was accomplished by varying the current in the electromagnet. A magnet current of 250 ma provided a maximum field flux of 7000 gauss. Provisions for either a manual or automatic sweep were built in the magnet regulator. Both the regulator, power supply and magnet were bought from Nuclide Corporation. Field flux was monitored more accurately with a RFL Gaussmeter utilizing a Hall effect indium-arsenide probe taped to the lower plate of the magnet.

The ion current was collected by a Faraday cup and amplified with a Cary vibrating reed electrometer. As mentioned previously, the entire collector assembly was shielded and grounded to diminish spurious background. The pre-amplifier-collector contact was found to be quite sensitive to vibrations in the table, thus the shielding box had to be securely bolted down. Read-out was accomplished by a Leeds and Northrup, 1-100 mv, recorder on 7-inch chart paper. The filament emission regulator, DC power supply, magnet power supply, and electrometer were all supplied from a constant voltage transformer in order to minimize signal variation caused by line voltage fluctuations.

B. Operating Parameters of the Mass Spectrometer

The equation given below describes the movement of ions in a sector-type mass spectrometer. It is derived from the electrical and magnetic forces acting upon a positive charge.

$$r^2 = \frac{2Vm}{eH^2}$$

where r = radius of curvature of path of ion, cm

V = accelerating potential, abvolts

m = mass of ion, g

e = charge of ion, abcoulombs

H = magnetic field strength, gauss

By focusing the mass spectrometer on mass 28 (CO^+) and measuring the magnetic field flux, an empirical radius of curvature of 4.14 inches was obtained. Deviations from the nominal 4.5 inch radius of curvature result from fringing field effects of the magnet and misalignment of the source and collector slits due to slight glass-blowing errors during construction of the tube and in the actual positioning of the tube with respect to the magnet.

Substituting the appropriate conversion factors for abvolts to volts and abcoulombs to coulombs, the following equation is then obtained for singly-charged ions deflected in a mass spectrometer of 4.14 inch radius:

$$M = 5300 \frac{H^2}{V}$$

where M = mass of ion, amu

H = magnetic field strength, kilogauss

V = accelerating potential, volts

Normally, the mass spectrometer was operated at an accelerating voltage of 2 KV. By lowering the accelerating voltage, however, heavy isotopes such as krypton and xenon could be

scanned within the range of the maximum magnetic field flux.

The operating parameters of the mass spectrometer for maximum sensitivity and resolution in the mass range 35-40 are given below:

trap current	25 μa
filament current	3.9 a
case voltage	36 v
case current	0.99 ma
trap voltage	147 v

There were two potentiometers which could be used to alter electron emission characteristics: one directly controlled filament current; the other, case voltage. A complex interrelationship existed between the above variables and other measurable electronic parameters of the source housing. In addition, filament current and case voltage controlled the signal strength of the collected ions. The optimum settings were empirically determined for each mass range of interest. To compound the problem, magnet current also affected the source characteristics, thereby introducing a small mass discrimination in the instrument. The isotopic ratio of air argon was used to check mass discrimination during operation.

Electrometer adjustments for read-out of ion current were set in order to reach a compromise between signal response and noise level. The background noise could be reduced by damping the signal; however, the time constant was thereby increased such that the mass range of interest had to be scanned

extremely slowly. During general operation, the noise level was approximately 2 mv corresponding to a current of 2×10^{-15} amperes. With a signal to noise ratio of 1:1, this limited the sensitivity of the mass spectrometer to about 7×10^{-10} std cc of argon. Sensitivity was determinied from the peak height of a known quantity of argon isotope.

Residual gases in the mass spectrometer varied depending upon whether the tube was being pumped or was isolated. When the valve was open to the ion pump and pressure maintained below 10^{-8} torr, the largest peaks represented mass 28 and 35. The former corresponds to CO^+, the latter is probably Cl^{35+} since the mass 37 peak was about one-third its height. Other ionic species noted in the background included H^+, H_2^+, He^+, C^+, CH^+, CH_2^+, CH_3^+, CH_4^+, OH^+, H_2O^+, Ar^{40+}, and CO_2^+. If the ion pump was turned off, many gases it had formerly pumped were desorbed to add to the residual background in the tube. Even when the tube was isolated from the pump, the background changed remarkably. Some of the residual gases were "pumped" into glass and metal surfaces by high voltage acceleration in the source section of the tube, while other species were released from such surfaces. In addition, other gases were "cracked" by the hot filament. The release of gases by ionic impact is termed a "memory effect" since it is largely governed by what elements were analyzed in previous runs. This subject will be treated in greater detail in section I.4.

C. Description of Gas Extraction System

1. General Design and Construction

The purpose of the gas extraction system was not only to collect the gases evolved from the mineral or rock samples, but also to remove contaminating gases from argon. For protection of the sensitive electronics of the mass spectrometer, the extraction system was situated in another part of the building, thus the gas samples had to be contained for storage and transport.

Figure 5 is a schematic representation of the gas extraction system. All components were constructed of Pyrex tubing unless otherwise noted. The system was mounted on a table approximately 3 x 2½ feet and supported within a framework of one-half inch stainless steel rod by stainless steel clamps specifically designed for this purpose. Brass clamps of the same design were originally used, but these warped upon repeated baking at 400°C. The table was built of Equipto steel angles. The top was one-half inch transite over which was bolted three-quarter inch Maranite on the front portion of the system.

A Welsh Duoseal mechanical pump was placed beneath the table and attached to a three-stage mercury diffusion pump by a rubber hose. The diffusion pump, in turn, was connected by Pyrex tubing to the cold trap which was maintained at -77°C by dry ice/acetone. After about one year of operation, a U-trap was added above the table in order

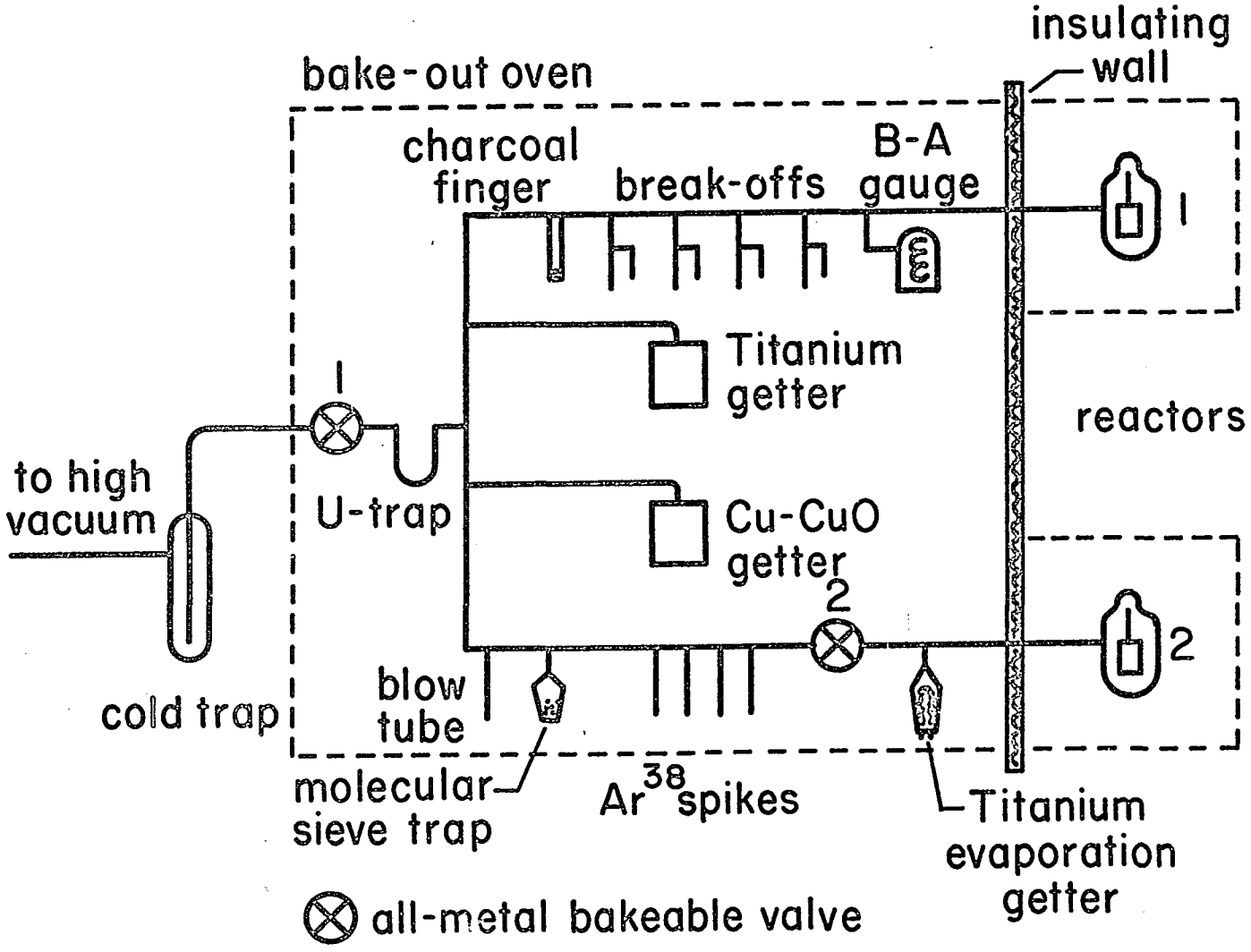

Figure 5 Gas Extraction System

to provide a bakeable trap for liquid nitrogen coolant. The valves were all metal, bakeable, ultra-high vacuum valves, the same type used in the mass spectrometer system. Glass bellows were used to dissipate thermal stresses set up in the glass system during bake-out.

The manifold was constructed of 17 mm OD Pyrex tubing. Up to eight break-off tubes and an equal number of tubes containing argon-38 spikes could be attached to the manifold. A Bayard-Alpert gauge was utilized to check system pressure. A quartz finger containing 0.1-0.2 g of activated charcoal was used to move the gases about in the system. This was accomplished merely by adsorbing the gases onto the charcoal at liquid nitrogen temperatures where all gases save hydrogen and helium are adsorbed. Also leading from the manifold were two reactors and the getters.

2. Description of the Gettering System

The function of the getters in the gas extraction system was to remove the chemically-active gases that were extracted, along with argon, from the mineral and rock samples. Three units essentially composed the gettering system: a titanium getter, a copper-copper oxide getter, and a molecular sieve trap. A titanium evaporation getter, similar to the one previously described in section II.A., was used occasionally.

The titanium getter was constructed from quartz tubing, 3.7 cm in diameter, and about 10 cm long, closed on

one end and connected through a quartz-to-Pyrex graded seal to the manifold. The tube contained approximately 10 g of -10 + 34 mesh titanium sponge (obtained from the U. S. Bureau of Mines, Boulder City, Nevada) enclosed in a quartz cup. Another getter, seldom used due to leakage, was fabricated from stainless steel pipe, 2½ inch OD, and 4 inches long. Top and bottom were heliarc welded. A piece of stainless steel tubing, ½ inch OD curved out of the top and was welded to a Kovar-to-glass seal. Vacuum-tight welding of stainless steel to Kovar was extremely difficult to attain. The stainless steel getter contained approximately 10 g of titanium sponge and two 3 x 24 inch strips of 8-mil titanium metal pleated to prevent overlap. A wire-wound resistance furnace was fitted around the getter to provide operating temperatures up to 1000°C. A chromel-alumel thermocouple was used to measure temperature.

The copper-copper oxide getter was made of stainless steel similar to the titanium getter described above. It contained 50-100 g of 20 mesh copper oxide rolled up in a copper screen. About 1-2 g of silver moss were added to a second copper-copper oxide getter. As with the titanium getter, a wire-wound resistance furnace maintained an operating temperature of 350-400°C.

The molecular sieve trap contained 10-15 g of one-sixteenth inch pellets of Linde molecular sieve 13X in a Pyrex bulb.

3. Description of Fusion Apparatus

Samples were contained in a molybdenum crucible suspended in a Pyrex reactor and melted by means of a 4 KW Lepel spark gap converter induction heater. A diagram of the fusion apparatus is shown in Figure 6. The reactor was made from 6.0 cm OD Pyrex tubing with a 3.7 cm OD neck. Total length was about 24 cm. The crucible was suspended in a molybdenum wire frame from a hook in the top of the reactor. The crucible was removed by breaking the neck of the reactor just below the hook.

The crucibles were fabricated from molybdenum sheet and were discarded after each run. The bottom was formed in a steel die from a circle of molybdenum metal 4 cm in diameter, cut from 5-mil sheet. The cup so produced was 2 cm in diameter with 0.5 cm lips. The collar was made from a 2 7/8 inch wide by 2 inch long piece of 5-mil sheet which was creased on each end and bent around a suitable mandrel. The ends were then fitted together to form a joint and squeezed tight with pliers. The top was formed in the same manner as the bottom, but with 3-mil molybdenum sheet. Holes were punched in the top after it was formed. The three pieces were then degreased in acetone and fitted together.

Temperatures as high as 1550°C could be attained with the induction heater operating at maximum power. The induction coil was made from 11 turns of ¼ inch copper tubing

Figure 6

Fusion Apparatus for Melting Rock and Mineral Samples

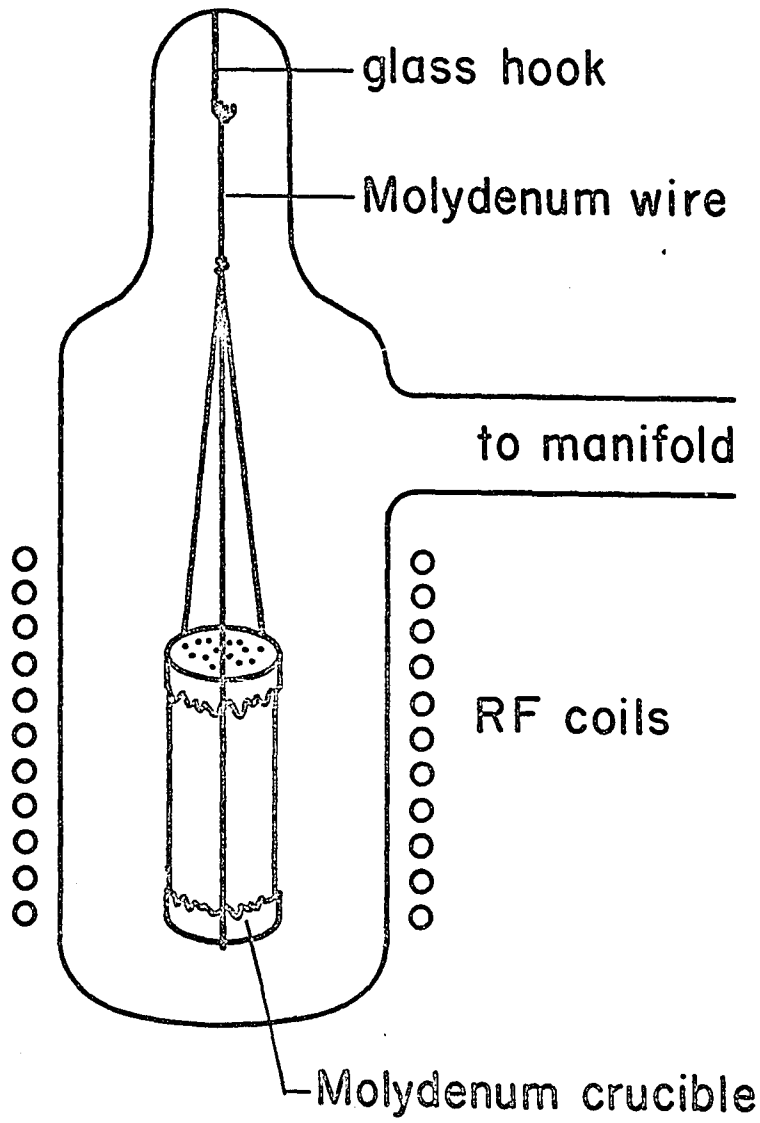

that had been flattened prior to coiling. In order to prevent the Pyrex reactor from softening due to radiative heating by the hot crucible, compressed air was blown around and through the induction coil. Figure 7 shows the reactor being cooled by air blown from a converted bunsen burner and an air gun.

4. Description of the Bake-out Ovens

Ordinarily, to attain a vacuum greater than 10^{-6} torr, it is necessary to bake the system to desorb gases from the walls of the apparatus. The higher the bake-out temperature, the less time to achieve low operating presures. The bake-out ovens used for the extraction system and the mass spectrometer vacuum system were constructed from 3/4-inch thick Maranite. The walls were cut such that they could be fitted together with bolts to form boxes of varying dimensions. The inside of the walls and covers were coated with aluminum foil. Heating was accomplished with 9 inch, 500 watt quartz infra-red lamps mounted on firebrick near the middle of each wall and top. The top of the oven was fitted with a female plug. This led to a terminal box which fed a number of wires that connected to the IR lamps with bulldog clips. Up to four lamps were connected in parallel and regulated from a 20 ampere potentiometer. Bake-out temperatures of $400^{\circ}C$ were easily and quickly attained despite a rather loose-fitting oven caused by warpage of the Maranite.

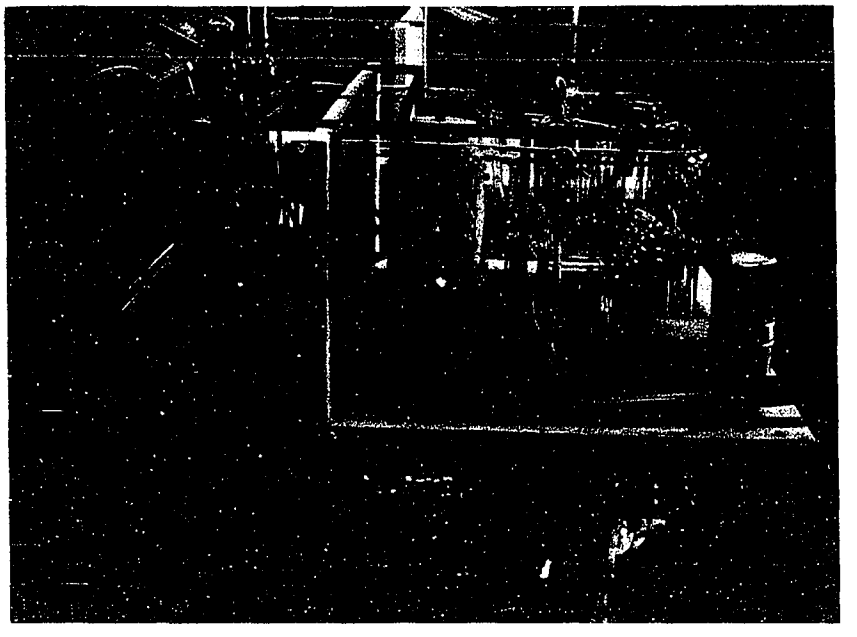

Figure 7

Gas Extraction System

5. Description of Crushing Apparatus

In a number of experiments, argon was released from the sample by mechanical crushing rather than fusion. Two types of crushers were utilized: a vibrating "wiggle-bug" (Figure 8), and a hammer crusher (Figure 9).

The wiggle-bug was the least efficient and the most troublesome of the two crushers. It was made of a stainless steel cylinder with screw caps on each end to which were attached brass rods with a cylindrical piece of soft iron soldered on the end. A concave silicon carbide disc was fitted inside each cap and an 8 mm silicon carbide ball was placed in the cylinder. A Pyrex container was constructed to fit the wiggle-bug with springs holding against each armature. By placing ordinary washing machine solenoids outside the protruding glass shafts next to the armatures and setting a motor-driven rotating disc to actuate a microswitch, alternating power to the solenoids drove the cylinder back and forth against the springs. The force of the ball hitting each carbide disc was sufficient to pulverize a portion of most samples.

The maximum sample load for each crusher was one gram. The initial particle size of the sample depended upon its friability; for example, rather flexible micas necessitated small (< 1 mm) mesh samples, whereas brittle olivines were easily pulverized from grains up to 4 mm in dimensions.

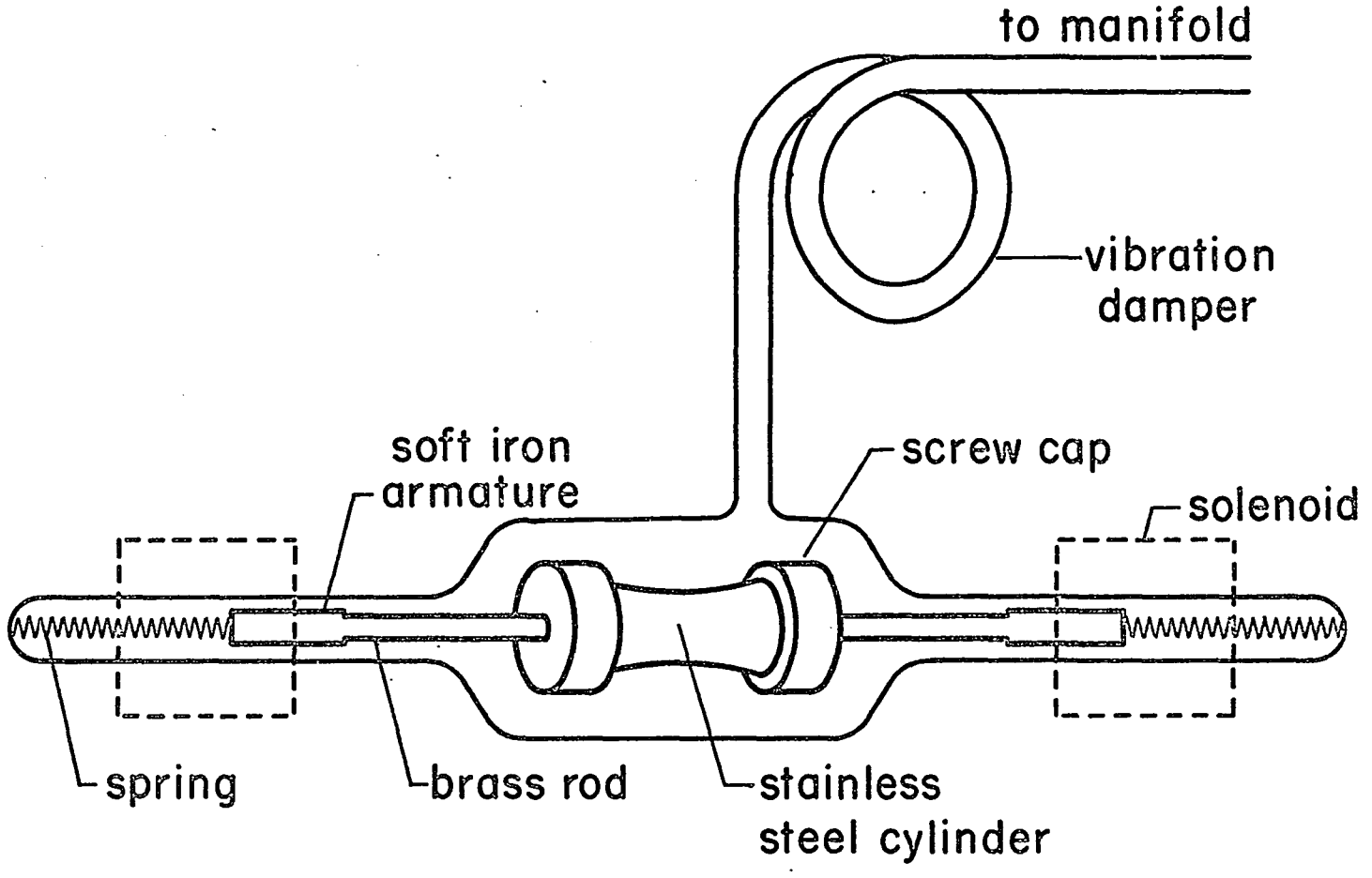

Figure 8

"Wiggle-bug" Crusher

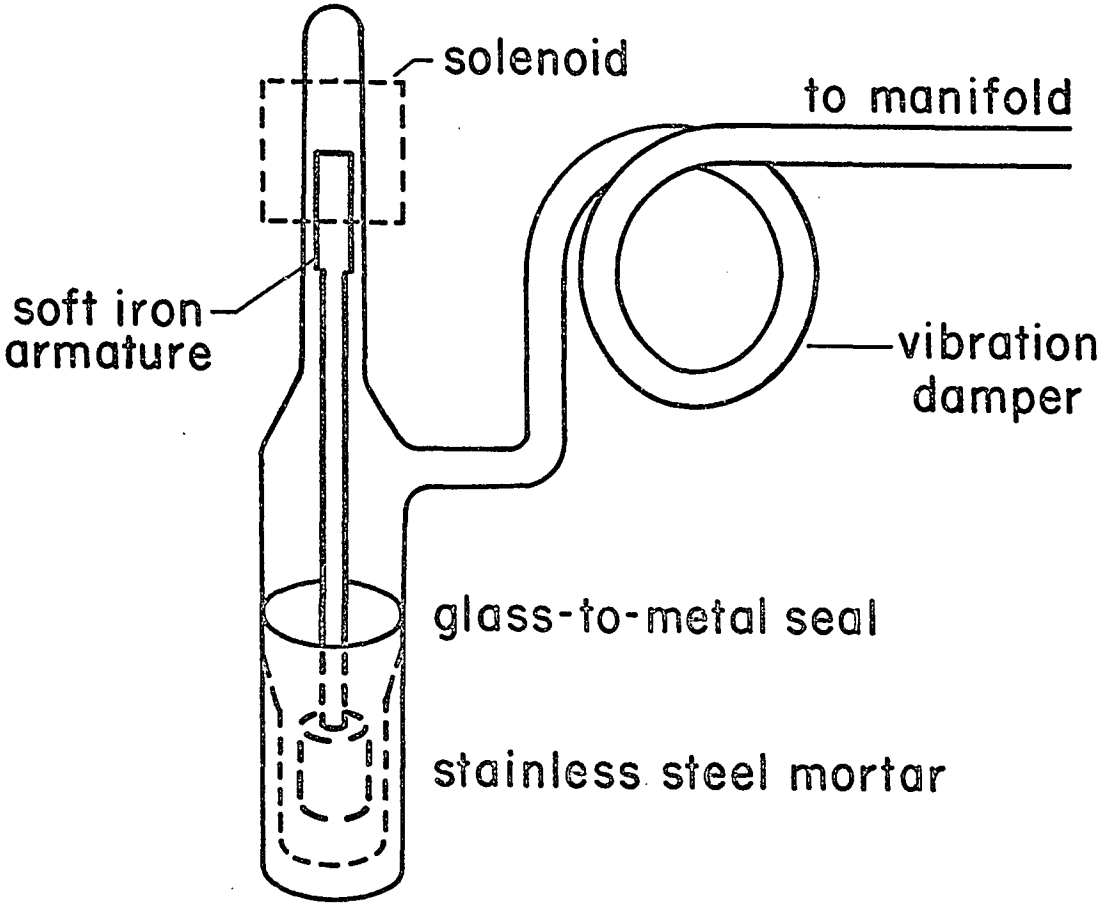

Figure 9

Hammer Crusher

D. Preparation of Argon-38 and Air Argon Spikes

1. Source and Purity of Argon-38

Argon-38 spikes for isotopic dilution analysis were prepared from a 0.1 std cc sample of argon-38 purchased from the Institute of Physical Chemistry, University of Zurich, Switzerland. The isotopic composition was given as:

$$0.01^{5}\ \%\ Ar^{40}$$

$$99.98^{2}\ \%\ Ar^{38}$$

$$0.00^{3}\ \%\ Ar^{36}$$

Six aliquots were prepared from the original argon-38 sample, each contained in a sealed glass tube and holding approximately 7×10^{-4} std cc argon-38.

2. Argon-38 Spike Preparation

The spike system was set up to prepare a large number of spikes at one time as simply and accurately as possible. Three separate sets of argon-38 spikes were prepared for a total of 83 spikes. With each preparation, small improvements were made both in the apparatus and the method.

A Pyrex break-off tube, 1 cm OD, with a 4 cm length of 1 mm ID capillary neck served as a spike container. The neck was connected about 6 cm up from the break-seal, and two marks, exactly one centimeter apart, were scratched in the neck. Attached to the other end of the capillary was a 3 cm length of glass tubing. The volume of each container, approximately 3 cc, was determined to the nearest 0.01 cc from the weight of carbon tetrachloride required to fill the

tube up to the top scratch. The density of the carbon tetrachloride at the filling temperature was taken from a handbook and corroborated with a Westphal balance. The tubes were filled using a hypodermic syringe.

The calibrated spike tubes were blown onto a manifold which was separated from the pumping system by a stopcock. See Figure 10. Leading off the manifold, through a U-trap and stopcock, was a 2.4-liter capacity McLeod gauge. A Bayard-Alpert gauge, a titanium evaporation getter, a break-off for collecting unused argon-38, and the argon-38 reservoir were attached to the other end of the manifold.

3. Argon-38 Spike Preparation

An operating pressure of less than 10^{-6} torr could only be achieved after prolonged pumping, flaming the apparatus with a hand torch, degassing the filaments of the pressure gauge and getter, and repeatedly turning the stopcocks. With liquid nitrogen in both the U-trap and cold trap, pressures in the 10^{-8} torr region could be attained. If the McLeod gauge was not isolated from the manifold by a liquid nitrogen trap, the pressure rose to about 2×10^{-4} torr due to the vapor pressure of mercury.

When it was ascertained that a pressure of less than 10^{-6} torr could be maintained in the closed manifold with the McLeod gauge valve open, the necks of all the spike tubes were preheated just below their softening point in order to desorb gases which would ordinarily contribute to total

Figure 10

Argon-38 Spike Preparation System

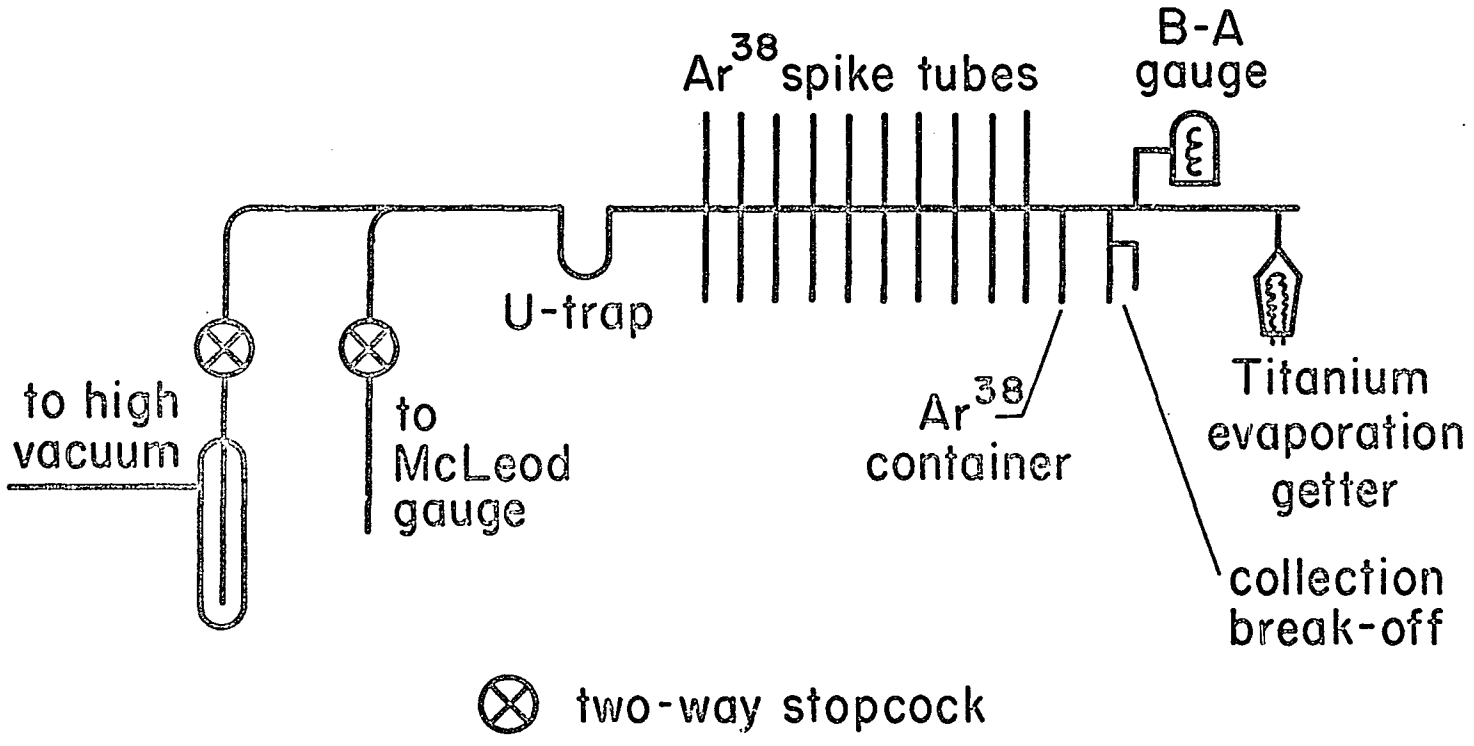

system pressure when the glass was sealed. This simple operation was found to be quite necessary in all cases when glass was later to be sealed. An indication of the degassing efficiency of this step can be seen in the following example: In a closed volume of about one liter, the pressure rose from 2×10^{-7} to 2×10^{-6} torr when the neck of one spike tube was heated. After pumping one-half hour, the same capillary was reheated in the closed system with a resultant pressure rise from 1.5×10^{-7} to 3.0×10^{-7} torr.

The argon-38 reservoir was broken in the closed manifold and titanium evaporated from the getter for about 10 seconds. Pressure was estimated by the Bayard-Alpert gauge which was kept on for only a few seconds in order to minimize ion pumping. The stopcock to the McLeod gauge was then opened and the gas was allowed to equilibrate for at least ten minutes before the first pressure measurement was taken. A number of spikes were removed by sealing at the top scratch with a small, hot flame. After several seconds of titanium evaporation, pressure was again determined with the McLeod gauge. This procedure was followed until all the spikes had been removed. The remaining argon-38 was adsorbed onto the charcoal of the break-off, and this was sealed off and used as the argon-38 reservoir for the next batch of spikes. A slight readjustment of spike volume was made when sealing did not take place at the designated scratch mark.

With the first batch of spikes, the capillaries were not previously degassed, thus the pressure rose from 3.65 x 10^{-4} to 5.40 x 10^{-4} during removal of the spikes. In the second preparation, the pressure remained constant at 2.2 x 10^{-4} mm Hg while 33 spikes were removed. During the third operation, the pressure fell from 1.46 to 1.43 x 10^{-4} mm Hg during the removal of 30 spikes. Each spike contained 5 to 14 x 10^{-7} std cc argon-38 depending upon its volume and filling pressure.

It was originally believed that the only error in determining the quantity of argon-38 in each spike resulted from uncertainties in volume calibration (0.1%), filling pressure (3%), and gas expansion during sealing operations (estimated 0.5%). However, subsequent investigation with the mass spectrometer indicated that (1) the spikes were not consistant from batch to batch, (2) within at least one batch, significant variations in the partial pressure of argon-38 occurred, (3) although the relative amount of argon-38 in all the spikes could be estimated within at least 3%, the absolute amount of argon-38 could only be determined by comparison to a standard spike or rock sample.

4. Air Argon Spike Preparation

Air argon spikes were prepared in order to determine if any mass discrimination occurred in the mass spectrometer by comparing the measured isotopic ratios with those reported by other investigators.

Initially, a set of air argon spikes was made up in the same manner and on the same system as that used for the preparation of argon-38 spikes. The air argon was obtained from a bulb of reagent-grade argon supplied by Air Reduction Co. In order to adjust the pressure of the argon in the manifold, the pump valve was cracked several times. Spikes from this batch subsequently yielded Ar^{40}/Ar^{36} ratios unusually high. These results were attributed to isotopic fractionation which occurred when a portion of the argon was pumped away. Assuming molecular flow, the Ar^{40}/Ar^{36} ratio in the manifold was estimated to be 312 instead of the normal 296.

Another batch of air argon spikes were prepared on the gas extraction system. A break-off tube was sealed at atmospheric pressure and attached to the extraction system. By trapping portions of the sample, then expanding and equilibrating, retrapping and pumping, the amount of air argon was reduced to a workable level while the oxygen and nitrogen were gettered. The spike tubes were then removed.

E. Sample Preparation

1. Sample Collection

The specimens analyzed in this work were, for the most part, collected by the writer during field trips. The remaining samples were generously donated by a number of people at the Hawaii Institute of Geophysics. A list of all samples collected with a petrographic description and

sampling site is given in Appendix 2. A map of northwestern Oahu indicating sample locations is also appended.

The suitability of each sample for potassium-argon analysis was adjudged from a petrographic examination of a thin section. Samples exhibiting extensive secondary alteration were discarded.

2. Preparation of Whole Rock Samples

Samples selected for whole-rock analysis were slabbed to remove weathered and contaminated portions. After enough rock for a thin section had been cut, the remainder was broken up into chunks small enough to fit into an iron mortar and pestle. Appropriate sieve fractions were saved for analysis. The sieve fraction ultimately used for analysis depended upon the size of the phenocrysts in the rock. Non-representative samples are sometimes rather easily obtained from certain size fractions due to the different friability of the minerals and groundmass of a rock. Generally, the -10 + 16 mesh fraction was used. No other pretreatment of whole-rock samples was judged necessary in most cases.

3. Mineral Separation

Mineral separates were analyzed whenever possible. Feldspar phenocrysts were hand-picked as were pyroxene and olivine crystals. For the more fine-grained rocks, magnetic and heavy-liquid separations were resorted to. The purity of each mineral fraction was determined from grain counts.

The Mauna Kuwale rhyodacite posed a special problem in separation since it was desired to resolve apparent age anomalies by analyzing each mineral constituent of this rock. Different size fractions from 100 to 300 mesh were selected for separation. Magnetite was removed with a hand magnet. The heavy minerals, biotite and hornblende, were concentrated with a Franz Isodynamic Separator, and then separated from the lighter material in tetrabromoethane. Hornblende was separated from the mica by shaking on an inclined paper. The flat, platelike biotite crystals did not roll off the paper as easily as the more cylindrical hornblende grains. The finer sieve sizes also tended to be greatly enriched in the more friable hornblende. Plagioclase phenocrysts were separated from the intermediate fraction of a carefully-adjusted acetone-tetrabromoethane mixture; while the groundmass, consisting predominantly of fine-grained plagioclase, alkali feldspar and glass, was skimmed off the top. All mineral fractions were copiously washed with anhydrous methanol immediately after immersion in the tetrabromoethane.

4. Chemical Pretreatment

Certain whole-rock samples were found to contain minor quantities of secondary alteration products. Amygdaloidal calcite was dissolved with dilute nitric acid. Certain feldspar and whole-rock samples were treated with 5% hydrofluoric acid for 20-30 minutes to remove any porous

alteration products and contaminants.

F. Potassium Analysis

As stated in the introduction, there are many methods of determining potassium in silicates; however, the primary problem is one of either removing interfering elements or predicting their effects. Analysis by flame photometry was chosen for this work for two reasons: (1) instrumentation was simple, already assembled and readily accessible; (2) the instrumental procedure was capable of being routinely handled by inexperienced undergraduate assistants.

The problem of interfering elements, ie, cations affecting the degree of potassium emission, was another matter, and a number of techniques were tried before a "standard" procedure was evolved. The analytical results are tabulated in section III.

1. Flame Photometry

Despite the different methods of working up the sample, the basic analysis by flame photometry was the same. A Beckman DU Spectrophotometer, Model 2400, with a flame photometer attachment, was used for all analyses. Rather than use the null meter, a Leeds and Northrup Speedomax recorder (Type G), with a 20 mv scale deflection, was connected to the output of the spectrophotometer. Spectral energy was recorded as peaks on 10-inch wide chart paper. Operating conditions were as follows: oxygen pressure, 14 psi; hydrogen pressure, 4.5 psi; red phototube; resistor #1; sensitivity, 0.1; wavelength for potassium analysis, 767 mμ;

slit width, 0.04 mm except for solutions less than 1 ppm K.

All standards were made from a 4489 ppm K stock solution which had been prepared from Merck reagent grade K_2SO_4 (dried overnight at 515°C) and deionized distilled water. This solution was stored in a capped and taped polyethylene bottle. Standard solutions were made up from about 0.2 to 8 ppm K. Emission energy (peak height) versus concentration was linear up to around 8 ppm where the slope started to decrease due to self-absorption effects.

The analytical procedure was as follows: five ml polyethylene cups were filled with the sample solution and several standards, and an estimated potassium content in the unknown obtained by comparing peak heights. Two standard potassium solutions were then selected to bracket the sample solution. With the more concentrated potassium standard in the flame, the wavelength selector was adjusted to maximum emissivity and the peak adjusted to 90% of full scale deflection with the spectrophotometer potentiometer and recorder sensitivity control. The three solutions were then consecutively aspirated into the flame as quickly as possible, but long enough to draw a line through the noise at the top of each peak. Seven sets of three peaks each were recorded, going from low-potassium standard to unknown to high-potassium standard, then high-potassium standard to unknown to low-potassium standard. Gas pressures were carefully maintained and any base line drift was duly noted.

The difference in peak heights in each set of peaks corresponded to differences in potassium concentration of the solutions, so:

$$\text{ppm } K_u = K_{sl} + \frac{\Delta k \Delta_{u-sl}}{\Delta_s} \qquad (1)$$

or

$$\text{ppm } K_u = K_{sh} - \frac{\Delta k \Delta_{u-sh}}{\Delta_s} \qquad (2)$$

where K_{sl} = ppm K in low-potassium standard, K_{sh} = ppm K in high-potassium standard, Δk = difference in potassium content of the two standards, Δ_{u-sl} = difference in peak height between unknown and low-potassium standard, Δ_s = difference in peak height between the two standards. When $\Delta_{u-sl} \leqslant \Delta_{u-sh}$, then equation 1 was used. The seven results were averaged and percent potassium in the sample was calculated from the following equation:

$$\%K = \frac{kV}{10W}$$

where K = ppm K in sample, V = total volume of sample solution in cc, W = weight sample in mg.

2. Separation by Ion Exchange

Barnes[111] used a zirconium phosphate ion exchange column to separate potassium from interfering elements prior to flame photometric analysis. He obtained good precision and accuracy on the few rock and mineral samples analyzed; therefore, this method, with minor modification, was utilized in the initial analysis,

The sample was ground to a fine powder with an agate mortar and pestle, and weighed into a platinum evaporating

dish. One ml H_2SO_4 (1:5) and 5 ml concentrated HF were added. The dish was heated overnight on low heat. The residue was dissolved in 25 ml HNO_3 (1:5) which was evaporated to SO_3 fumes. The residue was taken up with not more than 25 ml 0.05 N HCl and placed on the column.

The column was prepared in the same manner as described by Barnes--from 50 to 100 mesh of zirconium phosphate manufactured by Bio-Rad Laboratories. Elution was started with 50 ml 0.1 N HCl, then 100 ml of 0.3 N HCl were added and finally 400 ml 1.0 N HCl. The first 150 ml eluant contained sodium and was discarded, the next 400 ml were diluted to 500 ml and analyzed for potassium. Other cationic constituents were eluted during column rejeneration. Total elution time was about 2-2½ hours. Consistantly low results were obtained which led to an investigation of the separating efficiency of the column and the effect of HCl strength on potassium emission intensity.

It was found that passing the initial sample solution through filter paper at the top of the column caused tailing of the potassium peak before any separation occurred. By removing the filtering step and increasing acid strength of the 1.0 N eluant to 1.5 N HCl, fairly efficient separation was accomplished for relatively high-potassium samples (> 1% K). Figure 11 indicates the separation of sodium and potassium versus elution volume for the rhyodacite sample, HK-121 (3.2% K). There was still some tailing and also slight

Figure 11

Sodium-Potassium Separation on Zirconium Phosphate
Ion Exchange Column

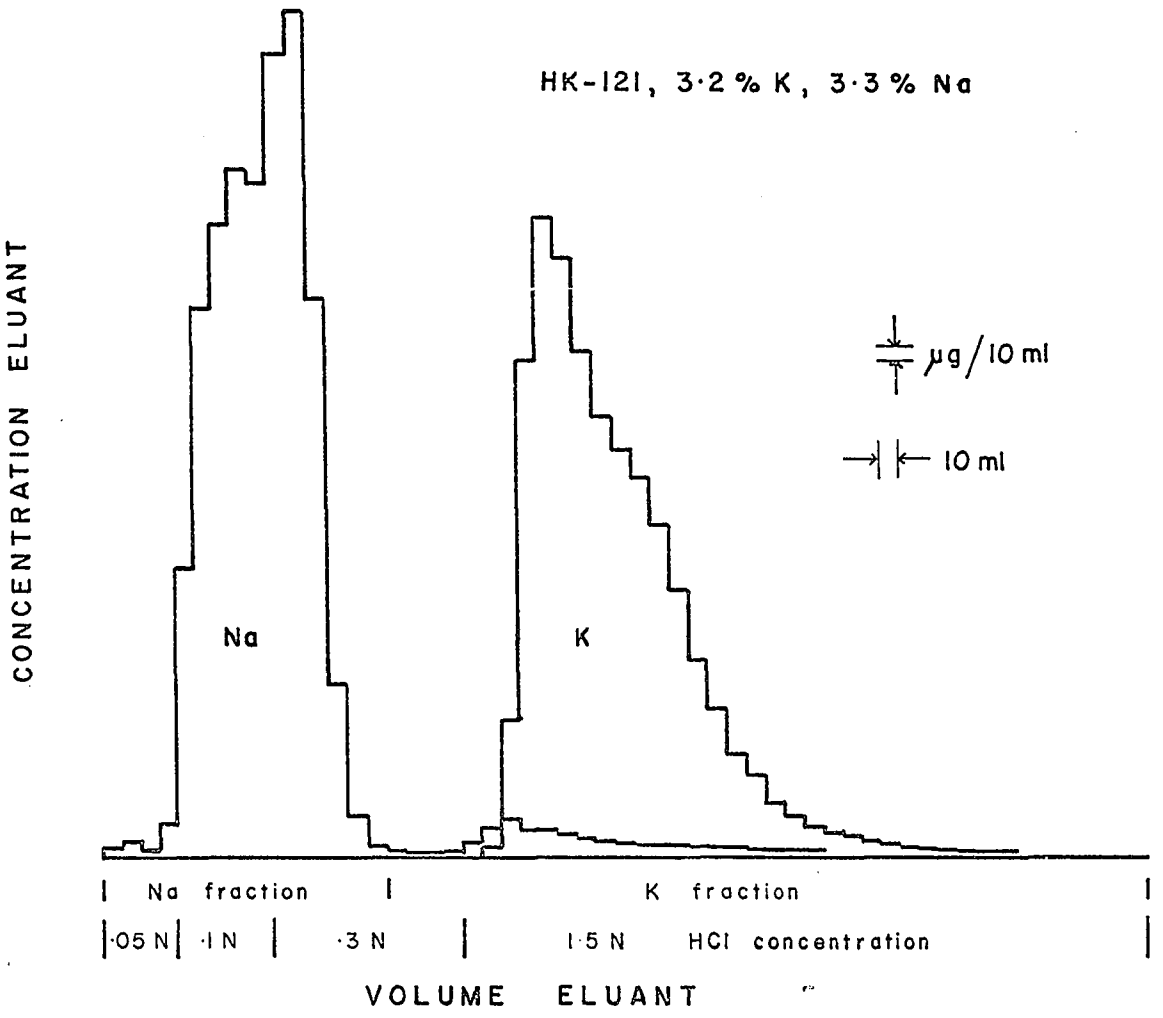

sodium contamination in the potassium fraction; however, results consistant with previous analyses were obtained with good precision.

With rocks of lower potassium content, results were again low and exhibited poor precision in many cases. It was noted that the potassium fraction of the eluant was colored yellow for several samples indicating the presence of Fe^{+++}. Apparently, samples with large iron, magnesium, or aluminum to potassium ratios caused overlapping elution peaks such as was reported by Sweet et al[112] for Dowex columns.

The effect of hydrochloric acid concentration on potassium emission can be seen from Figure 12. The suppression of alkali metal emission by HCl is well known and is attributed to the formation of stable metal chlorides.[113] The degree of suppression is dependent upon potassium concentration and flame temperature.[113] Such data accentuates the necessity of close control on acid strength both in standard solutions and unknowns.

3. R_2O_3 Precipitation

Iron, aluminum, some magnesium and calcium were precipitated as hydroxides and carbonates by a method similar to that described by Cooper.[114] The procedure was the same as described in the previous section, except the residue was taken up with water rather than 0.05 N HCl. Four drops of bromcresol green were then added and the solution neutralized

Figure 12

The Effect of Hydrochloric Acid Concentration on Potassium Emission

4.49 ppm K

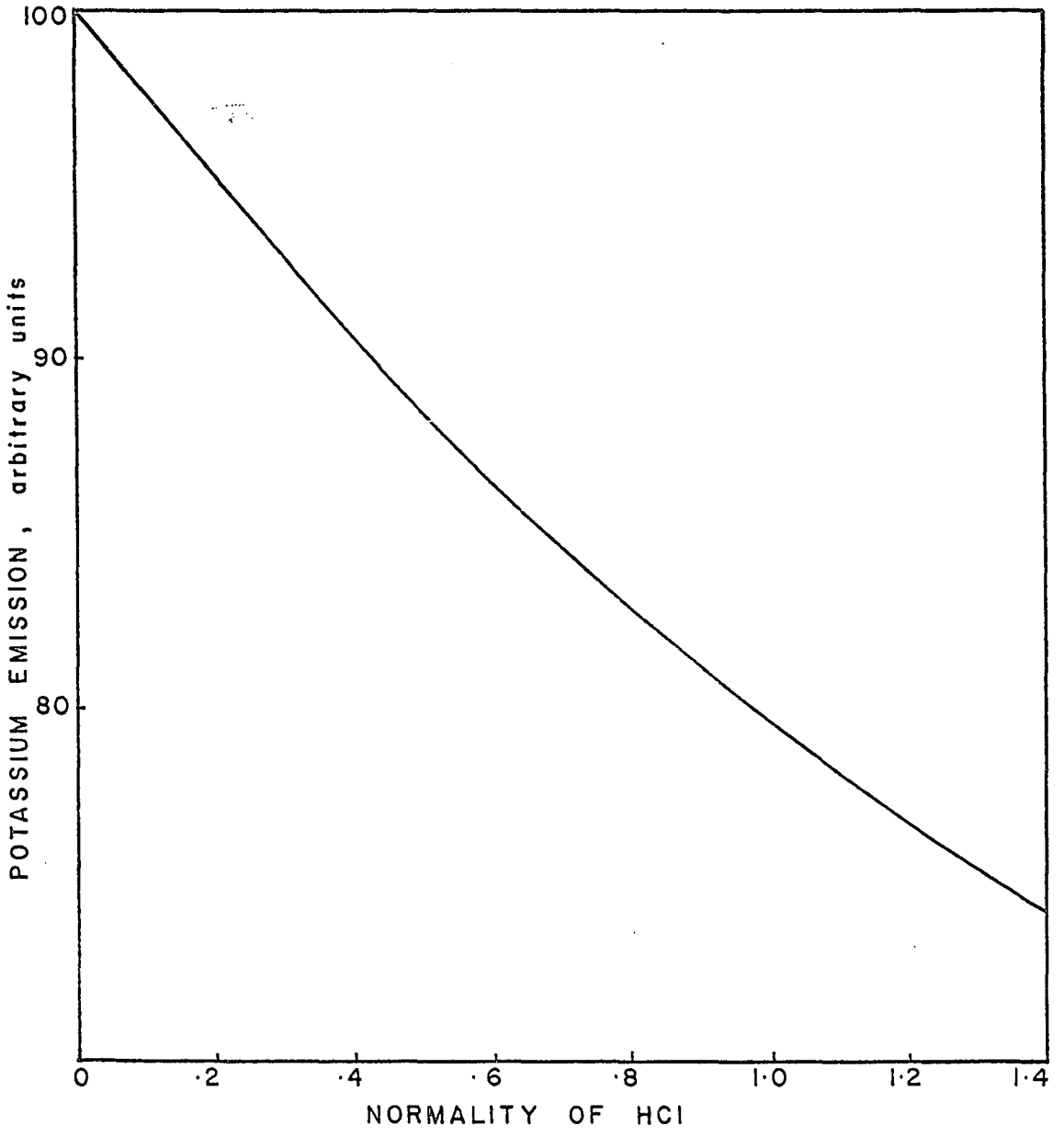

to a blue color with ammonia. Five ml of 10% $(NH_4)_2CO_3$ were added, the solution was warmed, cooled, and allowed to stand one hour before filtering through a pre-washed Whatman #41 filter paper. The filtrate was made up to volume and run on the flame photometer with an appropriate set of standards. Several samples were buffered with 500 ppm Na and compared with similarly-buffered standards.

Several problems arose with this method of separation. The precipitate was, with most samples, voluminous and gelatinous and, therefore, extremely difficult to filter and wash. A centrifuge large enough to accomodate the entire sample and precipitate in one tube was not available at the time. The reagents needed in this procedure contributed to a high potassium blank--the Na_2SO_4 for the buffer was especially high in potassium. Despite these difficulties, this method appeared to give precise and accurate results for the few basalts analyzed. There was no apparent difference in results between buffered and unbuffered sample solutions.

4. No Separation--"Standard" Procedure

Ultimately, a procedure was derived for potassium analysis that involved no separation of interfering cations at all. This method was simplest, quickest and most accurate for rocks and minerals containing more than 0.1% K, and it was also used for low-potassium ultra-basic specimens.

The procedure was again the same as described in

section F.2, except the residue was taken up in 0.65 N HCl. The solution was then transferred directly to a volumetric flask and made up to volume with 0.65 N HCl. In most cases, small amounts of a fine white precipitate remained undissolved, probably either $BaSO_4$ or $SrSO_4$.[115] The solutions were run off in the normal manner on the flame photometer using standards carefully adjusted to 0.65 N HCl. If the flame photometer analysis was not performed within several hours after sample preparation, then the solutions were transferred to polyethylene bottles. Initial sample weight and dilution volume were adjusted between 0.03-0.20 g and 50-250 ml respectively such that the final potassium concentration fell between 4-7 ppm. For low-potassium ultrabasic specimens (< 0.1% K), sample weights as high as 0.5 g were used necessitating repeated $HF-H_2SO_4$ dissolution steps. The flame photometer procedure was also modified slightly, whereby the average background radiation at 760 and 777 mu was subtracted from the potassium peak at 767 mu.

Generally, four analyses were performed at one time. These were scheduled such that a blank was usually included, a primary potassium standard occasionally included, and no more than two samples of the same specimen were dissolved on the same day.

It was somewhat surprising that reliable results were obtained from minerals and rocks of so widely varying composition without prior separation of interfering elements,

although a search of the literature revealed at least one investigator who also had no trouble from interferences in the potassium analysis of silicates and glasses.[116] It is well known that certain cations can alter the intensity; however, the degree of suppression or enhancement is dependent upon a number of experimental, instrumental, and sometimes, seemingly occult variables. With this in mind, the effect of specific cations on the spectral emission of potassium was briefly investigated in the following manner: the appropriate amount of cation chloride was dissolved in a sample solution of the rhyodacite (HK-121) containing 5.22 ppm K. The resulting solution was then diluted with more sample to make varying weight ratios of cation to potassium. Small corrections were made to account for potassium contamination from the salts. The chemical analysis of HK-121[46] indicated that the residual cation constituents would contribute only a small amount to the cation-potassium ratio as prepared. The salt + sample solutions were bracketed between the sample solutions in the flame photometric analysis. The degree of enhancement or suppression was expressed as a positive or negative deviation from the rhyodacite peak height. Results are listed in Table 3.

Emission enhancement is the dominant result of interelement interference and the effect is relatively small except for sodium. It is interesting to compare these results with those reported in the literature in which a Beckman DU

Table 3

Effect of Cations on Potassium Emission
(5.22 ppm K in 0.65N HCl)

Cation	Ratio $\frac{\text{cation}}{\text{potassium}}$	Change in Emission Intensity (%)
Na	100	+ 15
	50	16
	25	12
	12	10
	4	1
Ca	100	+ 3
	50	5
	25	6
	12	4
	6	4
Mg	100	0
	50	0
	9	0
Al	100	0
	50	0
	9	0
Fe	100	+ 5
	50	4
	25	4
	12	5
	4	- 2
	2	0
Ca, Mg, Al	33 each	0
Ca, Mg, Al, Fe	25 each	+ 2
Ca, Mg, Al, Fe, Na	20 each	+ 5
		4
	10	4
	5	3
	2	3
	1	4

Spectrophotometer with an O_2-H_2 flame was utilized. Cooper[114] reported no enhancement of potassium emission due to the presence of sodium in a 3 ppm K-H_2SO_4 solution, yet Grove et al[117] found over 20% enhancement for ratios of 30:1 and greater in an aqueous 15 ppm K solution. Cooper also noted relatively small depressant effects resulting from calcium, magnesium and aluminum, while Easton and Lovering[118] found up to 11% depression in a 10 ppm K-H_2SO_4 solution with a Mg/K ratio of 100:1. Iron was reported by Cooper to enhance potassium emission up to 50% at a ratio of 100:1 in a sulphuric acid solution. This effect was noted also by Easton and Lovering who attributed it to an increase in background radiation. Apparently, the many variables still involved in analysis preclude even qualitative comparisons, yet all data indicate that interference effects are not additive in mixtures. This may explain why no gross errors result from the varied constituents of the analytical samples.

Hamilton and Mountjoy[119] reported a flame photometric procedure for potassium analysis of ultrabasic rocks which was based upon the addition of a dilute "spike" (solution of known concentration of potassium) to an aliquot of the unknown solution. The concentration of the sample was calculated from the emission intensity of the sample and sample + spike, correcting for the reagent blank. Results for samples of pyroxene and olivine were less precise, but generally agreed with data obtained by the method described earlier in this section.

5. Separation by Distillation

Edwards and Urey[120] have described a procedure for separating volatile chlorides from silicates by distillation. The powdered sample is mixed with graphite and $CaCl_2$, transferred to a graphite crucible in a water-jacketed quartz reactor, and heated to 1350°C in a nitrogen atmosphere with an induction furnace. The alkali chlorides condense in the upper portion of the reactor and can subsequently be quantitatively recovered and analyzed with a flame photometer using sodium-buffered solutions.

This method was attempted for both high and low-potassium specimens, but with little success. Total condensation of the volatile chlorides could not be achieved even by passing the vapors through five inches of wet glass wool. Electrostatic precipitation of the chlorides also failed to effect quantitative recovery. Another problem dealt with high reagent blanks resulting from potassium contamination in the $CaCl_2$, and to a lesser extent, in the sodium buffer and graphite crucible.

6. Isotopic Dilution

Some of the rock specimens studied in this work were analyzed for potassium by mass spectrometry utilizing an isotopic dilution technique. Experimental details and analytical data are reported by Yamashiro.[121] It was hoped that this method of analysis could be utilized for low-potassium ultrabasic rocks; however, insufficient time pre-

cluded working out experimental details.

As mentioned earlier, the analytical results are given in section III. A comparison of the potassium content of selected rock samples obtained by several different investigators is also tabulated in the same section, while the accuracy of the results is assessed in section III.D.1.

G. Argon Analysis

1. Procedure for Argon Extraction

The amount of sample fused for argon release was governed by an estimate of its age and potassium content. Biotite from a young rock was sufficiently high in potassium to allow a charge of less than one gram, whereas 8-10 g of a young basalt were generally used. The sample was transferred to a previously degassed molybdenum crucible and the cover was replaced. The Pyrex reactor with the suspended crucible was sealed at the neck and then attached by glass blowing to the gas extraction system (reactor #1 in Figure 5). An empty crucible with cover was always held in reactor #2 for subsequent degassing. During sample loading operations, valve #1 was kept closed so the pumping system could be left on continuously. In order not to contaminate the pumps and cold trap, the system was rough pumped to about 0.01 mm Hg with a portable mechanical pump attached to the blow tube. After checking for leaks with a Tesla coil, the mechanical pump was isolated by sealing the blow tube, and valve #1 was opened.

The bake-out ovens were placed over the table and each reactor. The large Maranite oven was heated by four IR lamps regulated by a 20 ampere potentiometer while the temperature of each reactor oven was maintained separately by an 8 ampere potentiometer. The main portion of the extraction system and reactor #2, with the empty crucible, were baked at about 400°C, while the sample was baked at temperatures of 150-250°C depending upon the nature of the specimen; eg, whole-rock basalts and other retentive minerals were degassed at 200-250°C, while glass was degassed around 150°C. Bake-out time arbitrarily varied from 12-24 hours. The getters were turned on about half way through the bake; titanium at 800-850°C, copper-copper oxide at 340-360°C.

After the system had cooled, getter temperatures were adjusted to 780-790°C for the titanium, 340-350°C for the copper-copper oxide. Liquid nitrogen was placed on the U-trap, the Bayard-Alpert gauge was degassed, the charcoal finger and both the charcoal and neck of a break-off were flamed. The induction coil was fitted around reactor #1 and the blowers were emplaced. If the pressure was below 2×10^{-6} torr, both valves were closed and the liquid nitrogen taken off the U-trap.

Fusion of the sample was accomplished by intermittent heating and cooling cycles in order to maintain the reactor below the softening point of Pyrex. Generally, the induction coil was activated for 3-4 minutes and then turned off until

the glass was cool to the touch. This schedule was repeated for a total fusion time of 9-15 minutes. The argon-38 spike was broken immediately after heating was initiated. Liquid nitrogen was placed on the quartz charcoal finger after the first heating-cooling step. With samples of mica and small particle size rocks and minerals, the temperature of the crucible was intermittently raised slowly over 10-15 minutes in order to prevent decrepitation from blowing the sample out of the container.

After fusion, the liquid nitrogen was removed from the charcoal finger and the gases were gettered for 20-30 minutes before the titanium getter was turned off. The titanium was cooled with an air blower in 3/4-1½ hours. (Hydrogen is gettered by titanium only at temperatures below 400°C). The argon was collected in the break-off by placing liquid nitrogen around the charcoal finger for 20-30 minutes and then sealing the glass. The pressure of the system was measured in order to estimate the efficiency of gettering. Usually, it was 10^{-5} torr or less.

Preparation for the next run commenced by opening both valves and degassing the empty crucible in reactor #2 in the same manner as sample fusion. As soon as the glass was cool, valve #1 was closed and the system vented to the atmosphere. Reactor #2 was removed at the side arm, opened at its neck, and a new sample added. After sealing, it was reattached to the manifold in position #1. A clean reactor

with an undegassed crucible was placed in position #2 and the procedure for rough pumping and bake-out was carried out again.

2. Crushing Procedure

The same type of operation was performed in a crushing experiment except, of course, there was no fusion. The major exception to the procedure was the elimination of any prior degassing step to the empty crushing container. As mentioned earlier, the sample charge was limited to one gram. Crushing was accomplished in 1-3 hours with varying degrees of efficiency. Generally, all of the original sample was reduced in size, and greater than 30-40% was crushed finer than 300 mesh (ca 50 μ).

3. Mass Spectrometric Analysis

The gas samples from the extraction system were set aside until 10-20 had accumulated at which time they were attached to the sampling end of the mass spectrometer system. The sampling end was baked at 400°C while being pumped with a mechanical pump. A dry ice/acetone and liquid nitrogen trap in series were used to prevent migration and contamination by pump oil. Bake-out continued from 24-36 hours before the system was sealed off and the ion pump started. The mass spectrometer tube was baked twice during its two years of intermittent operation; the first time when it was newly assembled, the second after it had been accidentally broken open to the atmosphere. Oven temperature was main-

tained below 225°C for the second bake-out. A pressure of less than 10^{-8} torr could be attained in the sampling end only after ion pumping 2-5 days. The mass spectrometer portion of the system was maintained at 10^{-8} torr continuously since it was never vented.

The procedure of the mass spectrometer analysis of a gas sample follows in the order of actual operation. The filaments of the Bayard-Alpert gauge and titanium evaporation getter in the sampling end were degassed until very little pressure rise was noted. During this time, the gaussmeter was usually set to read 3.25 kG at the mass 28 peak and 3.65 kG at the mass 35 peak. A background spectrum in the region of mass 35-40 was run in the tube with the valve to the ion pump open. The sample end-pump valve was closed, pressure checked, sample broken, equilibrated for several minutes, and pressure checked again. The Bayard-Alpert gauge was operated at 0.1 ma emission current for a few seconds only whenever a sample was in the system. Longer operation caused appreciable ion pumping, about which more will be said later. If the pressure was greater than 1×10^{-4} torr, the sample was gettered by evaporating titanium for 30-60 seconds. This was repeated intermittently until sample pressure stabilized or was reduced below 5×10^{-5} torr.

The mass spectrometer-pump valve was closed and the middle valve opened for two minutes, the time of opening

being noted. The peaks at mass 36, 38, and 40 were scanned manually at least twice, going from lower to higher mass each time. Sensitivity of the electrometer and recorder was adjusted to create maximum deflection for each peak. The sample was then pumped out of the mass spectrometer tube and another aliquot analyzed, if necessary; otherwise, the sampling end was also opened to the ion pump. Recovery of operating background pressure depended upon the quantity of gas in the sample, but generally it took about ½-1 hour for the mass spectrometer portion and ½-6 hours for the sampling end.

"Time zero", the time at which the gas sample contacted the filament of the mass spectrometer, was marked on the recorder chart and the peaks of each mass number were extrapolated to this point. Peak heights were seldom constant; either increasing due to memory effect or decreasing from ion pumping. The zero-time peak heights were converted to millivolts deflection and recorded as such after subtracting background corrections.

4. Sample Age Calculation

The equation relating the age of a system to the radioactive decay of potassium-40 has been given in section D.1 of the introduction and is repeated here after substitution of the appropriate numerical constants.

$$t_{my} = 1887 \ln \left[1 + 9.130 \frac{Ar^{40}}{K^{40}} \right]$$

The volume of the radiogenic argon extracted from the specimen is given by the general equation:

$$V_R = V_T \left[\frac{\left(\frac{40}{38}\right)_T \left[1 - \left(\frac{38}{36}\right)_A \left(\frac{36}{38}\right)_S\right] - \left(\frac{40}{38}\right)_S \left[1 - \left(\frac{38}{36}\right)_A \left(\frac{36}{38}\right)_T\right] + \left(\frac{40}{36}\right)_A \left[\left(\frac{36}{38}\right)_S - \left(\frac{36}{38}\right)_T\right]}{\left[\left(\frac{36}{38}\right)_S \left(\frac{38}{36}\right)_A - 1\right]} \right]$$

where V refers to volume, T refers to tracer or spike, A refers to air, S refers to sample, and the number ratios imply argon isotopes of that mass number. Substituting the appropriate values calculated from the composition of atmospheric argon (see section I.C.2.h), the argon-38 spike (section II.C.1), and the mass discrimination factors (see section III.D.2.c), the following equation is obtained:

$$V_R = V_T \left[\frac{(.9833)\left(\frac{40}{38}\right)_S - (295.6)(1.017)\left(\frac{36}{38}\right)_S}{1 - \left(\frac{36}{38}\right)_S (0.187)(1.017)} \right]$$

The calculations involved in determining an age of a rock or mineral are best exemplified with actual data:

%K = 0.885

wt. sample = 9.0326 g

Ar^{38} spike #34 = 3.043 cc filled at 2.47×10^{-4} mm Hg

peak heights: Ar^{40} 19855 mv

Ar^{38} 3216

Ar^{36} 54.4

(1) Potassium-40

$$\frac{(1.22 \times 10^{-4})(0.885 \times 10^{-2})}{40} = 2.699 \times 10^{-8} \text{ moles/g}$$

where $K^{40}/K = 0.000122$ by weight

(2) Volume argon-38 spike

$$\frac{(3.043)(2.47 \times 10^{-4})}{760} = 9.890 \times 10^{-7} \text{ std cc}$$

(3) Volume of radiogenic argon

$$(9.890 \times 10^{-7}) \quad \frac{6.071 - 5.087}{1 - .0033} = 9.764 \times 10^{-7} \text{ std cc}$$

(4) Moles radiogenic argon

$$\frac{(9.764 \times 10^{-7})}{(9.033)(2.241 \times 10^{4})} = 4.824 \times 10^{-12} \text{ moles/g}$$

(5) Age

$$1887 \ln \left[1 + 9.130 \frac{4.824 \times 10^{-12}}{2.699 \times 10^{-8}}\right] =$$

$$(1887)(1.629 \times 10^{-3}) = 3.07 \text{ my}$$

(6) Air argon contamination

$$(54.4)(306) = 16600 \text{ mv } Ar^{40} \text{ from air}$$

where $306 = \left(\frac{40}{36}\right)$ measured for air

$$\frac{16600}{19860} \times 100 = 84\% \text{ air argon contamination}$$

H. Summary of Potassium-argon Age Determination

The complete procedure from sample to age is outlined below. The time needed to accomplish each step of the procedure is also given. It must be noted that the time is not actual working time but elapsed time and applies to one sample only. When additional samples were run in an assembly-line basis, so

to speak, the elapsed time per sample was reduced to one-third or less.

1.	Petrographic examination	1-2 hr
2.	Physical preparation of sample	1-4
3.	Potassium analysis	18-22
4.	Argon extraction	20-30
5.	Transfer to mass spectrometer and its preparation	50-72
6.	Mass spectrometric analysis	1
7.	Computation	1
	Total	92-132 hrs

I. Miscellaneous Effects Associated with Experimental Procedure

1. Gettering Conditions

The titanium getter on the gas extraction system was operated at 780-790°C. Previous studies by Patzlaff[122] indicated that argon was irreversibly desorbed from a quartz-contained titanium getter above 800°C, but no appreciable increase in argon partial pressure was noted below this temperature. In order to ensure minimum desorption of all gases from the titanium and quartz during an extraction, the titanium was degassed at temperatures above 850°C during bake-out. The rate of cooling did not influence the gettering of hydrogen which forms titanium hydride at temperatures below 400°C.

The copper-copper oxide getter was maintained around 350°C during an extraction. The rate of oxidation of

hydrogen and carbon monoxide by copper oxide is dependent upon temperature; however, above 400°C, the dissociation pressure of cupric oxide becomes appreciable,[58] thus the optimum pressure conditions are attained in the region of 350-400°C. In order to replenish the copper oxide, which is reduced to the metal after continual use, the getter was operated at 350-400°C at atmospheric pressure for several hours a week.

2. Re-emission of Gases from Titanium Ion Pumps

The VacIon pumps on the mass spectrometer system were the sole means of maintaining a low background pressure. They remove gases by ionization, sputtering, and chemical combination. The gas molecules and atoms are ionized by collisions with electrons and bombard the titanium cathode plates which are maintained at 3-4 KV above ground. This process knocks out titanium atoms which are deposited on the anode and cathode. The sputtered titanium reacts with the chemically-active gases and also physically buries the inert gases.

Three phenomena have been reported with titanium ion pumps: (1) argon instability, (2) hydrocarbon formation, (3) memory effect. Argon instability refers to the sudden release of argon from the cathode, and is caused by re-evolvement of previously pumped argon resulting from the continual action of ion bombardment. Only on one occasion was any argon instability noted. This occurred with the

VacIon pump on the sampling end of the mass spectrometer system and was manifested by sudden random pressure jumps observed on the pressure gauge of the ion pump power supply.

The formation of hydrocarbons, such as methane, ethane and propane, by titanium ion pumps has been reported by a number of investigators (see, for example, Lichtman,[123] Reich,[124]) and is attributed to the reaction of titanium carbide with water and/or hydrogen,[125,126] although it appears that the relatively unstable titanium hydride would be an active source of hydrogen for the reaction.

Hamilton[127] reported for a titanium triode getter ion pump that previously pumped gases were sometimes evolved when another gas was being pumped--essentially a replacement mechanism. He also noted large quantities of gas were given off after the pump was turned off.

The data shown as a bar graph in Figure 13 corroborates these earlier studies. The gases in the ion pump chamber had accumulated for 18 days with the pump off before being introduced to the mass spectrometer for analysis. The large increase in mass peaks 12 through 16 indicate the evolution of methane. The extremely large increase in the argon isotope peaks, which do not conform to the isotopic ratios of air argon, do indeed imply a memory effect, yet little to no background appears at the appropriate mass numbers when the ion pump is operating. Figure 14 indicates that significant argon re-emission occurs immediately after

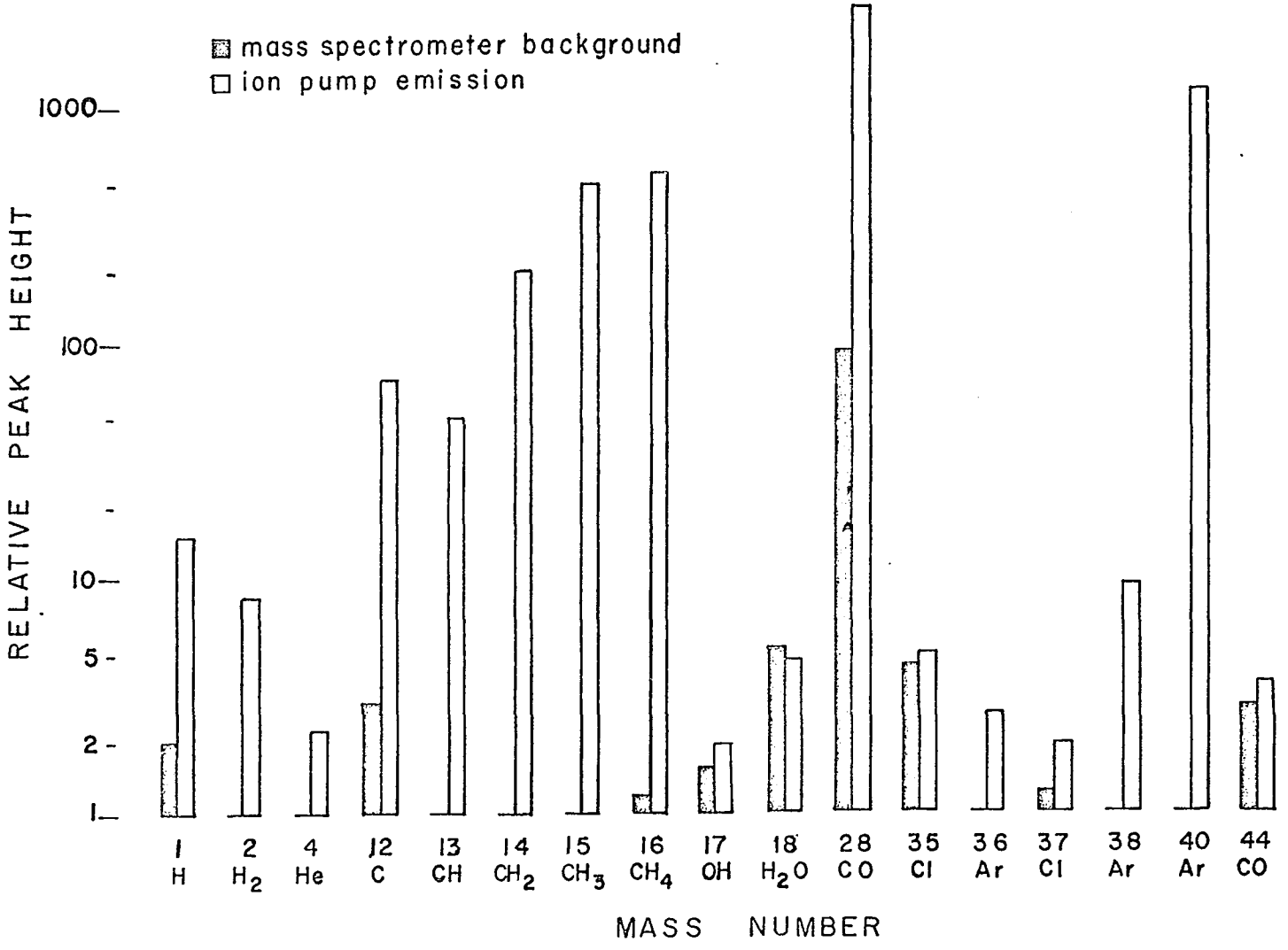

Figure 13 Gas Evolution from a Titanium Ion Pump

Figure 14

Argon Pumping and Re-emission by a Titanium Ion Pump

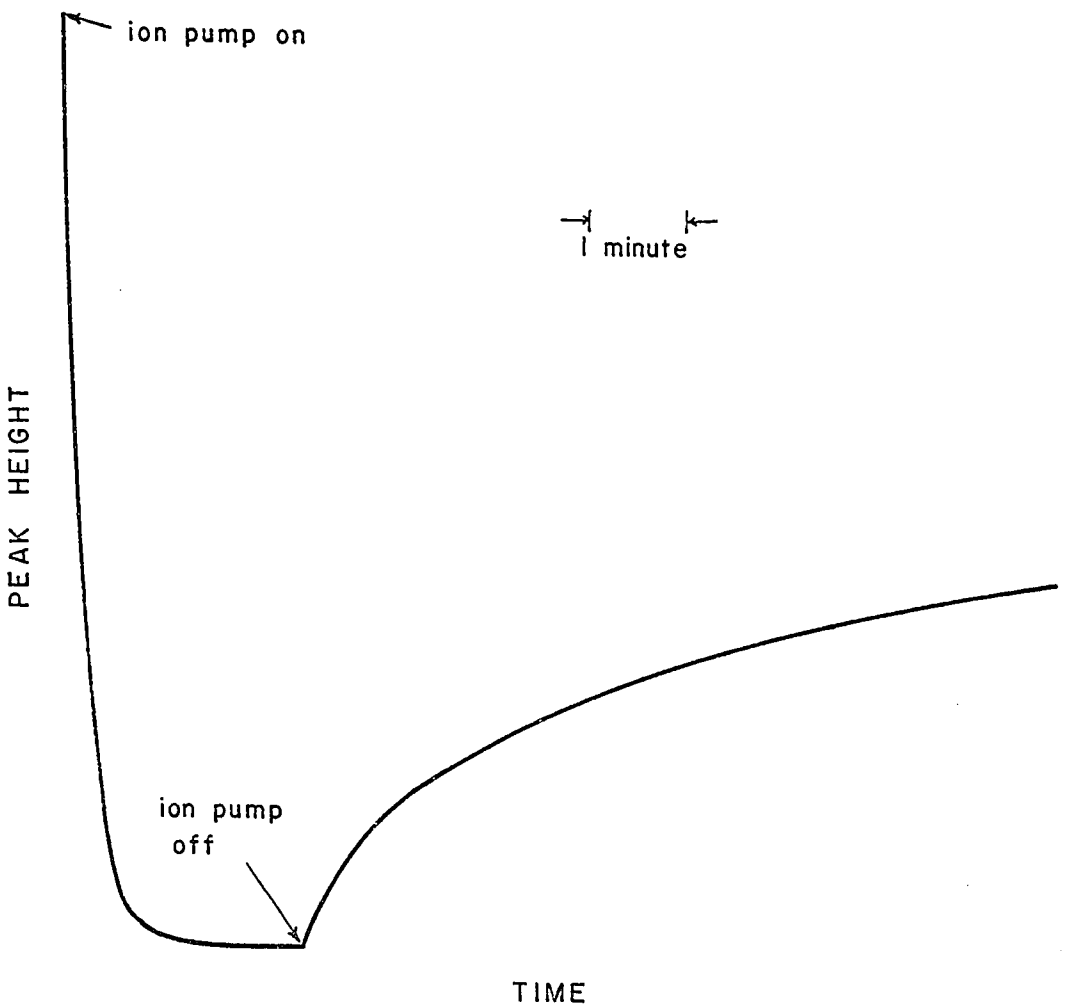

the pump is turned off despite the high pumping rate for the inert gas. It is interesting to note that water, carbon dioxide, and the mass 35 and 37 peaks are the only species not evolved from the ion pump or its surrounding surfaces.

The release of large quantities of argon and other gases underscores the necessity of isolating any ion pump from the analytical system when it is not in operation. Similar effects result from the operation of titanium evaporation ion pumps and, probably, to a much lesser degree, titanium evaporation getters of the type used on the sampling end of the mass spectrometer system.

3. Ion Gauge Pumping

The Bayard-Alpert gauge was the only pressure measuring device used on the isolated mass spectrometer and gas extraction systems. It served only to give an estimate of pressure since an accurate pressure determination would have involved the control of too many variables in gauge operation and conditions. The Bayard-Alpert gauge operates like a triode in which electrons, boiled off the filament, are accelerated by a helical grid and ionize gas molecules and atoms which are subsequently collected to produce an ion current. The ion current is directly proportional to pressure.

It has been known for over 100 years that gas is "cleaned up" when subjected to bombardment by energetic electrons. Investigations of pumping and re-emission of noble gases in the Bayard-Alpert gauge are numerous. It is

generally agreed that clean-up results from the interaction of ions with the glass envelope; however, the mechanisms involved and the quantitative aspects of gas removal are still disputed. A brief study was undertaken in connection with this research in order to determine how a pressure measurement would affect the quantity and isotopic composition of an argon gas sample. The Bayard-Alpert gauge on the sampling end of the mass spectrometer system was operated while monitoring the peak height of the argon isotopes. Some of the data is graphically presented in Figure 15.

The pumping curves generally conform to those previously reported and quantitatively described by equations of varying complexity.[57,128-130] Assuming all ions are irreversibly pumped, then

$$-\frac{dP}{dt} = \alpha P \qquad (1)$$

The proportionality constant, α, contains a sticking probability coefficient which is partially dependent upon ion mass so isotopes of greater mass should exhibit a slightly greater pumping speed.

The assumption of irreversible pumping is not valid, however. Three factors contribute to diminish the rate of clean-up until a dynamic equilibrium is attained with no net pressure change. Pumping is dependent upon "active" sites on the ion gauge surfaces which become depleted as clean-up progresses. Also spontaneous re-emission from these surfaces results from diffusion of the atoms already pumped.

Figure 15

Ion Gauge Pumping of Argon Isotopes

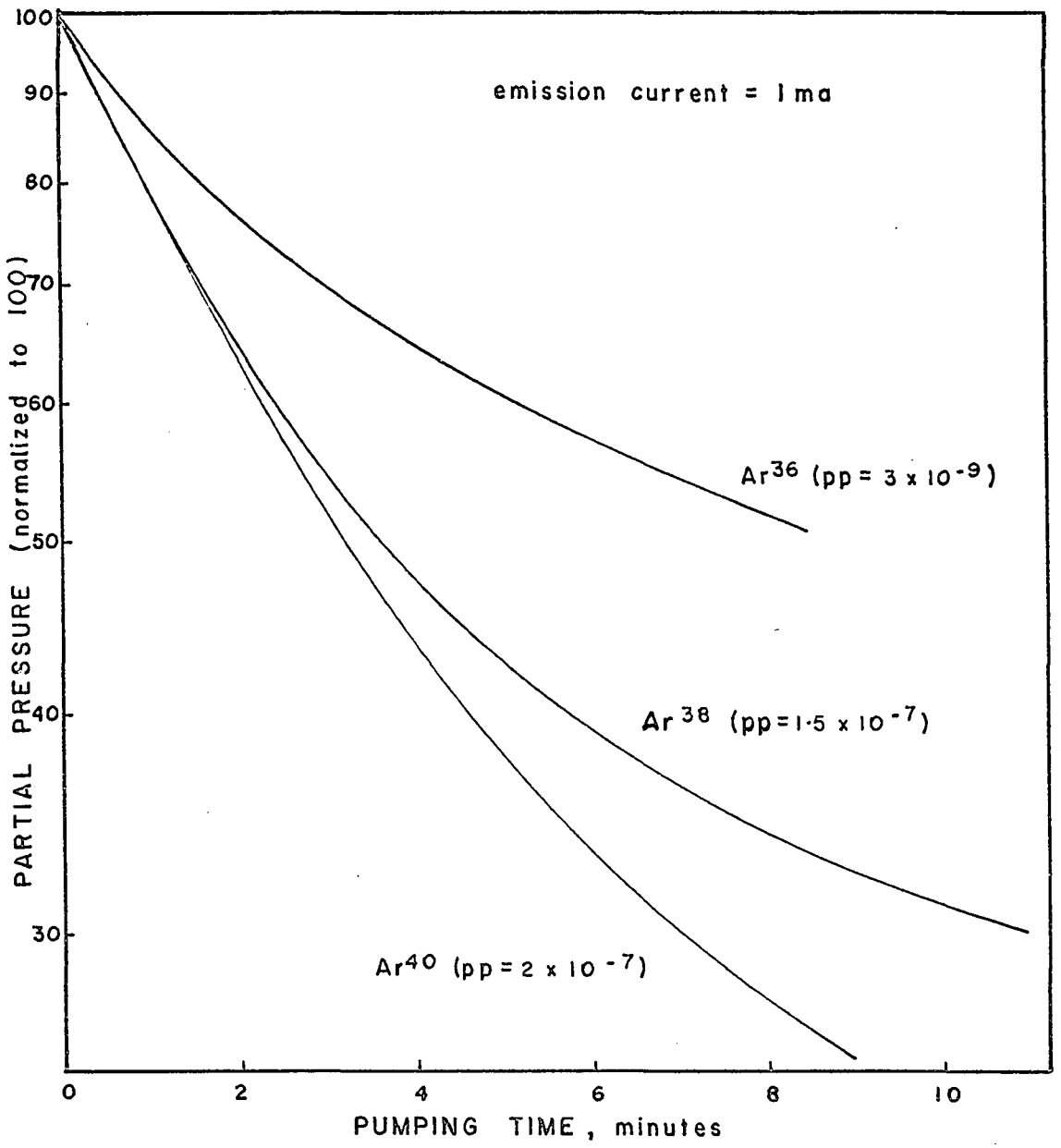

Re-emission can also be caused by ion bombardment; in some cases replacing one ionic species with another depending upon the gases previously pumped.[131] An equation, then, for describing the overall clean-up of one particular gas in an ion gauge would be composed of a number of terms:

$$-\frac{dp}{dt} = \underbrace{\alpha p}_{\text{pumping}} + \underbrace{\beta (P_0 - P)}_{\text{saturation}} + \underbrace{\gamma P (p_0 - p)}_{\text{induced re-emission}} + \underbrace{\delta (p_0 - p)}_{\text{spontaneous re-emission}}$$

where p = partial pressure at time t, P = total pressure, and the subscript refering to the initial pressure. The proportionality constant, γ, would also be mass dependent since ions of greater mass and equal kinetic energy would penetrate more deeply into the surface layers due to their greater momentum.

The departure from linearity of a pumping curve such as in Figure 15 can be ascribed to the increasingly greater effects of the last three terms of equation (2) as pumping progresses. Although the data tends to qualitatively support the proposed mechanisms, the curves should be interpreted with caution since peak heights (relative partial pressure) were not measured simultaneously but on separate runs for each isotope. Thus the degree of saturation of active sites and re-emission phenomena differ. Nevertheless, the fact remains that even in a "clean" Bayard-Alpert gauge there is a disturbing possibility of isotopic fractionation during pressure measurements causing enrichment of the lighter

isotopes. Also, "irreversible" pumping of significant quantities of argon can occur in relatively short periods of time. For example, 15-20% of total argon was lost in the first minute of operation at 1 ma emission current. This corresponds to a pumping speed of approximately 7×10^{-3} 1/s. After prolonged pumping, only slight recovery of argon was noted when the gauge was turned off. Little argon was recovered when the grid was outgassed at red heat for several minutes, yet almost total release occurred when the glass envelope of the ion gauge was gently flamed.

In order to alleviate pumping and possible fractionation effects, pressure measurements were made in less than five seconds and at a reduced emission current when possible (ie, 0.1 ma rather than 1 ma). Between runs, the Bayard-Alpert gauges were degassed well by flaming or bake-out.

4. Memory and Pumping in the Mass Spectrometer

As stated previously, mass spectrometer ion current was seldom constant, but either decreased or increased with time, thus necessitating the extrapolation of peak heights to time zero. The change of peak height with time was the net result of ion pumping and induced re-emission. The ion pumping is similar to that described for a Bayard-Alpert gauge except that ion energies are much larger and emission current much smaller. Induced re-emission causes a memory effect in that previously pumped atoms are dislodged by ion bombardment. The memory effect in mass spectrometer tubes

has seldom been mentioned in the literature, although a number of investigators[132-134] have studied induced re-emission by ion bombardment for metal and glass surfaces.

Pumping curves of argon isotopes in the mass spectrometer are similar in appearance to those presented in Figure 15. The initial pumping rate (exponential portion of the curve) for all isotopes was found to be about 8×10^{-5} 1/s. The rate of induced re-emission of argon atoms depended upon the quantity of gas previously pumped into the glass and metal surfaces of the mass spectrometer, and also on the total pressure in the tube during analysis. The data presented in graphical form in Figure 16 gives some indication of the magnitude of the memory effect for argon-40 and carbon monoxide. The mass spectrometer tube was isolated from the pump at a pressure of about 1×10^{-9} torr and the mass 40 and 28 peaks were measured versus time. For the carbon monoxide curve, the ordinate scale should be multiplied by 20 to keep the peak heights of the two gases relative. The source of the large quantities of carbon monoxide in the closed mass spectrometer is probably three-fold: induced re-emission by ion bombardment, the formation of carbon monoxide on the hot filament by oxygen-containing contaminating gases, and spontaneous desorption from the interior surfaces.

Too many variables preclude the quantitative evaluation of induced re-emission in the mass spectrometer;

Figure 16

Induced Re-emission of Argon-40 and Carbon Monoxide in the Mass Spectrometer Tube

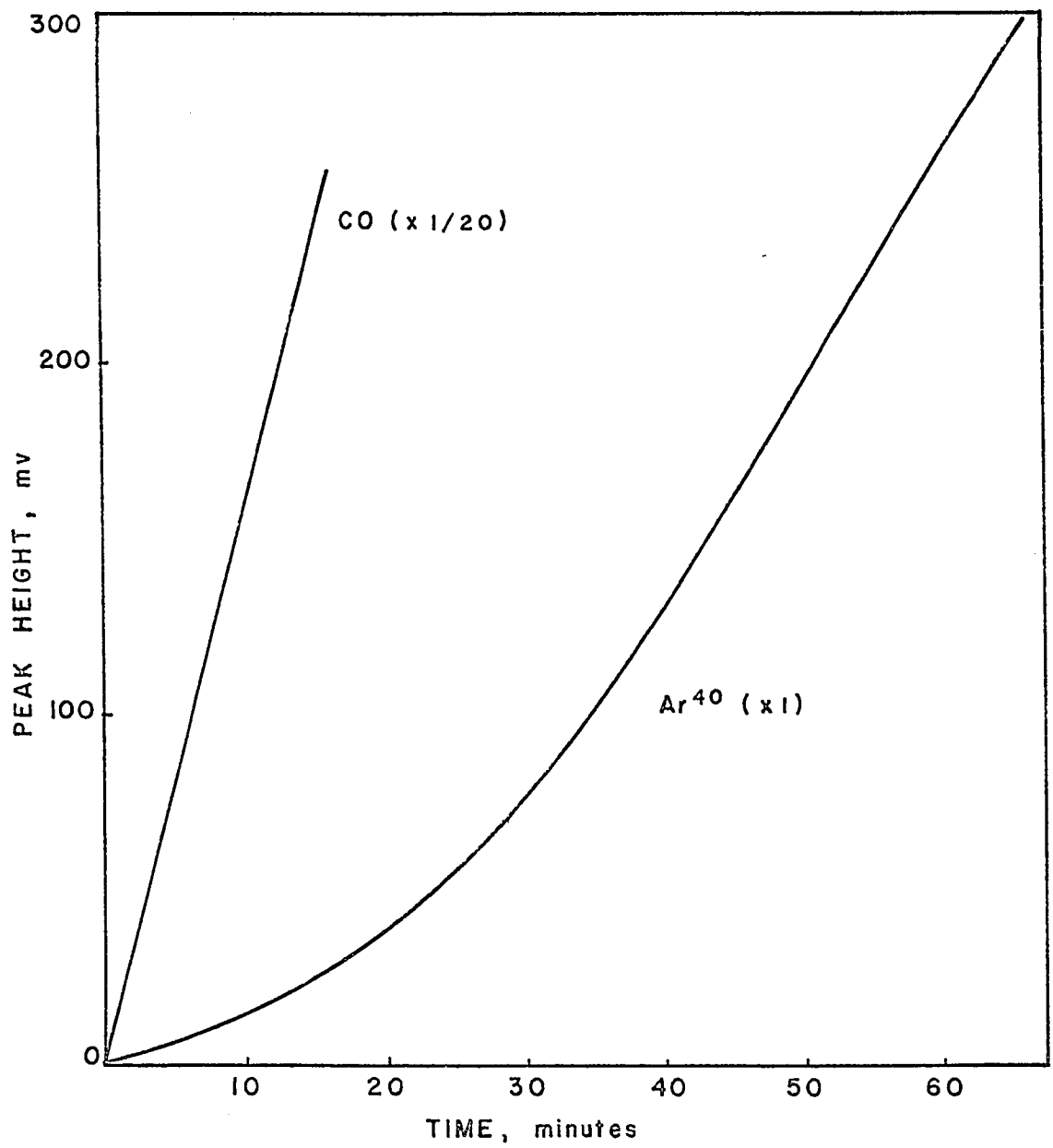

however, more can be learned about the memory effect from the interesting work of J. H. Leck and coworkers[133] at the University of Liverpool. Their studies of inert gas re-emission from bombarded glass surfaces indicate that all the pumped gas is not recoverable by ion bombardment, but can be quantitatively dislodged by baking at 400°C. They also found that the release efficiency of bombarding ions is a function of the adsorbed gas as well as the bombarding gas.

Ion pumping and induced re-emission are evils inherent in mass spectrometers utilizing high-voltage ion acceleration and operated in a static mode. The absence of any memory effect has been specifically reported by workers[135] employing an MS 10 mass spectrometer (Associated Electrical Industries) with low ion accelerating voltages (100 V). Other than changing machines or mode of operation, memory effects can be apparently removed only by regular bake-out of the mass spectrometer tube, although reduction of argon memory should occur by introducing substantial quantities of other gases in the ion source.

5. The Behavior of Argon in Vacuum Systems

No gross losses of argon during gas extraction were noted from the comparison of argon-38 spikes equilibrated with extracted gases and those directly introduced into the mass spectrometer; nevertheless, argon release and hold-up was investigated for a number of components making up the

gas handling systems.

As already mentioned in section II.D.3, heating glass evolves much gas, most of which is water with lesser amounts of carbon dioxide.[136] No evidence of argon release was found with the mass spectrometer during the heating or sealing of Pyrex glass.

No condensation of argon was noted when liquid nitrogen was placed on a cold finger in the mass spectrometer system, although Redhead[137] reported partial adsorption of argon at this temperature, and Barnes[111] found measurable quantities of argon trapped in U-traps in a high-vacuum system.

Titanium evaporated from a hot tungsten wire did not affect the quantity of argon in the system. Holdup of argon in molecular sieve and titanium sponge was not checked. Barnes[111] reported significant adsorption of argon by a titanium sponge getter; however, no large losses of argon were noted in the gas extraction system as stated above.

Activated charcoal was used extensively for the adsorption of gases in the high vacuum systems. Despite prolonged degassing, large quantities of gas were still evolved upon repeated flaming of charcoal fingers. A previously baked and flamed charcoal finger in a break-off tube evolved approximately 3×10^{-3} std cc of gas—from 15-20 mg of charcoal! A significant amount of argon-40 was found to be given off of a charcoal finger when it was gently flamed.

This particular charcoal had been in contact with many gas samples without any subsequent degassing; however, it had been subjected to pumping of less than 10^{-8} torr for 12 straight days prior to flaming. It is believed that little argon is lost on activated charcoal by normal operating procedures during argon analysis, but this remains to be verified.

III. RESULTS AND DISCUSSION

A. Age of the Waianae Range

The results of the potassium-argon age work on Hawaiian extrusive rocks are tabulated in Table 4. A petrographic description and sampling site for each specimen is given in Appendix 2. The uncertainty for each age is based on the experimental errors and the air argon correction (see section III.D.2.b and Figure 30). The data obtained from the Mauna Kuwale rhyodacite are treated in more detail in the next section.

The ages of the different members of the Waianae Range are in general agreement with those of McDougall[38] and Naughton.[40] McDougall reported an age of 8.36 my for a biotite fraction separated from the Mauna Kuwale rhyodacite. This age appears to be abnormally high in view of the present work which indicates that Mauna Kuwale is contemporaneous with the upper member of the Waianae Volcanic Series. The possible causes of the discordance are treated in the next section.

The results obtained from HK-123, a vesicular olivine basalt classified as lower Waianae, are clearly anomalous. The high degree of air argon contamination for this specimen contributes to the large uncertainty; however, this does not fully explain the wide variation in the results. Thin section examination as well as microscopic inspection of hand samples and granular fractions indicated no abnormal mineral components or alteration products. The basalt contains a large number of very small vesicles which probably contain entrapped air. This

Table 4

Potassium-Argon Ages of Hawaiian Extrusive Rocks

Specimen Number	Potassium (%)	Air Argon (%)	Age (my)	Remarks
HK-121	1.32 - 6.03	75 - 89	2.3±.4	Mauna Kuwale rhyodacite. Average of 11 determinations on whole rock and mineral fractions.
HK-119-1	1.43	49	3.3±.2	Dike through HK-121.
HK-119-2		50	3.0±.2	
HK-143-1f	0.206	91	4.3±1.1	Feldspar from flow overlying HK-121.
HK-122-3	0.885	88	2.3±.5	Flow underlying HK-121.
HK-122-4		84	3.1±.5	
HK-122-5	0.911	91	2.3±.6	Calcite removed.
HK-124-1	1.07	38	2.9±.1	Upper Waianae.
HK-126-1f	0.272	80	2.2±.2	Feldspar. Upper Waianae.
HK-126-2	0.970	37	2.7±.1	Whole-rock without feldspar.
HK-132-1f	0.238	65	2.2±.1	Feldspar. Upper Waianae.
HK-132-2	0.697	42	2.6±.1	Whole-rock.
HK-145-1	0.512	80	3.7±.4	Middle Waianae.
HK-145-2		77	3.5±.3	

Table 4 (Continued)

Potassium-Argon Ages of Hawaiian Extrusive Rocks

Specimen Number	Potassium (%)	Air Argon (%)	Age (my)	Remarks
HK-146-1	1.11	39	3.0±.1	Middle Waianae.
HK-146-2		39	2.9±.1	
HK-123-1	0.441	97	16.1±13.6	Lower Waianae.
HK-123-2		98	6.2±6.2	
HK-123-3	0.435	93	11.2±3.9	Powder sample.
HK-142-1	0.209	83	4.3±.6	Lower Waianae.
HK-142-2		82	4.9±.6	
HK-142-4	0.264	83	3.2±.4	Hydrofluoric acid treated.
HK-144-1	0.522	88	4.0±.8	Lower Waianae, Ewa drill
HK-144-2		90	3.5±.8	core.
HK-127-1	0.416	56	7.5±.4	Nihoa Island.
HK-107-1	1.04	57	11.3±.6	Necker Island.

is substantiated by the lower air argon correction for HK-123-3 which was ground to 100-180 mesh while the other two samples were analyzed as 10-16 mesh fractions. Of course, this sample could be 7-12 my old, but there is no confirmation from geological field evidence or other potassium-argon dates.

The ages obtained for HK-142, a lower Waianae olivine basalt, also show a range greater than that predicted from experimental uncertainties and the atmospheric argon correction. The potassium analysis on each fraction was confirmed. The hydrofluoric acid treatment may have contaminated HK-142-4 although this possibility appears unlikely because of the low potassium content of the hydrofluoric acid.

The basaltic dike (HK-119) cutting through the rhyodacite (HK-121) yields a high age relative to its host formation. The low air argon contamination in this specimen precludes any convenient overlap of ages within experimental error. No explanation of this discrepancy is offered at the present time.

The single determination on the feldspar (HK-143) from the flow overlying the rhyodacite should also be less than 2.3 $\pm$ .4 my. The feldspar phenocrysts were hand-picked from a weathered specimen and treated with hydrofluoric acid to remove the more easily soluble altered layers. Microscopic examination indicated pure plagioclase crystals with no alteration or contamination evident. The high atmospheric argon correction creates a large potential uncertainty in the 4.3 my date, and it is possible that an even greater error than acknowledged exists.

The variability in the degree of air argon contamination among the different samples is worth noting. Bake-out temperatures and time cannot be correlated with the quantity of air argon in each sample. A relatively large amount of air argon was present in the apparatus during the initial gas extractions, but any corrections for this would lower the atmospheric correction of HK-121 (whole rock) to a minimum of approximately 80%. As mentioned in section I.D.2.h, certain minerals have been found to hold inherently less air than others. This phenomenon apparently holds true for different whole-rock samples as well, and is probably related to the degree of microvesiculation of the basalts. The differences between feldspar separates and whole-rock samples is mostly attributable to the residual air argon in the extraction system which would predominate when smaller total quantities of radiogenic argon are released.

The two specimens in which feldspar and whole-rock ages can be compared indicate a possible loss of radiogenic argon from the plagioclase, yet Evernden and James[71] and Livingston et al[98] have reported that volcanic feldspars are quite retentive, especially for young rocks. It is most probable that during the 23-28 hours of bake-out at 210-240°C, some of the radiogenic argon was lost by diffusion, or that the lower ages are coincidental and result from experimental error.

Nihoa (Bird) Island is approximately 150 miles west-northwest of Kauai while Necker Island is about 180 miles beyond Nihoa. The ages of 7.5 my and 11.3 my, respectively, are

not surprising considering the progression of the age of the islands indicated by the data in Table 2 (ignoring the 8.36 my age of Mauna Kuwale).

The paucity of data and the large uncertainty in the age determinations preclude any generalizations regarding the duration of island growth or volcanism except to note that volcanic activity of the Waianae Volcano appears to have spanned well over two million years.

B. Discordant Ages of Hawaiian Extrusives

The relationship of Mauna Kuwale in the Waianae Volcanic Series is somewhat of an enigma. McDougall,[38] at Australian National University, reported an age of 8.36 my (two determinations, ± 3% error) on a biotite fraction separated from the rhyodacite, yet in his work no rocks older than 3.46 my were found among seven other Waianae samples. McDougall felt that the greater age of the rhyodacite corroborated the belief of Stearns and Vaksvik[43] that Mauna Kuwale represented the summit of an ancient volcano. No whole-rock analysis of the rhyodacite was performed by McDougall because of the suspect argon retentivity of the glassy microcrystalline groundmass.[138]

The results of this work indicate that Mauna Kuwale is 2.3 my old which would place it in the upper member of the Waianae Series in agreement with Macdonald's views;[44] however, McDougall's apparent discordant 8.36 my age and three anomalous ages, obtained from mineral separates, found in this work are left unexplained.

Potassium-argon age data for Mauna Kuwale are listed in Table 5. Rhyodacite samples were obtained from three different sites and the mineral fractions were not mixed. The number in parentheses indicates replicate analyses. Whole-rock analysis yielded an age of 2.1 my. The age of the different mineral fractions separated from the rhyodacite fall close enough to this value to substantiate an overall average age for the Mauna Kuwale flow of 2.3 my; however, there are three discordant ages, well outside of experimental error, which appear to occur randomly among the many mineral fractions analyzed. The concordance of the majority of the samples can best be seen in the isochron plot of Figure 17. For small Ar^{40}/K^{40} ratios, as found in young rocks, the age equation becomes linear such that a plot of radiogenic argon versus potassium describes a straight line of slope kt.

Another example of a clearly discordant age on a Hawaiian extrusive rock should also be dealt with here. Naughton[40] has reported an age of 2.8 my for a phlogopite fraction obtained from a hawaiite of the Laupahoehoe Series of Mauna Kea (Hawaii), the whole rock giving an age of 0.6 my.

It is believed that the discordant ages derived from the biotite and hornblende fractions of the rhyodacite and from the phlogopite of the hawaiite result from excess radiogenic argon held by these minerals. (The amount of excess argon held by these minerals is given in Table 8). Two alternative explanations for these anomalies exist, however. One, that the rocks

Table 5

Potassium-Argon Ages of Mauna Kuwale Rhyodacite

Sample Description	Potassium (%)	Air Argon (%)	Age (my)
Rhyodacite			
whole-rock (4)	3.21	88	2.1±.4
biotite (3)	3.68 - 6.03	77	2.4±.2
biotite (1)	5.96	80	4.5±.5
hornblende (1)	0.786	93	4.4±1.5
hornblende-biotite (1)	1.32	77	2.5±.2
hornblende-biotite (1)	1.38	82	4.4±.5
feldspar (1)	1.55	87	2.6±.5
groundmass (2)	3.76	87	2.3±.4
Basalt underlying rhyodacite (3)	0.894	88	2.6±.5
Dike through rhyodacite (2)	1.43	50	3.2±.2
Feldspar from flow overlying rhyodacite (1)	0.206	91	4.3±1.1

ISOCHRON PLOT FOR MAUNA KUWALE RHYODACITE

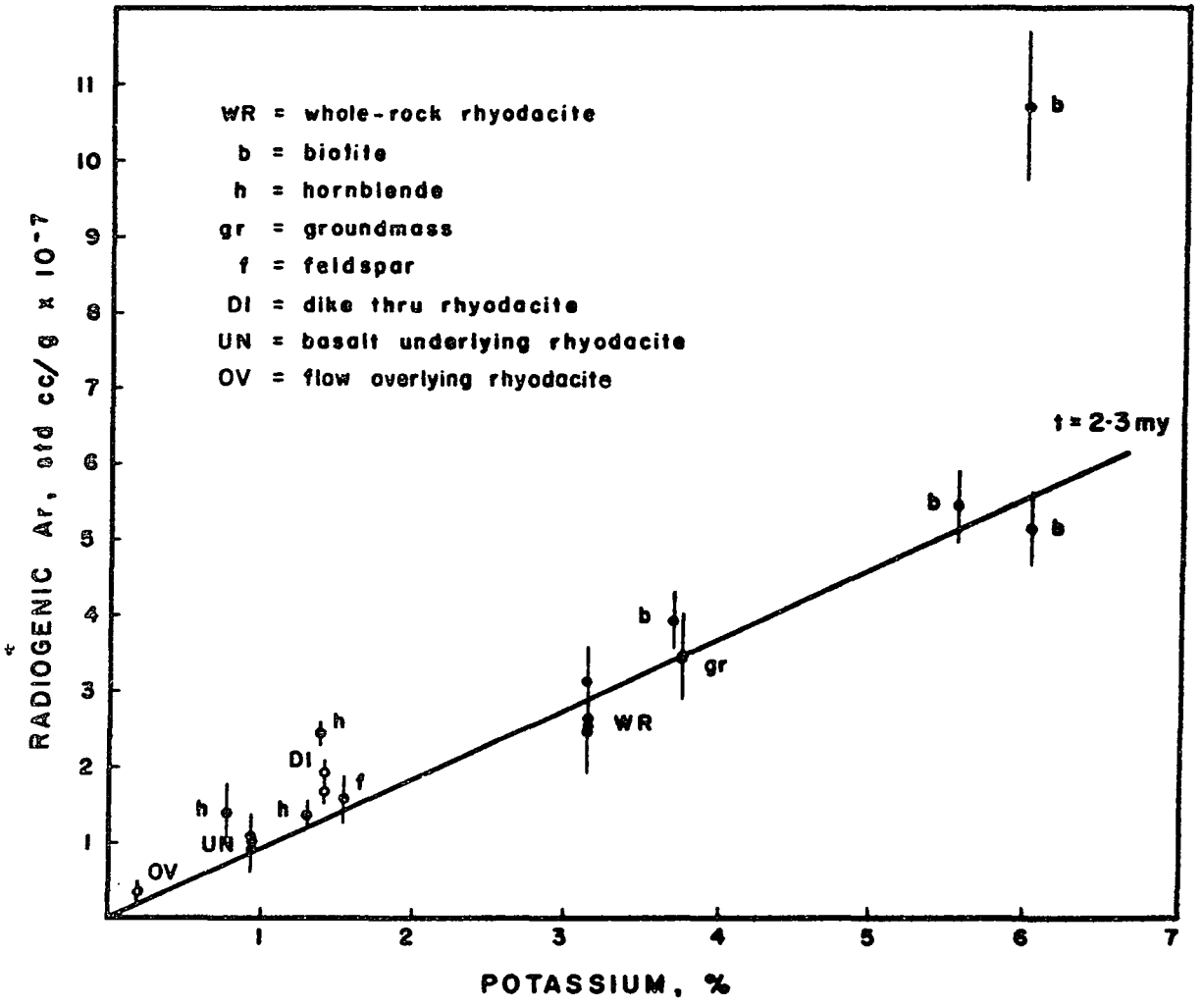

are older and have lost varying degrees of their radiogenic argon either by slow diffusion or in a violent thermal event at some specific time in the past; or two, that part of the potassium has been lost.

In the rhyodacite, it is difficult to find justification for the preferential loss of radiogenic argon from so many and diverse mineral fractions of varying retentivity and from different sampling sites. The observed concordancy of these samples and the underlying flow is evident from Figure 17; however, the three discordant ages of the rhyodacite minerals group about 4.4 my. Coincidentally, so does the feldspar age of the overlying flow (HK-143). If these flows are 4.3-4.5 my old, then the age of the dike (HK-119) is valid. Clearly, the argument is not conclusive based on these data alone.

In the hawaiite, the field relationships are not well defined; however, an age of 2.8 my for any part of the island of Hawaii appears excessive in view of potassium-argon ages and recent paleomagnetic results.[139]

Loss of potassium is considered unlikely without concomitant loss of the more mobile argon atoms, especially in light of research dealing with the weathering and leaching of potassium and argon from biotite.[67,68]

1. Excess Radiogenic Argon

There are several possible explanations for the presence of excess radiogenic argon observed in the particular mineral fractions: external or accidental contamina-

tion either from fluid inclusions or argon dissolution.

a) Accidental Contamination

The abundant ultra-basic xenoliths found throughout the Hawaiian Islands have been shown to contain relatively large amounts of excess radiogenic argon (section III.C). The xenoliths and inclusions are easily broken into small fragments and single crystals as evidenced by a close examination of the host rock. Xenocrysts, composed of pyroxene and olivine, would tend to sink with the mafic minerals during heavy liquid separation and thus be concentrated in the analytical fraction. According to Macdonald,[45] the lavas of the Laupahoehoe Volcanic Series contain many fragments of peridotite, thus a potential source of contamination exists for the phlogopite. No xenoliths have been noted, however, in the vicinity of Mauna Kuwale, although scattered occurrences have been reported in the alkali basalts of the upper member of the Waianae Series.[44]

The degree of contamination necessary to account for the discordant age of the phlogopite would amount to approximately one xenocryst per seven mica flakes assuming equal weights and that the xenocryst contained about 35×10^{-7} std cc Ar^{40}/g (see Table 8). Approximately one xenocryst for every forty hornblende crystals would provide sufficient argon-40 to give the anomalous age obtained. This order of contamination would surely have

been observed during microscopic examination and grain counts on each sample, thus it seems unlikely that accidental contamination of the mineral fractions can be responsible as a source of excess radiogenic argon.

b) Fluid Inclusions

Fluid inclusions are essentially holes in mineral crystals which contain gaseous and one or more liquid phases. They are formed by a growing crystal enveloping part of its environment (primary inclusions) or by the rehealing of cracks and imperfections after the crystal has developed (secondary inclusions). The size of these inclusions may range from several centimeters to below one micron. They have been studied sporadically over the last 150 years in an effort to learn more about the conditions of formation of rocks and minerals. F. G. Smith,[140] of the University of Toronto, has compiled an extensive bibliography of inclusion studies up through 1952, while Edwin Roedder,[141-144] of the U. S. Geological Survey, has been largely instrumental in developing the techniques used today in the investigation of small fluid inclusions.

Several generalizations concerning the appearance and conditions of formation of fluid inclusions are worth noting: (1) crystals formed slowly at high temperatures contain few or no inclusions; (2) the more rapid the rate of growth, the greater the number of

inclusions formed; (3) low-temperature crystals, especially those formed rapidly, may contain dendritic patterns of inclusions that have not reverted to a lower energy state by forming either spheres or negative crystals; (4) the number of inclusions in a crystal vary inversely as their size.

Excess radiogenic argon has been released from fluid inclusions by decrepitation and crushing. As early as 1956, Wahler[90] found evidence of argon in fluid inclusions in quartz crystals. Lippolt and Gentner[89] reported that the potassium-argon age of a fluorite sample decreased significantly when the specimen was reduced to a powder. Two Russian investigators[99,100] used a vacuum ball mill to crush large quantities of pneumatolytic and hydrothermal minerals. They postulated that the mineral-forming solutions contained CO_2, H_2, Ar and He which were occluded in fluid inclusions during crystal growth. The authors leave unexplained, however, the fact that large quantities of the same gases were found in the unaltered granite country rock some distance away from the quartz-feldspar vein. Rama et al[101] have released argon-40 from quartz and fluorite crystals by decrepitation. The amount of potassium in the fluid inclusions in some of the specimens studied had been previously investigated. Although the potassium concentration in a few inclusion fluids was relatively high,

radioactive decay could still not account for the large quantities of argon-40 released. The authors estimated that a partial pressure of the order of a few atmospheres would have been necessary to dissolve the measured amount of argon-40 in the pore fluids of one particular quartz specimen. Nesmelova[102] found excessive amounts of argon in gas inclusions in sylvite, while Hoy and coworkers[103] reported the presence of 0.4% argon in the gases from inclusions in a salt dome in Louisiana. They estimated the gases were held at 500-1000 atmospheres at $0^{o}C$ which would imply a partial pressure of argon of 2-4 atmospheres.

It is postulated that the excess radiogenic argon found in the ferromagnesian mineral fractions of the rhyodacite and hawaiite is contained in fluid inclusions in the mineral grains. This proposal is based upon the following observations: (i) abundant visual evidence of fluid inclusions; (ii) the random occurrence of inclusions and discordant ages; (iii) the release of radiogenic argon by crushing; (iv) synthesis of a mica containing inclusions.

(i) Visual Evidence of Inclusions in the Mauna Kuwale Rhyodacite

Figures 18 to 25 show a variety of inclusions in the minerals of the Mauna Kuwale rhyodacite (HK-121). Several distinct phases can be seen in a number of

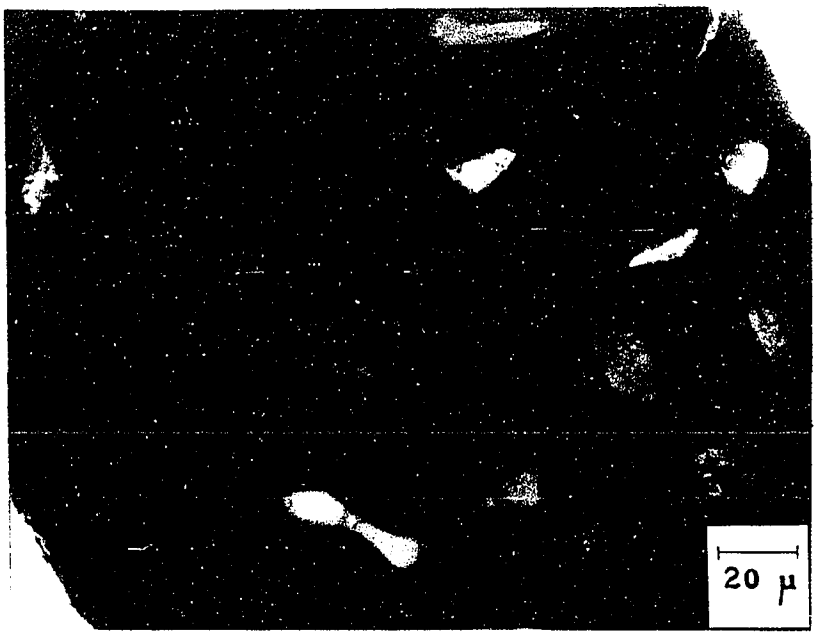

Figure 18

Fluid Inclusions in Biotite of Mauna Kuwale Rhyodacite

Figure 19

Multiple-Phase Inclusion in Biotite Crystal from Mauna Kuwale Rhyodacite

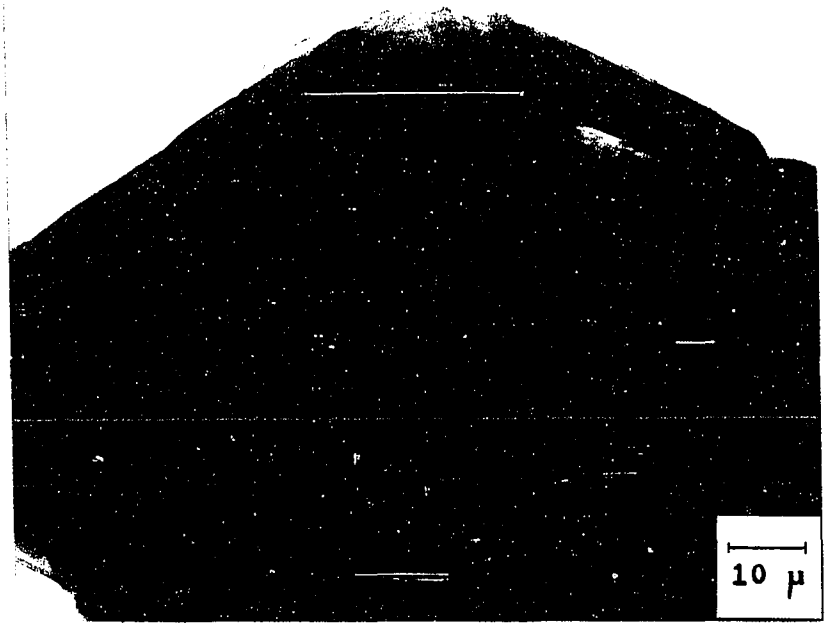

Figure 20

Fluid Inclusion in Biotite Crystal of Mauna Kuwale Rhyodacite

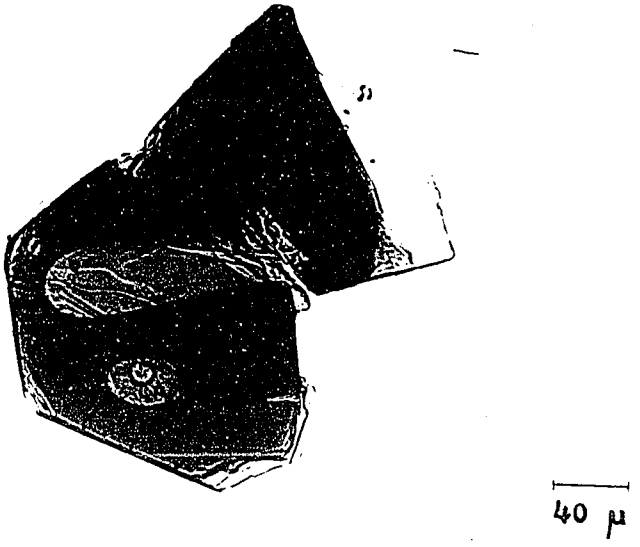

Figure 21

Large Fluid Inclusion in Biotite Crystal of Mauna Kuwale Rhyodacite

Figure 22

Multiple-Phase Inclusion in Biotite Crystal of Mauna Kuwale Rhyodacite

Figure 23

Rhyodacite Biotite Crystal with Multiple Primary Inclusions (Crossed Nicols)

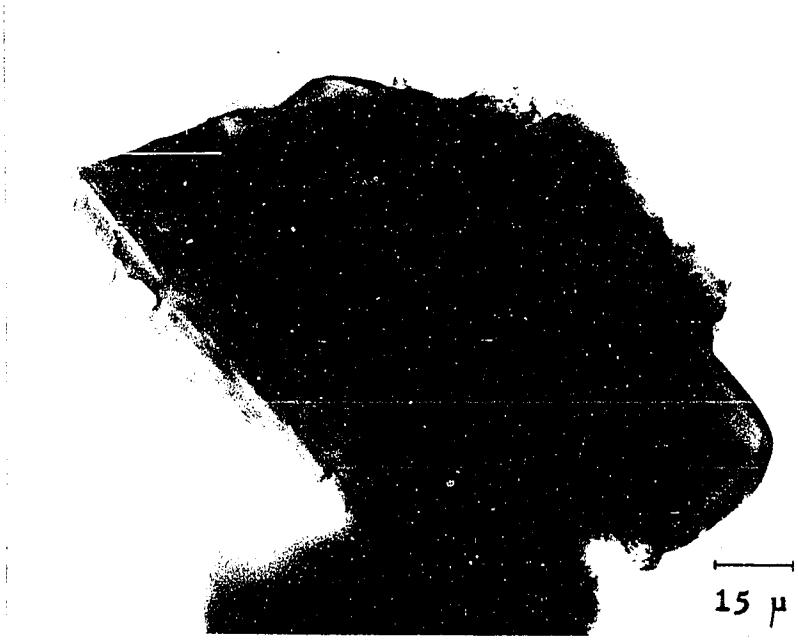

Figure 24

Fluid Inclusions in Hornblende Crystal of Mauna Kuwale Rhyodacite

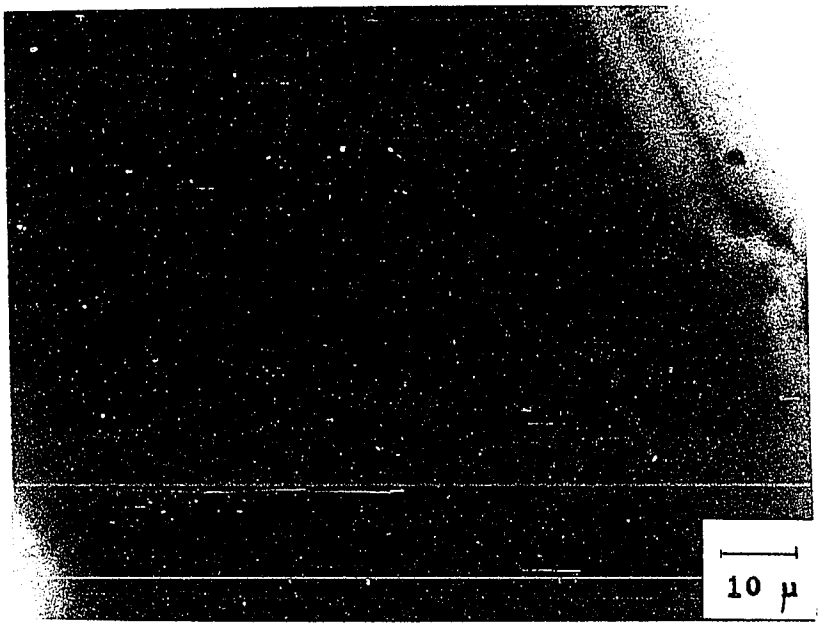

Figure 25

Inclusion with Liquid Bubble in Hornblende of Rhyodacite

inclusions which range in size from less than 5 μ to over 200 μ. Not all crystals were found to contain fluid inclusions however; for example, only approximately one in fifty of the biotite grains contained any inclusions at all as observed from a limited grain count, and those that did generally held more than two. In fact, some of the biotite was extremely variegated as may be seen in Figure 23. In this photograph, the inclusions follow definite crystalline planes of growth and are primary. Many of the inclusions observed in the biotite flakes appeared to be crystals of apatite, while others contained glass. The hornblende also exhibited the random occurrence of fluid inclusions; however, observation was more difficult due to focussing problems with the thick and uneven crystals. Many of the feldspar phenocrysts were deeply embayed and contained abundant dendritic inclusions of a pale brown glass, while very few others held what Zirkel has described as "glassy inclusions with fixed bubbles".[140]

(ii) Random Occurrence of Inclusions and Discordant Ages

As stated above, only an occasional mineral grain contained any fluid inclusions, thus if excess radiogenic argon is held in such sites, the quantity released during fusion or crushing depends upon the number of heterogeneous crystals in that particular sample. Each biotite sample contained on the order of 10^6 individual grains,

thus is was impossible to estimate the total number of inclusions per sample; however, the random occurrence of the crystals containing inclusions suggests the haphazard appearance of measurable excess argon. It is not surprising, then, to find an abnormally high age from only three of seven biotite and/or hornblende samples.

(iii) Release of Argon-40 by Crushing

A number of biotite, hornblende, and mixed biotite-hornblende samples were crushed in the "wiggle-bug" and hammer crusher previously described (section II.G.2). If reasonable assumptions are made regarding the argon released from the lattice through the surfaces exposed by crushing, it can be shown that a negligible amount of the radiogenic argon held in lattice sites in crystals and homogeneously dissolved would be released by crushing, whereas fluid inclusions would be preferentially opened up. In fact, Naughton, using a hammer crusher, had found selective release of adsorbed air argon-40 versus the radiogenic isotope from a volcanic glass and a mica sample.[108] The efficiency of crushing left much to be desired, but generally over 40% of the sample was pulverized sufficiently to pass through a 300 mesh (50 μ) screen after 3 hours of crushing.

The crushing data is listed in Table 6. The observed Ar^{40}/Ar^{36} ratios have been corrected for a mass discrimination of 306. Here again, excess radiogenic

Table 6

Argon-40/Argon-36 Ratios of Vacuum-Crushed Rhyodacite Minerals

Sample Description	Ar^{40}/Ar^{36}
Air Argon	296
Biotite (2)	296
Hornblende (1)	289
Hornblende-biotite (1)	293
Hornblende-biotite (1)	325

argon appears to occur randomly. The main point, however, is that radiogenic argon was released from only one sample which would tend to indicate that the argon-40 component derived from potassium decay is located in a different site from the non-air argon-40 liberated. Another fraction of the same sample, incidentally, also contained excess argon and yielded an age of 4.4 my.

(iv) Synthesis of a Mica with Inclusions

In an independent, yet related experiment, Clyde Noble synthesized a fluoromica according to the procedure of Kohn and Hatch.[145] The ingredients consisted of 1.60 g MgO, 2.34 g SiO_2, 0.44 g Al_2O_3, and 1.08 g K_3AlF_6. The charge was placed in a platinum crucible, blanketed continuously with argon, and heated to about 1400°C for one day. The temperature was lowered at a rate of 2°/hr to 1200° whereupon faster cooling was initiated. The synthesis of a mica was confirmed by x-ray diffraction and optical analysis.

A photograph of one crystal is shown in Figure 26. There is unmistakable evidence of abundant inclusions in this grain, yet many of the fluoromica flakes were clear, while others contained only several rows of primary inclusions.

Although this point is rather indirect and even circumstantial evidence for the presence of argon-40 in fluid inclusions, its importance lies in the fact that

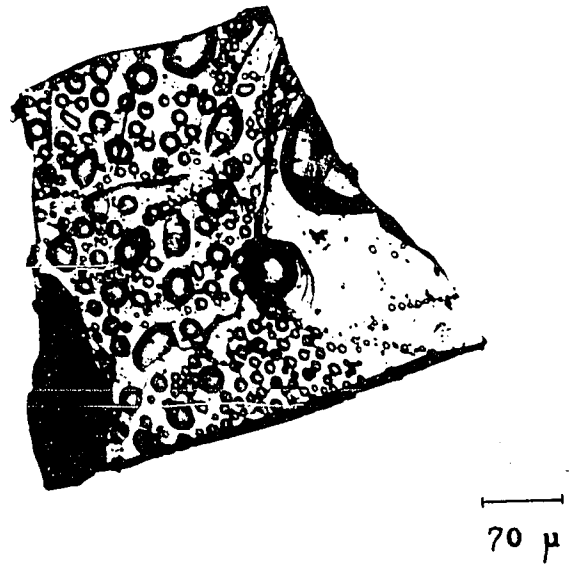

Figure 26

Inclusions in a Synthetic Fluoromica

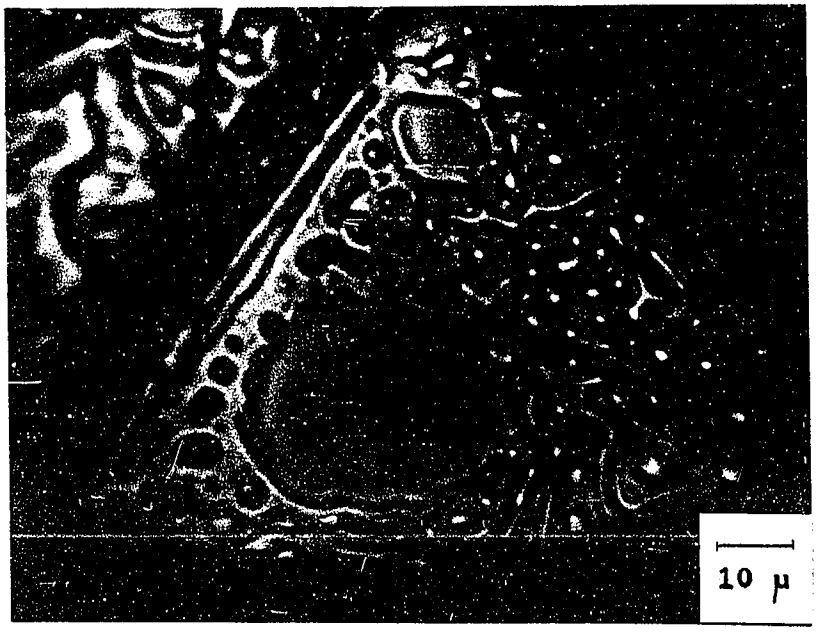

Figure 27

Dendritic Inclusions in a Dunite from Hualalai, Hawaii

inclusions were easily, yet randomly, produced in a mineral under anhydrous and geologically low-pressure conditions not intuitively conducive to their formation.

Water appears to be the primary component of the fluid inclusions observed in the rhyodacite minerals. Crushing a biotite sample and sweeping the gases released into a gas chromatograph evinced only the presence of water. Heating and cooling several inclusions while under microscopic observation again implied that the observed bubbles were an aqueous phase. No polyphase inclusions were studied. Breaking inclusions immersed in oil by squeezing between two glass plates indicated little pressure difference between the inclusions and the atmosphere.

Macdonald and Katsura have reported that the Mauna Kuwale rhyodacite is the end-stage differentiate of the tholeiitic suite of Hawaiian lavas.[46] They postulate that the high-silica rhyodacite may have been enriched in oxygen by the upward migration of water from the deeper levels of the main magma chamber. It is not unlikely that argon-40, generated by the degassing of the primary magma and wall rocks, would rise with the water and other volatiles to the relatively shallow chamber of the derivative magma. (The presence of radiogenic argon in magma chambers and volcanic vents is substantiated by argon-40 enrichment in volcanic gases and

emanations. See, for example, references 146 and 147.) The magma, enriched in silica and alkalies, would be very viscous. Possibly through local pockets of supersaturation, some of the ferromagnesian minerals would crystallize at such a rate as to incorporate a relatively large amount of their bubbling environment in many primary inclusions. During eruption, the temperature of the lava must have been sufficiently low and/or the water pressure great enough to prevent decrepitation of the inclusions, loss of structural water from the biotite, and peripheral magmatic resorption of the mineral grains.

According to Bowen's reaction series, the oligoclase feldspar phenocrysts of the rhyodacite should have crystallized at the same time as the biotite. Why there were so few inclusions evident in this mineral may be a result of it possessing a less hydrophillic surface for the polar volatiles, whereas the structural hydroxyl groups of the biotite and hornblende presented a more receptive surface to water vapor.

The total pressure of the volatiles in the magma chamber may be crudely estimated from the stability curves of biotite and hornblende assuming a temperature around 800°C and a magma chamber of only a few kilometers in depth. A water pressure of approximately 400 bars (395 atmospheres) would seem reasonable, correspond-

ing to a depth of 1-2 kilometers. Assuming a water:argon-40 ratio in the chamber of 10^3 to 10^4 (based on the total weight of the water in the hydrosphere to total weight of argon-40 in the atmosphere and the ratio of water to argon in composite samples of volcanic gases), an average partial pressure of argon-40 of 30-300 mm Hg would exist in the presence of the crystallizing magma.

Superficial microscopic examination of the phlogopite from the hawaiite (HK-103) indicated no heterogeneity in the crystals; however, careful scrutiny at 1000X revealed areas that appeared to be composed of many small bubbles and dendritic patterns. Most of the crystals examined contained such "disturbed" areas which covered roughly 1/10 to 1/4 of each flake, thus if excess radiogenic argon is held in inclusions, it would be essentially homogeneously distributed. Although Naughton[110] only analyzed the phlogopite and hawaiite in duplicate, and these from the same sample fraction, vacuum crushing performed by the writer on another sample of the phlogopite did not release any measurable amount of radiogenic argon. Thus the results from this limited number of samples imply that the excess argon is homogeneously distributed throughout the phlogopite in small amounts.

The phlogopite must have been formed at the surface during the final stages of consolidation of the magma since large crystals were only prevalent along

fissures and fractures in the lava flow.[148] The volatile-rich residual gases escaping from the magma served to transport the necessary chemical constituents for development of the phlogopite. The deuteric solutions must have been enriched in argon-40 which was incorporated into the growing mica crystals either in the crystal lattice or in the observed microinclusions. Extraordinary argon-40 enrichment in the magma chamber could occur by the assimilation of argon-rich peridotite and dunite fragments associated with the Laupahoehoe volcanic series.

c) Argon Dissolution

In the laboratory, argon has successfully been dissolved or injected in several mineral species under high pressure. Karpinskaya and her coworkers[149] introduced argon into muscovite at pressures of 3000-5000 atmospheres and temperatures of 750-850°C. They concluded from the thermal diffusion characteristics that the argon was entrapped in the crystal lattice of the mica. Roy et al[150] dissolved approximately 0.15 wt % argon in glass at an argon pressure of 2 kb at 750°C. Refractive indices of the glass at varying argon concentrations suggested that the gas was held in structural holes rather than in replaced ion positions. The glasses were microscopically homogeneous with no indication of bubbles by electron microscope replica examination. Schreyer and Yoder[151] produced synthetic

cordierites which incorporated as much as 2 wt% at 900°C and 10 kb argon pressure; however, the argon was probably located in the open structural channels common to minerals of this type.

The fact that the excess radiogenic argon in the rhyodacite minerals is not homogeneously distributed and can be released by crushing tends to invalidate a dissolution mechanism for its incorporation. Although the excess argon appears to be homogeneously distributed in the phlogopite of the Laupahoehoe hawaiite, it is difficult to conceive how argon could be dissolved in the crystal structure under the deuteric conditions of phlogopite formation, notwithstanding the premise that sufficient argon could probably be incorporated in a mineral, as it was in the laboratory, except over longer periods of time and at lower partial pressures of argon.

2. Conclusions

It is postulated that the random discordant ages of the rhyodacite minerals and the hawaiite phlogopite result from inherited radiogenic argon contained in fluid inclusions.

The major significance of these results is the implication that mica, a standard potassium-argon dating mineral, can contain excess argon-40 which would yield unusually high ages in young rocks.

C. Excess Argon in Hawaiian Xenoliths

1. Introduction

An investigation of several Hawaiian ultra-basic xenoliths and nodules was prompted by the discordant results from the rhyodacite and hawaiite minerals. It was known at the time that minerals in Hualalai nodules contained fluid inclusions, and when investigators at Australian National University obtained an abnormally high age for a pyroxene from a Salt Lake Crater inclusion, it appeared there might be a correlation between fluid inclusions and excess argon in the xenoliths and, by analogy, in the extrusive minerals.

Xenoliths and inclusions are found in alkali and nepheline basalts throughout the State of Hawaii. The xenoliths are predominantly dunite and peridotite although some grade into gabbro; also so-called "eclogites" are found in one location on Oahu. Hawaii is not unique in its possession of ultrabasic xenoliths. Approximately seventy localities throughout the world are known for their dunite and peridotite inclusions in basaltic rocks. The chemical and mineral composition of these pervasive fragments is remarkably uniform.[152]

There are two major schools of thought concerning the origin of dunite and peridotite xenoliths: one, that they are unmelted parts of the peridotite layer from which the primary magma is thought to originate, ie, upper mantle material;[153,154] the other belief is that these fragments represent heavier differentiates of primary magma that have accumulated by gravity in shallow intrusive bodies.[153]

The eclogite facies is based upon the association of garnet and omphacite, a pyroxene grading between diopside and jadeite. There is general agreement that these very dense rocks crystallize at great depth and at high temperatures, and thus must originate in either the lower crust or upper mantle.[154]

It was thought that a brief investigation on the potassium-argon ages of some Hawaiian xenoliths might indicate the presence of excess argon and perhaps aid in determining its source. As early as 1936, Holmes and Paneth[157] calculated several uranium-helium ages on eclogitic and ultramafic xenoliths from the South African kimberlite pipes. They found eclogite ages up to 398 my in a host rock of 60-70 my. The xenolith ages were considered minimal due to loss of helium; thus, it was felt that the eclogites, at least, were not segregations of the original magma, but part of the lower crust or upper mantle. Recently, however, Lovering and Morgan[158] have felt that the uranium concentrations found by Holmes and Paneth were too high in view of more sensitive determinations on other eclogites. In 1964, Lovering and Richards[93] reported potassium-argon ages on minerals from eclogites collected at Salt Lake Crater, Oahu, from a kimberlite pipe in South Africa, and from a breccia pipe in New South Wales, Australia. An apparent age of 1407 my was obtained from the clinopyroxene of an "olivine eclogite" from Salt Lake. The other two samples also yielded

ages older than those of the host intrusion. The amount of argon-40 over and above that required to give an age of the host rock was calculated by Lovering and Richards and their results are tabulated in Table 9 along with those of other investigators. From their results, they concluded it was not possible to decide whether the excess argon was included in the minerals during crystal growth, was accumulated radiogenically, or was forced in at some subsequent time by a high partial pressure of argon-40.

McDougall and Green[96] reported a number of potassium-argon ages of tectonic peridotites and eclogites from lenses in the Nordfiord region of Norway. Again, most all the minerals analyzed had anomalously high ages; one, a diopside from a garnet peridotite, gave an age of 8100 my! There was no age correlation between rock types of localities or even minerals from one sample. In contrast, it is worth mentioning that Miller and coworkers[159] dated a clinopyroxene from an eclogite from Scotland and obtained an age of 1515 my which they considered reasonable for that area of the countty.

2. Sampling Sites

The ultrabasic xenoliths studied in this work were obtained from two sampling sites: Hualalai Volcano, Hawaii and Salt Lake Crater, Oahu.

Nodules, consisting predominantly of dunite and periodite, but including gabbro, were erupted in the 1800-01 Kaupuleha flow from Hualalai Volcano, Hawaii.[160] They range

in size from less than an inch to over one foot in diameter, and are scattered throughout the flow in vast quantities.[161]

At Salt Lake Crater, nodules of peridotite appear to grade continuously into "eclogite" or garnet peridotite. Although there is no doubt that many of these inclusions contain garnet, some petrologists have not found omphacite present while others apparently have, or at least continually refer to the inclusions as "eclogites". The Salt Lake nodules vary in size from a fraction of an inch to over 8 inches in diameter, and are imbedded in a tuff belonging to the Honolulu Series of late Pleistocene and recent times.[162]

3. Discussion of Results

Potassium-argon ages on a number of Hualalai and Salt Lake samples are given in Table 7. It is readily apparent that the derived ages are abnormally high, and similar to McDougall and Green's results on Norwegian xenoliths, there is no age correlation between nodules or even among the individual minerals in the nodules.

It is believed that the excess radiogenic argon in these samples also is held in fluid inclusions, based on visual evidence and crushing and decrepitation experiments.

a) Visual Evidence of Fluid Inclusions

Figures 27-29 show several types of inclusions in the minerals of the Hualalai samples. No gas or liquid bubbles are apparent in the inclusions in the olivine of Figure 27, but this is a good example of the

Table 7

Potassium-Argon Ages of Hawaiian Xenoliths

Sample	Potassium (%)	Age (my)	Air Argon (%)
HK-128 (garnet pyroxenite)	0.052	232	23
HK-129 (dunite)	0.0034	> 2040	18
HK-130 (pyroxenite)			
pyroxene	0.014	960	29
HK-134 (pyroxenite)	0.015	1500	7
HK-135 (dunite)	0.0028	> 1580	19
HK-137 (olivine gabbro)			
feldspar	0.11	160	16
pyroxene	0.013	2470	16
		2960	72
olivine	0.014	> 791	51
HK-138 (peridotite)			
enstatite	0.0082	3300	5
chromian diopside	0.036	2020	4
olivine	0.0023	> 925	33

Figure 28

Dendritic Inclusions in a Hualalai Pyroxenite

Figure 29

Fluid Inclusions in an Olivine Crystal of a Hualalai Xenolith

dendritic stage of growth of inclusions before they "squeeze off" to form spherical cavities. In most all the minerals observed from both sampling localities, small ($< 5\mu$) inclusions were extremely abundant. Many contained liquid carbon dioxide bubbles that continually bounced about due to Brownian movement. Roedder[163] has noted some mineral grains from the Hualalai nodules with up to 3 vol % inclusions!

b) Crushing and Decrepitation Experiments

Selected samples of minerals were subjected to crushing and decrepitation. The excess argon-40 extracted in this manner is given in Table 8. The olivines could not be melted at the maximum power output of the induction furnace; however, sufficient decrepitation of the fluid inclusions occurred at 1550°C to release contained argon, although subsequent microscopic examination revealed that not all the inclusions were broken. This corroborates Roedder's observation that inclusions 0.8 mm from the basalt contact of the nodule were still intact,[163] and explains the apparent lack of outgassing of the xenoliths by the magma on their way up to the surface.

4. Conclusions

The minerals from many of the ultra-basic xenoliths found in the Hawaiian Islands contain excess radiogenic argon. The location of argon-40 in fluid inclusions in-

Table 8

Excess Radiogenic Argon in Hawaiian Rocks

Sample	Method of Argon Release	Excess Argon (std cc/g x 10^{-7})
HK-121		
biotite	fusion	5.0
hornblende	fusion	0.65
hornblende-biotite	fusion	1.5
hornblende-biotite	crushing	0.56
HK-103		
phlogopite	fusion	5.0[a]
HK-128		
garnet pyroxenite	fusion	4.44
HK-129		
olivine	decrepitation	4.99
	crushing	4.75
HK-130		
pyroxene	fusion	6.97
	crushing	1.56
HK-134		
pyroxenite	fusion	12.8
HK-135		
olivine	decrepitation	2.74
HK-137		
feldspar	fusion	7.47
pyroxene	fusion	27.2, 37.1
	crushing	10.8
olivine	decrepitation	5.29
HK-138		
enstatite	fusion	29.5
	crushing	22.5
chromian diopside	fusion	51.5
olivine	decrepitation	1.07

a Reference 40

dicates that these ages are apparent only and are not derived from potassium decay in situ. The radiogenic argon was incorporated either during primary crystal growth or during secondary crystallization. Roedder[163] has estimated a carbon dioxide pressure of 2.5-5.0 kb during trapping of secondary inclusions which would correspond to a depth of 8-16 kilometers of basaltic magma. This is very close to the mantle; however, the results still do not indicate whether this material is of direct mantle origin or if is a heavy differentiate of the primary magma that has settled within a magma chamber.

The fact that excess argon was found in fluid inclusions suggests that such sites may also furnish the inherited argon reported by other investigators (Table 9) not only for peridotites and eclogites, but also for minerals that have undergone high-grade metamorphism.

As mentioned earlier, contamination of lava flows by ultrabasic xenocrysts and fragments can be a very real problem in potassium-argon geochronology of young basalts. Fortunately, these nodules only occur in alkali basalts so the much greater proportion of tholeiitic material should not have to be closely scrutinized for possible contamination.

D. Precision and Accuracy of Potassium-argon Ages

All too often, radiometric ages are assigned to geologic formations with no mention of the estimated accuracy or possible deviation. The geologist many times will accept the data at

Table 9

Excess Argon in Rocks and Minerals

Mineral	Excess Argon (std cc/g x 10^{-7})	Reference
Beryl	450 - 320,000	91
Cordierite	680 - 8000	91
Tourmaline	110 - 1160	91
Hornblende	"definite evidence"	91
	0 - 0.65	a
Plagioclase	3.4 - 27	164, 165
Pyroxene	30 - 90	92
	3	93
	ca 700	94
	ca 220	95
Albite	13 - 15	164
	4.5 - 27	165
Muscovite	0 - 4800	97
Biotite	0 - 2200	97
	0 - 5.0	a
Phlogopite	5.0	40
	96 - 272	93
Quartz-feldspar vein	2500 - 89,000	100
Pegmatitic		
feldspar	7800 - 27,000	99
quartz	16,500 - 75,000	99
apatite	7000	99
amethyst	34,000	99
Quartz	0.4 - 120	101

Table 9 (Continued)

Excess Argon in Rocks and Minerals

Mineral	Excess Argon (std cc/g x 10^{-7})	Reference
Fluorite	2	101
	1.0 - 3.8	89
Thucholite	up to ca 1400	166
Xenoliths and Inclusions:		
Salt Lake	19	93
	up to 51.5	a
Hualalai	up to 37.1	a
Norwegian eclogites and peridotites	14 - 115	96

a This work

face value for his interpretations and conclusions, yet sometimes the uncertainty may span an entire epoch. D. B. McIntyre, a geologist, has written a chapter in The Fabric of Geology[167] in which he has used lead-alpha and potassium-argon dates taken from the literature to emphasize the need of a quantitative evaluation of reported radiometric ages. He states the problem most succinctly: "A date quoted for a rock is no better than its precision; hence readers are entitled to expect every author to pass on, in unambiguous terms, his best quantitative evaluation of this date."

1. Potassium Analysis

It is surprising that potassium, ranked seventh in the elemental abundance of crustal rocks, is so difficult to analyze precisely and accurately. The uncertainty in potassium analysis has caused potassium-argon geochronologists much concern (see, for example, the article by Pinson, reference 168). Several standard samples have been distributed to laboratories engaged in potassium-argon work; unfortunately, however, these have all been micas with high potassium content (> 6%). Even so, although intralaboratory precision is generally about 1% or less (standard deviation) and interlaboratory precision is approximately 1.5%, the range in values exceeds 5%.[169,170] No low-potassium standards have been used by geochronology laboratories except U. S. Geological Survey rocks G-1 and W-1. Interlaboratory precision on diabase W-1 was 2.6%

standard deviation as determined from the data in Fleischer and Stevens.[171]

Selected results of potassium analyses are given in Table 10. The number of replicate analyses is indicated in parentheses. The precision of potassium analysis which was performed by the procedure described in section II.F.4 varied randomly. Generally, standard deviation was less than 2% except for the low-potassium ultrabasic samples which showed a standard deviation of less than 10% in most cases.

The accuracy of the potassium analyses can be assessed in a general way by comparing with other results. Yamashiro's results,[121] determined by isotopic dilution, agreed within 2% of the flame photometric analyses reported here in 3 out of 6 samples. The greatest deviation was 21% (Table 10, HK-123). Of five potassium analyses determined by Barnes[172] by ion-exchange-flame photometry, all fell within 4% of the reported results. Comparison with standard rock samples reveals that the potassium analyses from this work are generally lower--4.7% being the greatest deviation, unaccountably in the highest potassium sample.

No standards suitable for very low-potassium (<0.05%) analysis were available, thus the accuracy of the analysis of the ultrabasic minerals can only be crudely estimated. The greatest source of error would result from cation interference in the emission intensity of potassium during flame photometric analysis. In the search for a rapid and

Table 10

Precision and Accuracy of Potassium Analyses

Sample	This Work	Percent Potassium Flame Photometry Ion Exchange[a]	Isotopic Dilution[b]	Standard Value
HK-121	3.21±.05 (1.6%) (9)	3.20±.03 (0.9%) (10)	3.07±.02 (0.6%) (7)	-
HK-121 biotite	5.96±.035 (0.6%) (5)	-	5.90±.26 (4.4%) (3)	-
HK-123	0.441±.0059 (1.3%) (4)	0.456±.0049 (1.1%) (9)	0.350±.006 (1.7%) (7)	-
NBS #98 Plastic Clay	2.58±.072 (2.8%) (8)	-	-	2.64[c]
NBS #99 Soda Feldspar	0.319±.012 (3.8%) (16)	-	0.343 (1)	0.33[c]
W-1 Diabase	0.511±.0096 (1.9%) (7)	-	-	0.54[c]
G-1 Granite	4.56±.067 (1.4%) (4)	-	4.54 (1)	4.55[c]
P-207	8.20±.19 (2.3%)	-	-	8.60[d]

a Reference 172
b Reference 121
c Reference 173
d Reference 170

efficient method of potassium analysis, potential interfering elements were either removed or nullified by several different methods. The results of these analyses indicate only a random deviation not exceeding 30% among the different procedures. It can be stated, then, that the analyses of the ultrabasic samples are probably "true" within $\pm$ 30%, while for samples with potassium above 0.1%, an accuracy of 3% appears valid.

2. Argon Analysis

a) Errors in the Physical Constants

Aldrich and Wetherill[6] have reviewed the status of the decay constants and believe the value of 0.585×10^{-10} yr^{-1} for the electron capture decay constant, λ_{β} , is within 5% of the true value. The direct beta decay of potassium-40 to calcium-40 is more easily measured, thus λ_{β} is more accurately known that λ_{γ}, however, the potassium-argon age of a rock is not very dependent upon the accuracy of λ_{β}. In fact, for very young rocks, the age varies directly with λ_{γ}, thus a 5% error in this decay constant is transmitted directly to the resulting age. Since most all laboratories now involved in potassium-argon geochronology use the same constants, no discrepancies in age result from this source of error.

The interesting possibility that beta decay is dependent upon time has been raised by Dicke.[175] Aside from the difficulty in proving such a hypothesis, the change in potassium-argon or rubidium-strontium ages would amount to

no more than 6-7% for the oldest known rocks on the earth.[176]

b) Precision and Accuracy

The two standard samples most widely used by potassium-argon laboratories have been prepared by Hurley's group at MIT and Lanphere and Dalrymple at U. S. Geological Survey, Menlo Park. Nine interlaboratory analyses of the MIT biotite, B-3203, give 3.88×10^{-4} std cc Ar^{40} (r)/g with a standard deviation of 0.36% and a range of 3.6%.[169] Data from ten laboratories on the USGS muscovite, P-207, indicate that it contains 2.839×10^{-5} std cc Ar^{40} (r)/g with a standard deviation of 2.2% and a range of 3.5%.[170] Both these samples are relatively old, high-potassium minerals for which air argon contamination is low.

In some very recent work, Dalrymple and Hirooka[174] have analyzed a young basalt (2.6% K, 3 my) a number of times. The precision of ten replicate potassium analyses by flame photometry was 0.35% with a total spread of 1.16%, ten argon analyses gave a precision of 1.84% with a range of 6.76%, while the age was determined with a precision of 1.90% and a spread of 7.60% (average air argon correction 28%). These authors have raised the important point of sample heterogeneity. The range of potassium values in different sections of a hand sample was found to be 3.11%. Intraflow analytical variations were even greater. The same flow

was sampled in seven different locations over a distance of nearly 3 km. Although the standard deviation and range in the age was similar to that from the hand sample, the spread in potassium and argon analyses was about 20-25% with a standard deviation of about 7% each.

For young rocks, especially with low potassium content, the amount of contamination by atmospheric argon-40 is the limiting factor in the precision, and accuracy, attained. The subject of air argon contamination has been treated in section I.D.2.h. The magnitude of the uncertainty in the age of a rock as a function of the air argon correction can be seen from Figure 30.

Five replicate analyses were performed on the standard muscovite, P-207. The average was then used to standardize the argon-38 spikes employed in this work so the results cannot be used to compare the accuracy of analysis; however, the data do indicate the precision of measurement when air contamination is minimal. Standard deviation was 2.0% with a range of 4.9%, atmospheric argon contamination averaged 7.7% which, from the equation on page 30, would contribute only 0.2% uncertainty to the result.

Standard deviation in the age of four replicate analyses of HK-121 whole rock is 11% (88% air argon). Averaging 11 analyses of HK-121 including whole rock and

Figure 30

Standard Error in Age of Young Rocks as a Function of Air Argon Contamination

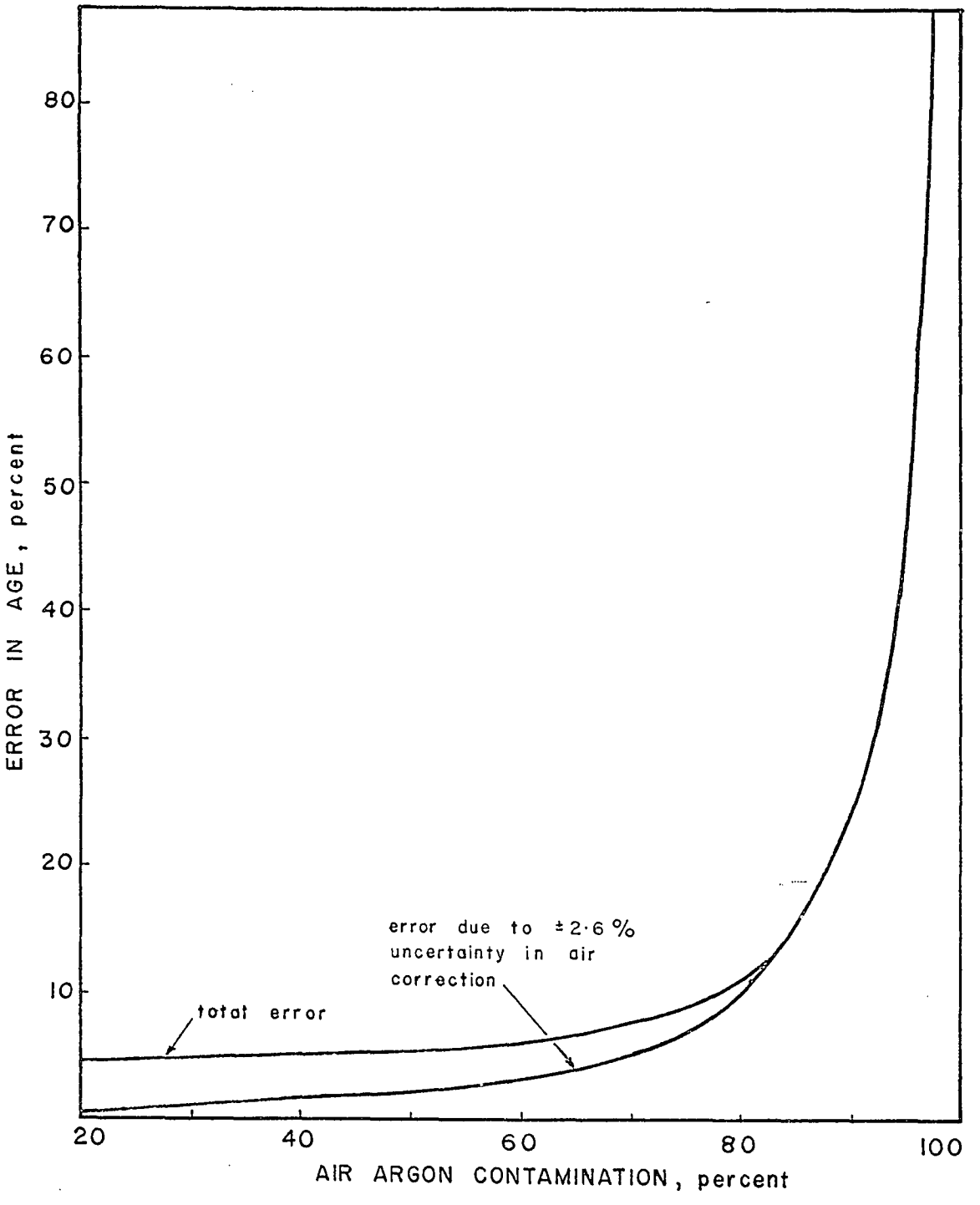

mineral constituents gives 2.29 $\pm$ .25 (11%) my with a total spread of 30%. Accuracy, of course, is impossible to determine, but the limits dictated by air argon contamination appear to give a reasonable range of uncertainty in view of the precision involved. Figure 30 can be used to assess the total uncertainty in the age of individual samples of young rocks.

c) Experimental Errors

As mentioned earlier, the argon-38 spikes were prepared in three separate batches. The last one was standardized against P-207 while the others were related to the last batch through mass spectrometer sensitivity, ie, x std cc argon-38 produces y mv deflection. The standard deviation of the analysis of P-207 (2%) probably reflects the variations in the amount of argon-38 in each spike within the one batch and this is taken as the uncertainty in spike preparation for batch #3. The error in the spikes of the earlier two preparations is related to that in the spikes of batch #3 and the uncertainty in the mass spectrometer sensitivity (2%) yielding a total error of approximately 3%.

Throughout the year and a half of mass spectrometer operation, six isotopic ratios were measured on air argon. A ratio of 306 $\pm$ 8 (2.6%) compared to the normal 296 for Ar^{40}/Ar^{36} indicated that discrimination

occurred in mass spectrometric analysis. In the radiogenic argon calculations, this discrimination has been accounted for (see sample age calculation, section II. G.4), nevertheless, the uncertainty in the degree of discrimination creates a possible error in the amount of radiogenic argon-40. The magnitude of this error is dependent upon the difference in the ratios of Ar^{40}/Ar^{38} and Ar^{36}/Ar^{38}; therefore, it is difficult to assess without applying it to a specific example. However, for the sake of simplicity, the uncertainty in the argon-40 calculation due to the observed discrimination is estimated at 2.5%.

3. Improvements in Precision and Accuracy

Although air argon contamination is the greatest cause of the uncertainty in the young ages reported here, it is desirable, as in perfecting any analytical technique, to minimize any and all errors in experimental procedure.

There does not appear to be any way to improve the precision of the potassium analysis without destroying the simplicity and rapidity of the present procedure. Most of the observed uncertainty in precision results from the flame photometric procedure as indicated by replicate runs on the same sample solution. Thus the sensitivity of the emission intensity must be increased without a concomitant rise in noise and instability. One method of achieving this result would be the use of a radiation buffer or organic solvents

to enhance the emission intensity of potassium. Analysis of low-potassium ultrabasic minerals could perhaps be better accomplished by a method which is less influenced by the extremely large quantities of potential interferents. Isotopic dilution utilizing mass spectrometry or atomic absorption spectrometry might well be the answer.

The preparation of argon-38 spikes used in this work leaves much to be desired. Argon-38 pressure of the first two batches, as measured with a McLeod gauge, were in error by 28% and 10%. The causes of such errors are not presently known. Variations in filling pressure in each individual spike became apparent during subsequent mass spectrometer analysis, most probably resulting from sealing off the spike tubes. It is suggested that future spike preparations be patterned after the procedure and apparatus used at the University of California at Berkeley by Curtis and Evernden.[177] The break-off tubes are sealed straight up from a horizontal, branched manifold to which is attached a mercury reservoir through a large-bore valve. The manifold portion of the system is baked at 400°C in order to achieve pressures below 10^{-8} torr. The argon-38 is released from the reservoir in the closed system, pressure measured with a McLeod gauge, and then the mercury is introduced into the manifold to such a level as to seal off each individual tube. Thus all spikes are at the same pressure which remains constant during sealing. Over 100 spikes are generally

prepared at one time. Randomly-selected spikes are subsequently calibrated against either a known volume of argon or a standard mineral sample. It is estimated that argon-38 spikes prepared in this manner are accurate to 0.5%.[177]

The discrimination of 2.6% observed in the mass spectrometric analysis of air argon is believed to result from an increase in the filament current as the magnet current is raised during scanning of the argon isotope peaks. The direct relationship between these two variables is somewhat obscure. It may result from an inductive current transmitted from the magnet coils by the conductive coating of the tube into the ion source. If so, better isolation may be possible. An alternative remedy might be to use a collimating magnet for the electron beam--this would also serve to increase the sensitivity of the mass spectrometer.

The uncertainty resulting from air argon contamination can be reduced by decreasing the error in the determination of the isotopic ratios. Increasing the sensitivity of the mass spectrometer would not necessarily effect this result. A good part of the 2.6% standard deviation observed in measuring air Ar^{40}/Ar^{36} probably is caused by non-linear peak height fluctuation brought about by the memory effect of the mass spectrometer tube. Baking out the tube after several analyses would tend to reduce the memory effect.

A portion of the atmospheric argon-40 contamination is contributed by the residual gases in the extraction

system. In the early days of operation, the air argon blank was 1.22×10^{-5} std cc. After a year and a half of operation and improvements, the blank was reduced to 1.86×10^{-7} std cc Ar^{40}, yet even this value makes up a large portion of the air correction for very young rocks of low potassium content. Further reduction of residual air argon could probably be accomplished by replacing the quartz titanium getter with one of stainless steel.

E. Summary of Conclusions

1. The potassium-argon ages determined on the Waianae Volcano confirm those reported by other investigators with one notable exception.

2. Mauna Kuwale is contemporaneous with the upper member of the Waianae Volcanic Series contrary to previously-reported results.

3. The problem of dating young volcanic rocks include high air argon contamination, secondary alteration of rocks and minerals, excess radiogenic argon, and accidental contamination.

4. Deep-seated ultramafic xenoliths are subject to large excesses of radiogenic argon.

5. The precision of the young potassium-ages reported herein was found to be approximately 11% (standard deviation). Air argon contamination of over 75% contributes markedly to an overall uncertainty in the accuracy of such results.

IV. SUMMARY

A Reynolds mass spectrometer, gas extraction system, spike preparation system, and associated apparatus has been assembled in order to perform potassium-argon age determinations on young, low-potassium rocks typically found in the Hawaiian Islands. Techniques have been perfected for the routine analysis of potassium by flame photometry with a precision of approximately 3%, and the analysis of radiogenic argon by isotopic dilution with a precision of about 4%. The accuracy in the ages of young basaltic rocks was found to be severely limited by the high degree of atmospheric argon contamination.

The Waianae Volcano Range of Oahu, Hawaii has been systematically dated in order to apply the techniques and instrumentation of potassium-argon analysis to a specific problem. The results corroborate earlier work by other investigators, ie, the Waianae Range is approximately 2.3±.4 my, with one exception: Mauna Kuwale was found to be 2.3 my rather than 8.4 my as reported elsewhere, and thus is contemporaneous with the upper member of the Waianae volcanic series.

Discordant ages of certain ferromagnesian minerals from young Hawaiian extrusives result from excess radiogenic argon. It is postulated that the inherited argon-40 is held in fluid inclusions in the mineral crystals. This belief is substantiated by visual evidence, vacuum crushing experiments, the synthesis of a fluoromica that contained inclusions, and, indirectly, by the analogous phenomena observed with Hawaiian xenoliths mentioned below.

Several ages determined on basalts from islands northwest of

Kauai confirm the already abundant evidence that the age of the Hawaiian Island chain progressively increases from southeast to northwest.

Abnormally high potassium-argon ages (160-3300 my) were found for several samples of ultrabasic xenoliths that are scattered throughout the Hawaiian Islands. No correlation is evident between the ages of different nodules or even among the different minerals of the same xenolith. It is believed that these ages are apparent only and are caused by exogenous argon-40 contained in the abundant fluid inclusions observed in these rocks. Vacuum crushing data further substantiate this belief.

The problems encountered in dating young volcanics, ie, a high atmospheric argon correction, secondary alteration, excess radiogenic argon, and possible contamination by ultramafic xenocrysts, emphasize the need of multiple, yet selective, sampling of a suite of rocks. Judiciously-selected, whole-rock samples and, preferably, several different mineral separates should then be utilized for analysis in order to obtain geologically significant ages.

APPENDIX 1

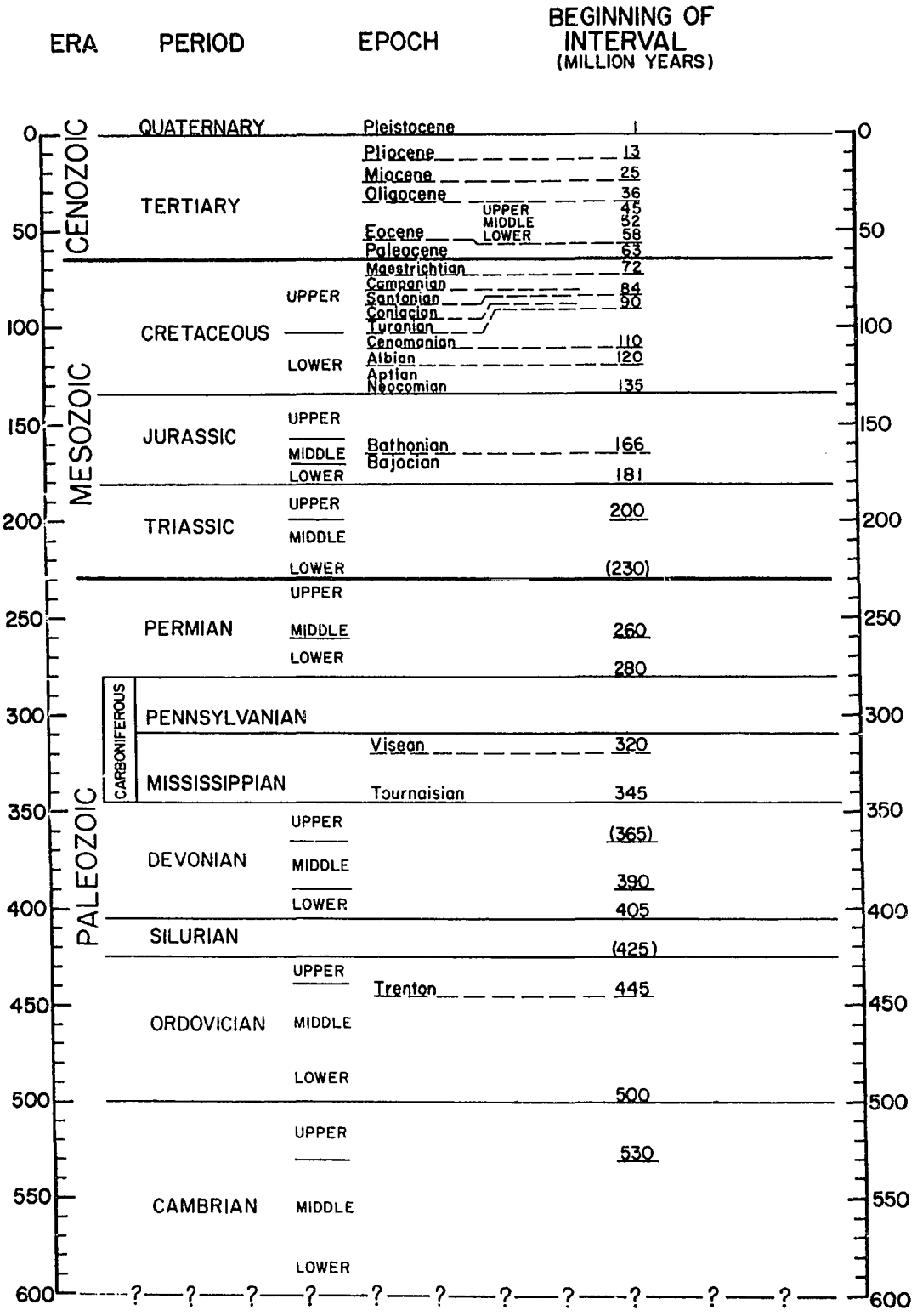

Geologic time scale.

APPENDIX 2

Description of Rock and Mineral Specimens

HK-103 Hawaiite. Laupahoehoe Series of Mauna Kea, Hawaii. Collected from Paauito Quarry. Examination of a hand sample indicates this to be a medium-grey, dense andesine andesite (hawaiite) with unusually large and abundant phlogopite crystals.

HK-107 Olivine basalt collected from a sill on Necker Island. A fine-grained, dense, olivine basalt trending towards an alkalic basalt. Hand sample examination only.

HK-119 Two foot dike of basalt in rhyodacite (HK-121). Collected from quarry at the southwest end of Mauna Kuwale, Waianae Range. Rare phenocrysts of plagioclase occur in an intersertal groundmass of plagioclase, monoclinic pyroxene, magnetite, ilmenite, and glass. A few small former grains of olivine are wholly altered to goethite (?) while some of the glass is altered to fine serpentinous material.

HK-121 Hornblende-biotite rhyodacite from quarry at southwest end of Mauna Kuwale, Waianae Range. Collected at an altitude of about 200 feet. Dark grey, massive rock with oligoclase phenocrysts, euhedral to subhedral crystals of biotite, basaltic hornblende, and magnetite in a fine-grained groundmass with fluidal texture. The groundmass consists of tiny microlites of plagioclase in a matrix of alkali feldspar and glass. See reference 44, p. 82, for a more complete petrographic description and reference 46, p. 116 (sample TK-1501) for a chemical analysis.

HK-121b was taken from the same quarry, but in a different area and at a later date.

HK-121c was collected from the north side of Mauna Kuwale at approximately 350 feet above sea level. It is the same as the other two samples, except the bulk specimens exhibit a purple-red tinge due to slight weathering and the matrix is a little finer-grained and glassier.

HK-122 Olivine basalt flow beneath the rhyodacite. Collected from the east end of Mauna Kuwale at an elevation of about 200 feet. Phenocrysts of plagioclase and augite lie in an intersertal groundmass of plagioclase, monoclinic pyroxene, magnetite, ilmenite, and purplish-brown glass. Former microphenocrysts of olivine are completely altered to serpentine while some of the glass is altered to yellow secondary products. Some vesicles are filled with calcite.

HK-123 Tholeiitic olivine basalt. Lower Waianae. Collected at the mouth of Makua Cave, Kaena Point, at an elevation of 100 feet. A vesicular pahoehoe with phenocrysts of olivine much altered to iddingsite set in a fine-grained intergranular to intersertal groundmass consisting of plagioclase, monoclinic pyroxene, magnetite, ilmenite, and glass.

HK-124 Alkalic olivine basalt. Upper Waianae. From Pacific Rock Company quarry at south end of Waianae Range. Microphenocrysts of olivine in an intergranular groundmass of plagioclase, monoclinic pyroxene, olivine, and magnetite. Olivine extensively altered to iddingsite. For a chemical analysis, see reference 46, p. 116 (C-30).

HK-126 Alkalic olivine basalt from dike in roadcut in Kuaokola Game Management Area, Kaena Point. Elevation 1000 feet. Porphyritic, with rounded and embayed phenocrysts of calcic plagioclase up to one centimeter across in a fluidal intergranualr groundmass of labradorite, pyroxene, and olivine.

HK-127 Olivine basalt from a dike on Nihoa Island. Labradorite, pyroxene, olivine largely altered to iddingsite or goethite, ilmenite, magnetite, and interstitial glass some of which is altered to a chloritic material.

HK-128 Xenolith of garnet peridotite from the palagonite tuff of Salt Lake Crater, Oahu. Small crystals of clinopyroxene, garnet, olivine, and spinel.

HK-129 Dunite nodule, approximately 3 inches in diameter, from the 1800-01 Kaupulehu flow, Hualalai, Hawaii.

HK-130 Pyroxenite nodule from 1800-01 Kaupulehu flow, Haulalai, Hawaii. Composed mostly of augite.

HK-132 Alkalic olivine basalt from Mokuleia trail, northwestern part of the Waianae Range. Upper Waianae. Large feldspar phenocrysts up to one centimeter across , very similar in appearance to HK-126. Hand sample examination only.

HK-134 Pyroxenite nodule from 1800-01 Kaupulehu flow, Hualalai, Hawaii. Composed predominantly of clinopyroxene with less than 10% olivine.

HK-137 Olivine gabbro nodule, 6 x 6 x 12 inches, from 1800-01 Kaupulehu flow, Hualalai, Hawaii. Composed mostly of olivine (65%) with large phenocrysts of feldspar (10-15%) and pyroxene (augite?) crystals (20-25%).

HK-138 Composite sample of 3-4 peridotite inclusions ranging from 1-3 inches in size. From the palagonite tuff of Salt Lake Crater, Oahu. Composed of 60-80% olivine, 15-20% enstatite, 5% chromian diopside, and < 5% spinel.

HK-142 Tholeiitic olivine basalt. Lower Waianae. Collected 14 feet above sea level just south of Kaluakauila Stream, Waianae Range. An intersertal groundmass composed principally of labradorite and monoclinic pyroxene, with lesser amounts of magnetite, ilmenite, and interstitial glass, scattered grains of olivine and augite grading in size to microphenocrysts. Secondary serpentine and iron oxides and possibly other secondary minerals are present as cavity fillings and stains, and as alterations of olivine.

HK-143 Basalt from the flow overlying the Mauna Kuwale rhyodacite (HK-121), collected just southwest of Mauna Kuwale along Paheehee Ridge at an elevation of approximately 350 feet. A prophyritic olivine basalt with abundant phenocrysts of feldspar and some olivine. Very vesicular and somewhat altered. Hand sample examination only.

HK-144 Tholeiitic basalt. Lower Waianae. Core sample taken from lower portion of a seven-foot flow of basalt at 1081-foot level of Ewa I drill hole, located at the southeast section of USCGS station at Barbers Point, Oahu. Intergranular rock composed of labradorite and monoclinic pyroxene with lesser amounts of magnetite and ilmenite, and a few phenocrysts of olivine, slightly rounded and embayed by resorption and altered around the edges to iddingsite. A little secondary iron oxide is present in places.

HK-145 Tholeiitic basalt. Middle Waianae. From ridge on north side of Nanakuli Valley, Waianae Range. Elevation 1410 feet. A fairly coarse-grained rock composed of labradorite, slightly brownish pyroxene (augite and pigeonite), magnetite, ilmenite, scattered grains of olivine, and a little interstitial glass. Some of the olivine grains are partly altered to goethite(?), and a little secondary iron oxide and serpentine are present. See reference 46, p. 116 (C-48) for a chemical analysis.

HK-146 Hawaiite. Middle Waianae. Taken from ledge at 1920 feet on the same ridge as HK-145, Nanakuli Valley, Waianae Range. Phenocrysts of plagioclase (labradorite), augite and olivine in a fine-grained intergranular groundmass of andesine, augite, olivine, magnetite and ilmenite. The olivine phenocrysts show slight alteration to iddingsite or goethite. See reference 46, p. 116 (C-52) for a chemical analysis.

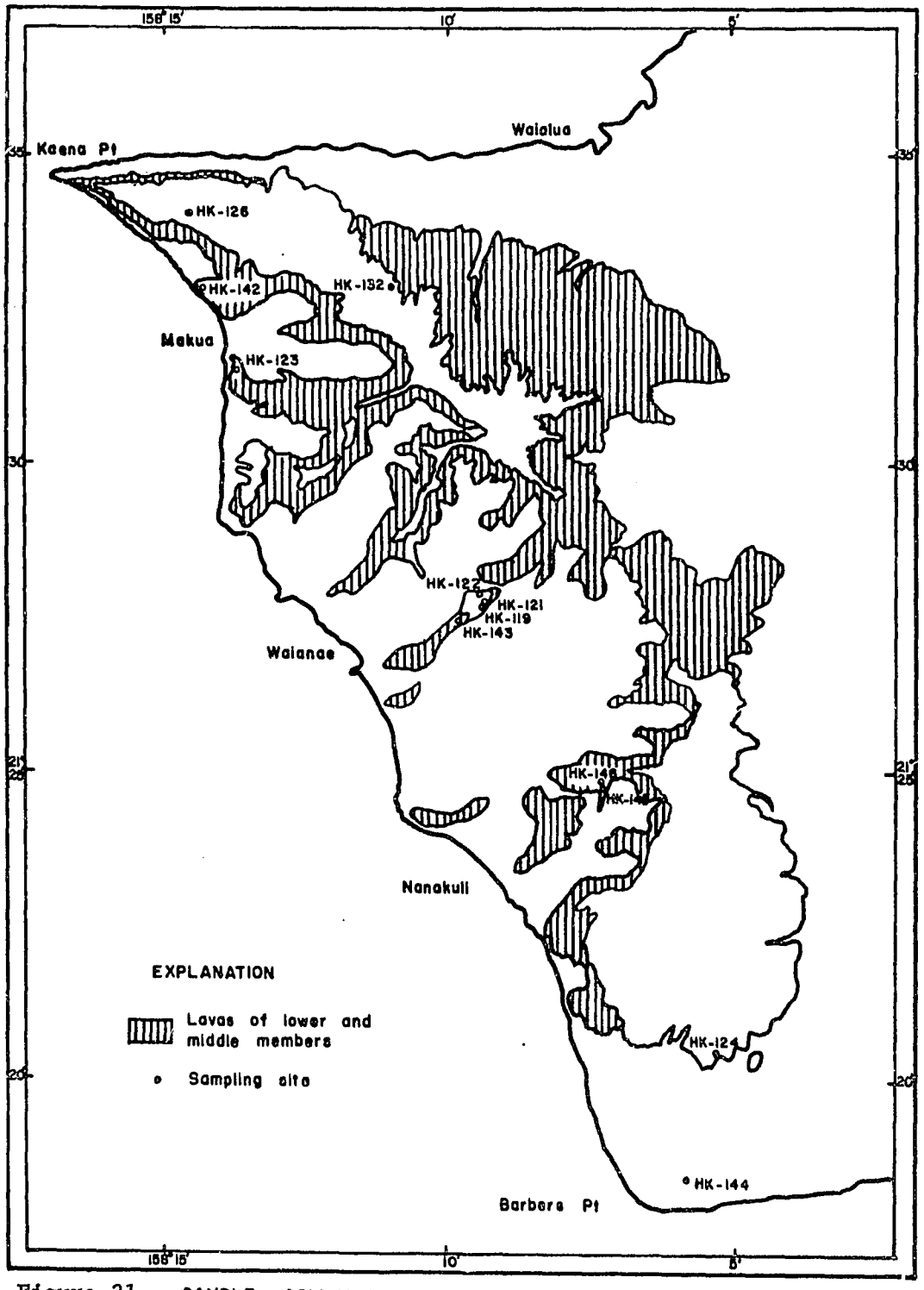

Figure 31. SAMPLE COLLECTION SITES IN THE WAIANAE RANGE

BIBLIOGRAPHY

1. W. J. Sollas, The Age of the Earth and Other Geological Studies, Dutton, New York, 1905.

2. J. Barrells, "Rhythms and the measurements of geologic time", Geol. Soc. Amer. Bull. 28, 745-904 (1917).

3. B. B. Boltwood, "On the ultimate disintegration products of the radioactive elements", Am. J. Sci. 23, 77-88 (1907).

4. J. L. Kulp, "Geologic time scale", Science 133, 1105-1114 (1961).

5. E. S. Hamilton, M. H. Dodson, N. J. Snelling, "The application of physical and chemical methods of geochronology", Int. J. Appl. Rad. Isot. 13, 587-610 (1962).

6. L. T. Aldrich, G. W. Wetherill, "Geochronology by radioactive decay", Ann. Rev. Nucl. Sci. 8, 257-298 (1958).

7. A. Knopf, "Measuring geologic time:, in Study of the Earth, ed. J. F. White, Prentice-Hall, New Jersey, 1962, pp. 41-62.

8. A. O. Nier, "The isotopic constitution of radiogenic leads and the measurement of geological time, II", Phys. Rev. 55, 153-163 (1939).

9. A. O. Nier, R. W. Thompson, B. F. Murphy, "The isotopic constitution of lead and the measurement of geological time, III", Phys. Rev. 60, 112-116 (1947).

10. O. Hahn, E. Walling, "Über die Moglichkeit geologischer Altersbestimmungen Rubidiumhaltiger Mineralen und Gesteine", Z. anorg. u. allgem. Chem. 236, 78-82 (1938).

11. L. H. Ahrens, "Determination of the age of minerals by means of the radioactivity of rubidium", Nature 157, 269 (1946).

12. D. G. Brookin, P. M. Hurley, "Rb-Sr geochronological investigation in the middle Haddon and Glastonbury Glastonbury Quadrangles", Am. J. Sci. 263, 1-16 (1965).

13. W. F. Libby, "Atmospheric helium-3 and radiocarbon from cosmic radiation", Phys. Rev. 69, 671-672 (1946).

14. L. T. Aldrich and A. O. Nier, "Argon^{40} in potassium minerals", Phys. Rev. 74, 876-877 (1948).

15. E. J. Zeller, "New developments in the thermoluminescence method of geologic age determination", Radioactive Dating, International Atomic Energy Agency, Vienna, 1963. pp. 73-85.

16. N. M. Johnson, "Thermoluminescence in contact metamorphosed limestone", J. Geol. 71, 596-616 (1963).

17. B. E. Sabels, "Age studies on basaltic lava flows using natural alpha activity and thermoluminescence", Radioactive Dating, International Atomic Energy Agency, Vienna, 1963. pp. 87-102.

18. A. Cox, R. R. Doell, G. B. Dalrymple, "Reversals of the earth's magnetic field", Science 144, 1537-1543 (1964).

19. H. D. Holland, "Radiation damage and its use in age determination," in Nuclear Geology, ed. H. Faul, J. Wiley and Sons, New York, 1954, pp. 175-180.

20. H. W. Fairbairn, P. M. Hurley, "Radiation damage in zircon and its relation to ages of Paleozoic igneous rocks in northern New England and adjacent Canada", Am. Geophys. Un. Trans. 38, 99-107 (1957).

21. S. Deutsch, P. Kieffer, E. Picciotto, "Pleochroic halos and the artificial coloration of biotites by β particles: II". Nuov. Cim. 10, 797-810 (1957).

22. S. R. Titley, P. E. Damon, "Investigation of color centers in fluorite with application to geologic time", J. Geophys. Res. 67, 4491-4495 (1962).

23. P. B. Price, R. M. Walker, "Fossil tracks of charged particles in micas and the age of minerals", ibid, 68, 4847-4862 (1963).

24. R. L. Fleischer, P. B. Price, "Techniques for geological dating of minerals by chemical etching of fission fragment tracks", Geochim. et Cosmochim. Acta 28, 1705-1714 (1964).

25. P. M. Hurley, "The helium age method and the distribution and migration of helium in rocks", in Nuclear Geology, ed. H. Faul, J. Wiley and Sons, New York, 1954. pp. 301-329.

26. R. J. Strutt, "Helium and radioactivity in rare and common minerals", Proc. Roy. Soc. (London) A80, 572-594 (1908).

27. P. E. Damon, W. D. Green, "Investigations of the helium age dating method by stable isotopic-dilution technique", Radioactive Dating, International Atomic Energy Agency, Vienna, 1963. pp. 55-71.

28. O. A. Schaeffer, "Helium-uranium ratios for Pleistocene and Tertiary fossil aragonites", Science 149, 312-316 (1965).

29. H. L. Volchok, J. L. Kulp, "The ionium method of age determination", Geochim. et Cosmochim. Acta 11, 219-246 (1957).

30. J. K. Osmond, J. R. Carpenter, H. L. Windom, "Th^{230}/U^{234} age of the Pleistocene corals and oolites of Florida", J. Geophys. Res. 1843-1847 (1965).

31. B. Hirt, W. Herr, W. Hoffmeister, "Age determinations by the rhenium-osmium method", Radioactive Dating, International Atomic Energy Agency, Vienna, 1963. pp.35-43.

32. W. Herr, E. Merz, "The natural racioactivity of letetium-176 and its possible application to geological age determination", Radioisotopes in Scientific Research, Vol. II, ed. R. C. Extermann, Pergamon Press, London, 1958. p. 571.

33. R. Davis, Jr., O. A. Schaeffer, "Chlorine-36 in nature", Ann. N. Y. Acad. Sci. 62, 105-122 (1955).

34. G. O. S. Arrhenius, "Sedimentation on the ocean floor", Researches in Geochemistry, ed. P. H. Abelson, J. Wiley and Sons, New York, 1959. p. 14.

35. D. L. Thurber, Jr., "Anomalous U^{234}/U^{238} in nature", J. Geophys. Res. 67, 4518-4520 (1962).

36. I. Friedman, R. L. Smith "A new dating method using obsidian", Amer. Antiquity 25, 476-522 (1960).

37. C. K. Wentworth, "Estimates of marine and fluvial erosion in Hawaii", J. Geol. 35, 117-133 (1927).

38. I. McDougall, "Potassium-argon ages from lavas of the Hawaiian Islands", Geol. Soc. Amer. Bull. 75, 107-128 (1964).

39. J. F. Evernden, D. E. Savage, G. H. Curtis, G. T. James, "Potassium-argon dates and the Cenozoic chronology of North America", Am. J. Sci. 262, 145-198 (1964).

40. J. J. Naughton, A. O. Schaeffer, "Some preliminary age determinations on Hawaiian Lavas", abstract of paper presented at International Symposium on Volcanology, Tokyo, May 9-19, 1962.

41. R. Moberly, Jr., "Rate of denudation in Hawaii", J. Geol, 71, 371-375 (1963).

42. H. W. Menard, E. C. Allison, J. W. Durham, "A drowned Miocene terrace in the Hawaiian Islands", Science 138, 896-897 (1962).

43. H. T. Stearns, K. N. Vaksvik, "Geology and groundwater resources of Oahu, Hawaii", Hawaii Div. Hydrography Bull. 1, p. 67 (1935).

44. G. A. Macdonald, "Petrography of the Waianae Range, Oahu" in H. T. Stearns, "Supplement to the geology and groundwater resources of the island of Oahu, Hawaii," Hawaii Div. Hydrography Bull. 5, 63-91 (1940).

45. G. A. Macdonald, "Hawaiian Petrographic Province," Geol. Soc. Amer. Bull. 60, 1541-1595 (1949).

46. G. A. Macdonald, T. Katsura, "Chemical composition of Hawaiian lavas," J. Petrol. 5, 82-133 (1964).

47. N. R. Campbell, A. Wood, "The radioactivity of the alkali metals," Proc. Cambridge Philos. Soc. 14, 15-21 (1906).

48. F. C. Thompson, S. Rowlands, "Dual decay of potassium," Nature 1952, 103-104 (1933).

49. C. F. Von Weizsacker, "Uber die Möglichkeit eines dualen - zerfalls von Kalium," Z. Physik 38, 623-635 (1937).

50. W. R. Smythe, A. Hemmendinger, "The radioactive isotope of potassium," Phys. Rev. 51, 178-182 (1937).

51. A. O. Nier, "Evidence for the existence of an isotope of potassium of mass 40," Phys Rev. 48, 283-284 (1935).

52. A. O. Nier, "A redetermination of the relative abundances of carbon, nitrogen, oxygen, argon and potassium," Phys. Rev. 77, 789-793 (1950).

53. F. Smits, W. Gentner, "Argonbestimmungen an Kalium Mineralen I. Bestimmungen an tertiaren Kalisalzen," Geochim. et Cosmochim. Acta 1, 22-27 (1950).

54. M. G. Inghram, H. Brown, C. Patterson, D. C. Hess, "The branching ratio of K^{40} radioactive decay," Phys. Rev. 80, 916-917 (1950).

55. D. R. Carr, J. L. Kulp, "Use of Ar^{37} to determine argon behavior in vacuum systems," Rev. Sci. Instr. 26, 379-381 (1955).

56. D. Alpert, "New developments in the production of high vacuum," J. Appl. Phys. 24, 860-876 (1953).

57. J. H. Reynolds, "High sensitivity mass spectrometer for noble gas analysis," Rev. Sci. Instr. 27, 928-934 (1956).

58. S. Dushman, Scientific Foundations of Vacuum Technique, John Wiley and Sons, New York, 1962. pp. 629-634.

59. D. E. White, G. A. Waring, "Volcanic Emanations," USGS Professional Paper 440-K, pp. 10-11 (1963).

60. J. R. Stevens, H. A. Shillibeer, "Loss of argon from minerals and rocks due to crushing," Proc. Geol. Soc. Can. 8, 71-76 (1956).

61. S. S. Goldich, H. Baadsgaard, A. O. Nier, "Investigations in A^{40}/K^{40} dating," Amer. Geophys. Un. Trans. 38, 547 (1957).

62. E. K. Gerling, J. M. Morozova, V. V. Kurbatov, "The retentivity of radiogenic argon in ground micas," Ann. N. Y. Acad. Sci. 91, 227-234 (1961).

63. D. R. Carr, J. L. Kulp, "Potassium-argon method of geochronometry," Geol. Soc. Amer. Bull. 68, 763-784 (1957).

64. O. A. Schaeffer, D. Heymann, "Comparison of Cl^{36}-Ar^{36} and Ar^{36}-Ar^{38} cosmic ray exposure ages of dated fall iron meteorites," J. Geophys. Res. 70, 215-224 (1965).

65. A. A. Polkanov, E. K. Gerling, "K-A and Rb-Sr methods and age of Precambrian of USSR," Amer. Geophys. Un. Trans. 39, 713-715 (1958).

66. A. Y. Krylov, "The possibility of utilizing the absolute age of metamorphic and fragmental rocks in paleogeography and paleotectonics," Ann. N. Y. Acad. Sci. 91, 324-340 (1961).

67. H. Baadsgaard, G. L. Cumming, R. E. Folinsbee, J. D. Godfrey, "Limitations of radiometric dating," in Geochronology of Canada, Univ. of Toronto Press, Toronto, 1964. pp. 20-38.

68. J. L. Kulp, J. Engels, "Discordances in K-Ar and Rb-Sr Isotopic ages," Radioactive Dating, International Atomic Energy Agency, Vienna, 1963. p. 231.

69. W. A. Bassett, P. F. Kerr, O. A. Schaeffer, R. W. Stoenner, "Potassium-argon dating of the late Tertiary volcanic rocks and mineralization of Marysville, Utah," Geol. Soc. Amer. Bull. 74, 213-220 (1963).

70. G. B. Dalrymple, "Potassium-argon dates of some Cenozoic volcanic rocks of the Sierra Nevada, California," Geol. Soc. Amer. Bull. 74, 379-390)1963).

71. J. F. Evernden, G. T. James, "Potassium-argon dates and the Tertiary floras of North America," Am. J. Sci. 262, 945-974 (1964).

72. J. F. Evernden, G. H. Curtis, Personal communication to J. J. Naughton.

73. G. J. Wasserburg, R. J. Hayden, "A^{40}-K^{40} dating," Geochim. et Cosmochim. Acta 7, 51 (1955).

74. H. Baadsgaard, J. Lipson, R. E. Folinsbee, "The leakage of radiogenic argon from sanidine," Ibid. 25, 147-157 (1961).

75. S. R. Hart, "Mineral ages and metamorphism," Ann. N. Y. Acad. Sci. 91, 192-197 (1961).

76. G. R. Tilton, S. R. Hart, "Geochronology," Science 140, 357-366 (1963).

77. G. N. Hanson, "The effect of thermal metamorphism on the K-Ar and Rb-Sr ages of various minerals in the Snowbank stock," Amer. Geophys. Un. Trans. 45, 115 (1964).

78. J. L. Kulp, "Potassium-argon dating of volcanic rocks," Bull. Volcanologique 26, 247-258 (1963).

79. P. M. Hurley, H. Hughes, W. H. Pinson, Jr., H. W. Fairbairn, "Radiogenic argon and strontium diffusion parameters in biotite at low temperatures obtained from Alpine Fault uplift in New Zealand," Geochim. et Cosmochim. Acta 26, 67-80 (1962).

80. G. W. Wetherill, L. T. Aldrich, G. L. Davis, "Ar^{40}/K^{40} ratios of feldspars and micas from the same rock," Ibid. 8, 171-172 (1955).

81. S. R. Hart, "The use of hornblendes and pyroxenes for K-Ar dating," J. Geophys. Res. 66, 2995-3001 (1961).

82. I. McDougall, "Determination of the age of a basic igneous intrusion by the potassium-argon method," Nature 190, 1184-1186 (1961).

83. G. P. Erickson, J. L. Kulp, "Potassium-argon dates on basaltic rocks," Ann. N. Y. Acad. Sci. 91, 322-323 (1961).

84. O. A. Schaeffer, R. W. Stoenner, W. A. Bassett, "Dating of Tertiary volcanic rocks by the potassium-argon method, Ibid. 317-320.

85. J. F. Evernden, G. H. Curtis, J. Obradovich, R. Kistler, "On the evaluation of glauconite and illite for dating sedimentary rocks by the potassium-argon method," Geochim. et Cosmochim. Acta 23, 78-99 (1961).

86. P. M. Hurley, "Glauconite as a possible means of measuring the age of sediments," Ann. N. Y. Acad. Sci. 91, 294-297 (1961).

87. J. Hower, P. M. Hurley, W. H. Pinson, H. W. Fairbairn, "The dependence of K-Ar age on the mineralogy of various particle size ranges in a shale," Geochim. et Cosmochim. Acta 27, 405-410 (1963).

88. C. T. Harper, "Potassium-argon ages of slates and their geological significance," Nature 203, 468 (1964).

89. H. J. Lippolt, W. Gentner, "K-Ar dating of some limestones and fluorites," Radioactive Dating, International Atomic Energy Agency, Vienna, 1963. pp. 239-244.

90. W. Wahler, "Über die in Kristallen eingeschlossenen Flüssigkeiten und Gase," Geochim. et Cosmochim. Acta 9, 105-135 (1956).

91. P. E. Damon, J. L. Kulp, "Excess helium and argon in beryl and other minerals," Amer. Min. 43, 433-459 (1958).

92. S. R. Hart, R. T. Dodd, Jr., "Excess radiogenic argon in pyroxenes," J. Geophys. Res. 67, 2998-2999 (1962).

93. J. F. Levering, J. R. Richards, "Potassium-argon age study of possible lower-crust and upper-mantle inclusions in deep-seated intrusives," Ibid. 69, 4895-4901 (1964).

94. G. R. Evans, J. Tarney, "Isotopic ages of Assynt dykes," Nature 204, 638-641 (1964).

95. H. L. Allsopp, "Rb-Sr and K-Ar age measurements on the great dike of Southern Rhodesia," J. Geophys. Res. 70, 977-984 (1965).

96. I. McDougall, D. H. Green, "Excess radiogenic argon in pyroxenes and isotopic ages on minerals from Norwegian eclogites," Norsk. Geol. Tidsskr. 44, 183-196 (1964).

97. J. R. Richards, R. T. Pidgeon, "Some age measurements on micas from Broken Hill, Australia," J. Geol. Soc. Australia 10, 243-259 (1963).

98. D. E. Livingston, P. E. Damon, R. L. Mauger, R. Bennett, A. W. Laughlin, "Argon retentivity in cogenetic plagioclase, potash feldspar, and mica from plutonic and metamorphic rocks," Amer. Geophys. Un. Trans. 46, 547 (1965).

99. M. M. Elinson, V. S. Polykovskii, "Some characteristics of the process of formation of quartz crystal pegmatites as revealed by an investigation of gas inclusions in minerals and rocks," Geochemistry, No. 10, 977-987 (1961).

100. M. M. Elinson, V. S. Polykovskii, "The composition of gases in pneumatolytic-hydrothermal solutions," Ibid. No. 8, 799-807 (1963).

101. S. N. I. Rama, S. R. Hart, E. Roedder, "Excess radiogenic argon in fluid inclusions," J. Geophys. Res. 70, 509-511 (1965).

102. Z. N. Nesmelova, "Gases in potassium salts of the Bereznikovsk mine," Tr. Vses. Nauchn.-Issled. Inst. Galurgii, No. 35, 206-243 (1959).

103. R. B. Hoy, R. M. Foose, B. J. O'Niell, Jr., "Structure of Winfield Salt Dome," Am. Assoc. Petrol Geol. Bull. 46, 1444-1459 (1962).

104. Argon, Helium and the Rare Gases, Vol. 1, ed. G. S. Cook, John Wiley and Sons, New York, 1961. pp. 42-43.

105. J. Lipson, "Potassium-argon dating of sedimentary rocks," Geol. Soc. Amer. Bull. 69, 137-150 (1958).

106. G. B. Dalrymple, "Potassium-argon dates of three Pleistocene interglacial basalt flows from the Sierra Nevada, California," Geol. Soc. Amer. Bull. 75, 753-758 (1964).

107. K. I. Amirkhanov, S. B. Brandt, E. N. Bartnitsky, "Radiogenic argon in minerals and its migration," Ann. N. Y. Acad. Sci. 91, 235-275 (1961).

108. J. J. Naughton, "Possible use of argon-39 in the potassium-argon method of age determination," Nature 197, 661-663 (1963).

109. Y. M. Artimov, K. G. Knorre, V. P. Strizhov, "Isotopic dilution technique with a tracer introduced in the solid phase," Geochemistry, No. 12, 1213-1214 (1963).

110. J. J. Naughton, Personal communication.

111. I. L. Barnes, "An investigation of a new method for potassium-argon age determination," Ph.D. Thesis, University of Hawaii, 1963. pp. 21-30

112. R. C. Sweet, W. Rieman III, J. Beukenkamp, "Determination of alkali metals in insoluble silicates by ion-exchange chromatography," Anal. Chem. 24, 952-955 (1952).

113. J. A. Dean, Flame Photometry, McGraw-Hill, New York, 1960. p. 47.

114. J. A. Cooper, "The flame photometric determination of potassium in geological materials used for potassium argon dating," Geochim. et Cosmochim. Acta 27, 525-546 (1963).

115. G. H. Hoops, "The nature of the insoluble residues remaining after HF-H_2SO_4 acid decomposition (Solution B) of rocks," Ibid. 28, 405-406 (1964).

116. P. B. Adams, "Rapid flame photometric determination of alkalis in glasses and silicates, " Anal. Chem. 33, 1602-1605 (1961).

117. E. L. Grove, C. W. Scott, F. Jones, "Mutual radiation interference effects of the alkali elements and hydrogen upon the resonance line intensities of the alkali elements in flame spectrophotometry," Talanta 12, 327-342 (1965).

118. A. J. Easton, J. F. Lovering, "Determination of small quantities of potassium and sodium in stony meteorites material, rocks, and minerals," Anal. Chim. Acta. 30, 543-548 (1964).

119. W. Hamilton, W. Mountjoy, "Alkali content of alpine ultramafic rocks," Geochim. et Cosmochim. Acta 29, 661-671 (1965).

120. G. Edwards, H. C. Urey, "Determination of alkali metals in meteorites by a distillation process," Ibid. 7, 154-168 (1955).

121. C. Yamashiro, "Potassium analysis of selected rocks by solid source mass spectrometry," MS Thesis, University of Hawaii, 1965.

122. G. Patzlaff, "The gettering properties of titanium and zirconium at elevated temperatures," MS Thesis, University of Hawaii, 1966.

123. D. Lichtman, "Methane evolution in ion pump systems," Paper presented at the Amer. Phys. Soc. Annual Meeting, Jan. 27, 1960, New York City.

124. G. Reich. H. G. Noller, "Ionen-Getterpumpe für Niedrige Druck," Advances in Vacuum Science and Technology I, Pergamon Press, London, 1960. pp. 443-445.

125. A. Klopfer, W. Ermrich, "Erfahrungen mit Titan-Ionen-pumpen," Ibid. 427-429.

126. L. Holland, J. Laurenson, P. G. W. Allen, "Evolution of hydrocarbons in an ion pump system," Nature 192, 749-750 (1961).

127. A. R. Hamilton, "Some experimental data on parameter variations with the triode-getter ion pump," National Symp. Vac. Tech. Trans. 2, 388-394 (1961).

128. J. R. Young, "Electrical cleanup of gases in an ionization gauge," J. Appl. Phys. 27, 926-928 (1956).

129. R. N. Bloomer, M. E. Haine, "The electronic clean-up of gases in sealed-off vacuum systems," Vacuum 3, 128-135 (1953).

130. K. B. Blodgett, T. A. Vanderslice, "Electrical cleanup in ionization gauges," National Symp. Vac. Tech. Trans. 2, 400-405 (1961).

131. H. Schwartz, "Gasaufzehrung und Gasaustausch bei der Messung Niedrigster Druck im Ionisationsmanometer," Z. Physik 122, 437-450 (1944).

132. R. B. Burtt, J. S. Colligon, J. H. Leck, "Sorption and replacement of ionized noble gases at a tungsten surface," Brit. J. Appl. Phys. 12, 396-400 (1961).

133. L. H. James, J. H. Leck, G. Carter, "Ion bombardment induced emission of sorbed gas from glass surfaces," Ibid. 15, 681-689 (1964).

134. J. H. Carmichael, E. A. Trendelburg, "Ion-induced re-emission of noble gases from a nickel surface," J. Appl. Phys. 29, 1570-1577 (1958).

135. E. Farrar, R. M. MacIntyre, D. York, W. J. Kenyon, "A simple mass spectrometer for the analysis of argon at ultra-high vacuum," Nature 204, 531-533 (1964).

136. S. Dushman, op cit. pp. 469-491.

137. P. A. Redhead, E. V. Kornelsen, J. P. Hobson, "Ultra-high vacuum in small glass systems," Can J. Phys. 40, 1814-1836 (1962).

138. I. McDougall, Personal communication to J. J. Naughton.

139. R. R. Doell, A. Cox, "Paleomagnetism of Hawaiian lava flows," J. Geophys. Res. 70, 3377-3405 (1965).

140. F. G. Smith, Historical Development of Inclusion Thermometry, University of Toronto Press, Toronto, Canada, 1953. 149 pp.

141. E. Roedder, "Technique for the extraction and partial chemical analysis of fluid-filled inclusions from minerals," Econ. Geol. 53, 235-269 (1958).

142. _____, "Studies of fluid inclusions I: Low temperature application of a dual-purpose freezing and heating stage," Ibid. 57, 1045-1061 (1962).

143. _____, "Studies of fluid inclusions II: Freezing data and their interpretation," Ibid. 58, 167-211 (1963).

144. Roedder, B. Ingram, W. E. Hall, "Studies of fulid inclusions III: Extraction and quantitative analysis of inclusions in the milligram range," Ibid. 58, 353-374 (1963).

145. J. A. Kohn, R. A. Hatch, "Synthetic Mica Investigations, VI: X-ray and optical data on synthetic fluor-phlogopite," Amer. Mineralogist 40, 10-21 (1955).

146. G. Boato, G. Careri, G. Nencini, M. Santangelo, "Isotopic composition of argon in natural gases," Annali Geofisica (Rome) 4, 111-112 (1951).

147. G. J. Wasserburg, E. Mazor, R. E. Zartman, "Isotopic and chemical composition of some terrestrial natural gases," in Earth Science and Meteoritics. North Holland, Amsterdam (1963).

148. G. A. Macdonald, Personal communication.

149. T. B. Karpinskaya, I. A. Ostrovskii, L. L. Shanin, "Artificial introduction of argon into mica at high pressures and temperatures," Izv. Akad. Nauk SSSR, Ser. Geol. No. 8, 99-100 (1961).

150. D. M. Roy, S. P. Faile, O. F. Tuttle, "Effect of large concentrations of dissolved gas on properties of glass," Phys. and Chem. of Glasses 5, 176-177 (1964).

151. W. Schreyer, H. S. Yoder, Jr., "Synthetic hydrous and argon-bearing cordierites," Geol. Soc. Amer. Bull. 71, 1968-1969 (1961).

152. C. S. Ross, M. D. Foster, A. T. Myers, "Origin of dunites and olivine-rich inclusions in basaltic rocks," Amer. Mineralogist 39, 693-737 (1954).

153. I. Kushiro, H. Kuno, "Origin of primary basalt magmas and classification of basaltic rocks," J. Petrol 4, 75-89 (1963).

154. F. J. Turner, J. Verhoogen, Igneous and Metamorphic Petrology, McGraw-Hill, New York (1960) pp. 201-202.

155. G. A. Macdonald, "The lithological constitution of the crust and mantle in the Hawaiian area," Pac. Sci. 19, 285-286 (1965).

156. F. J. Turner and J. Verhoogen, op cit. 1st ed., p. 140 (1951).

157. A. Holmes, F. A. Paneth, "Helium-ratios of rocks and minerals from the diamond pipes of South Africa," Proc. Roy. Soc. London, A, 154, 385-413 (1936).

158. J. F. Lovering, J. W. Morgan, "Uranium and thorium abundances in possible upper mantle materials," Nature 197, 138-140 (1963).

159. J. A. Miller, A. J. Barber, N. H. Kempton, "A potassium-argon age determination from a Lewisian inlier," Nature 197, 1095-1-96 (1963).

160. H. T. Stearns, G. A. Macdonald, "Geology and ground-water resources of the island of Hawaii," Hawaii Terr. Div. Hydrography Bull. 9, (1946) p. 147.

161. D. H. Richter, K. J. Murata, "Xenolith nodules in the 1800-01 Kaupulehu flow of Hualalai Volcano and their petrologic implication," Proc. Hawaiian Acad. Sci. 35th Annual Meeting, 1960.

162. H. Winchell, "Honolulu Series, Oahu, Hawaii," Geol. Soc. Amer. Bull. 58, 1-48 (1947).

163. E. Roedder, "Liquid carbon dioxide in ultra-mafic xenoliths in Hawaiian basalts" (abstract), presented at Geochemistry Session, International Union of Geodesy and Geophysics, Berkeley, Calif., August 1963.

164. P. E. Damon, J. L. Kulp, "Argon in mica and the age of the Beryl Mt., N. H., pegmatite", Am. J. Sci. 255, 697-704 (1957).

165. P. E. Damon, "Correlation and chronology of ore deposits and volcanic rocks," Annual Prog. Rpt. COO-689-50 to U. S. Atomic Energy Commission, p. 37 (1965).

166. D. D. Bogard, M. W. Rowe, O. W. Manuel, A. K. Kuroda, "Noble gas anomalies in the mineral thucholite," J. Geophys. Res. 70, 703-708 (1965).

167. D. B. McIntyre, "Precision and resolution in geochronometry," C. C. Albritton, ed., The Fabric of Geology, Addison-Wesley, Reading Massachusetts (1963) p. 113.

168. W. H. Pinson, "The potassium-argon method: the problem of potassium analysis," Ann. N. Y. Acad. Sci. 91, 221-224 (1961).

169. P. M. Hurley, ed., Variations in Isotopic Abundance of Strontium, Calcium, and Argon and Related Topics, Mass. Instit. Technol. Dept. Geology and Geophysics, Tenth Ann. Progr. Rept. (1962) p. 151.

170. M. A. Lanphere, G. B. Dalrymple, "P-207. An interlaboratory standard muscovite for argon and potassium analysis," J. Geophys. Res. 70, 3497-3503 (1965).

171. M. Fleischer, R. E. Stevens, "Summary of new data on rock samples G-1 and W-1," Geochim. et Cosmochim. Acta 26, 525-543 (1962).

172. I. L. Barnes, Personal communication.

173. S. R. Taylor, P. Kolbe, "Geochemical standards," G & CA 28, 447-454 (1964).

174. G. B. Dalrymple, K. Hirooka, "Variation in potassium, argon and calculated age in a late Cenozoic basalt," J. Geophys. Res. 70, 5291-5296 (1965).

175. R. H. Dicke, "Principle of equivalence and weak interactions," Rev. Mod. Phys. 29, 355-362 (1957).

176. R. H. Dicke, "Dirac's cosmology and the dating of meteorites," Nature 183, 170-171 (1959).

177. J. R. Richards, Personal communication.